

THE
IIOAB
JOURNAL

VOLUME 3 : NO 2 : JULY 2012 : ISSN 0976-3104



Institute of Integrative Omics and
Applied Biotechnology Journal

Dear Esteemed Readers, Authors, and Colleagues,

I hope this letter finds you in good health and high spirits. It is my distinct pleasure to address you as the Editor-in-Chief of Integrative Omics and Applied Biotechnology (IIOAB) Journal, a multidisciplinary scientific journal that has always placed a profound emphasis on nurturing the involvement of young scientists and championing the significance of an interdisciplinary approach.

At Integrative Omics and Applied Biotechnology (IIOAB) Journal, we firmly believe in the transformative power of science and innovation, and we recognize that it is the vigor and enthusiasm of young minds that often drive the most groundbreaking discoveries. We actively encourage students, early-career researchers, and scientists to submit their work and engage in meaningful discourse within the pages of our journal. We take pride in providing a platform for these emerging researchers to share their novel ideas and findings with the broader scientific community.

In today's rapidly evolving scientific landscape, it is increasingly evident that the challenges we face require a collaborative and interdisciplinary approach. The most complex problems demand a diverse set of perspectives and expertise. Integrative Omics and Applied Biotechnology (IIOAB) Journal has consistently promoted and celebrated this multidisciplinary ethos. We believe that by crossing traditional disciplinary boundaries, we can unlock new avenues for discovery, innovation, and progress. This philosophy has been at the heart of our journal's mission, and we remain dedicated to publishing research that exemplifies the power of interdisciplinary collaboration.

Our journal continues to serve as a hub for knowledge exchange, providing a platform for researchers from various fields to come together and share their insights, experiences, and research outcomes. The collaborative spirit within our community is truly inspiring, and I am immensely proud of the role that IIOAB journal plays in fostering such partnerships.

As we move forward, I encourage each and every one of you to continue supporting our mission. Whether you are a seasoned researcher, a young scientist embarking on your career, or a reader with a thirst for knowledge, your involvement in our journal is invaluable. By working together and embracing interdisciplinary perspectives, we can address the most pressing challenges facing humanity, from climate change and public health to technological advancements and social issues.

I would like to extend my gratitude to our authors, reviewers, editorial board members, and readers for their unwavering support. Your dedication is what makes IIOAB Journal the thriving scientific community it is today. Together, we will continue to explore the frontiers of knowledge and pioneer new approaches to solving the world's most complex problems.

Thank you for being a part of our journey, and for your commitment to advancing science through the pages of IIOAB Journal.



Yours sincerely,

Vasco Azevedo

Vasco Azevedo, Editor-in-Chief
Integrative Omics and Applied Biotechnology
(IIOAB) Journal



Prof. Vasco Azevedo
Federal University of Minas Gerais
Brazil

Editor-in-Chief

Integrative Omics and Applied Biotechnology (IIOAB) Journal Editorial Board:



Nina Yiannakopoulou
Technological Educational Institute of Athens
Greece



Jyoti Mandlik
Bharati Vidyapeeth University
India



Rajneesh K. Gaur
Department of Biotechnology, Ministry of Science and Technology
India



Swarnalatha P
VIT University
India



Vinay Aroskar
Sterling Biotech Limited
Mumbai, India



Sanjay Kumar Gupta
Indian Institute of Technology
New Delhi, India



Arun Kumar Sangaiah
VIT University
Vellore, India



Sumathi Suresh
Indian Institute of Technology
Bombay, India



Bui Huy Khoi
Industrial University of Ho Chi Minh City
Vietnam



Tetsuji Yamada
Rutgers University
New Jersey, USA



Moustafa Mohamed Sabry Bakry
Plant Protection Research Institute
Giza, Egypt



Rohan Rajapakse
University of Ruhuna
Sri Lanka



Atun RoyChoudhury
Ramky Advanced Centre for Environmental Research
India



N. Arun Kumar
SASTRA University
Thanjavur, India



Bui Phu Nam Anh
Ho Chi Minh Open University
Vietnam



Steven Fernandes
Sahyadri College of Engineering & Management
India

PERFORMANCE OF LOW PRESSURE REVERSE OSMOSIS MEMBRANE TREATING SYNTHETIC NATURAL ORGANIC MATTER (NOM) AND ENDOCRINE DISRUPTING CHEMICAL (EDC)

Mohd Fadhil Md Din¹, Rafidah Shahperi¹ and Shreeshivadasan Chelliapan^{2*}

¹Institute of Environmental Water Resources and Management (IPASA), Faculty of Civil Engineering, Universiti Teknologi Malaysia, 81310 Skudai, Johor Bahru, MALAYSIA

²UTM Razak School of Engineering and Advanced Technology, Universiti Teknologi Malaysia (International Campus), Jalan Semarak, 54100, Kuala Lumpur, MALAYSIA

ABSTRACT

The current study describes the performance of low pressure reverse osmosis membrane (LPROM) treating synthetic wastewater containing dichlorodiphenyltrichloroethane, DDT (endocrine disrupting chemical, EDC) and glucose (natural organic matter, NOM) at various operating pressure and pH. The experimental results were compared to a modified design expert model using response surface method (RSM). Results showed up to 94.6% DDT and 85% glucose removal was achieved in the membrane system at an operating pressure and pH of 100 psi and 9, respectively, indicating efficient performance of the system. However, when the membrane system was operated at elevated pressure and low pH (120 psi and pH 5.5), the DDT and glucose removal efficiencies decreased to 91.2 and 75.5%, respectively, indicating operating pressure and pH affected the performance of the system. The design expert analysis for both DDT and glucose showed high removal efficiencies (93.67 and 81.70%) when the LPROM was operated at 114.14 psi, confirming that the LPROM is an excellent system for the treatment of EDC and NOM containing wastewater.

Received on: 10th-Sept-2011

Revised on: 2nd-Jan-2012

Accepted on: 9th-Feb-2012

Published on: 2nd-Mar-2012

KEY WORDS

Reverse osmosis (RO); low pressure reverse osmosis membrane (LPROM); endocrine disrupting chemical (EDC); natural organic matter (NOM); dichlorodiphenyltrichloroethane (DDT); glucose

*Corresponding author: Email: shreeshivadasan@ic.utm.my; Tel: 006-03-26154581; Fax: 006-03-26934844

[1] INTRODUCTION

Membrane technology is considered as one of the most effective process for water and wastewater treatment. It is a compact system, economically feasible and has high pollutant removal efficiency. The technology has been proven to be effective and offers an alternative system where better effluent quality was produced in wastewater treatment plant [1, 2]. In general, the membrane process can be divided into four major classifications: microfiltration (MF), ultrafiltration (UF), nanofiltration (NF), and reverse osmosis (RO). In the past, pressure-driven membrane processes such as RO had gained special attention due to its effective removal of pollutants, especially those with low concentrations.

The wastewater treatment and reclamation by RO has developed tremendously. These include enhancement in salt removal capabilities, chemical stability and perhaps most importantly, pressure requirements [3]. RO is a process that reversing natural phenomenon of osmosis by applying pressure on the concentrated solution in contact with a semi-permeable membrane. This pressure-driven process rejects dissolved constituents that present in the feed water due to size and charge exclusion and physical chemical interactions between

solute, solvent and membranes [4]. However, the use of RO is limited due to high operational cost especially when high pressure is applied. Therefore, low pressure reverse osmosis membrane (LPROM) has been introduced to water and wastewater industries in the past few years [5, 3, 6, 7].

Most of LPROM are multi-layer thin film composed of complex polymers. The active membrane surface layer normally consists of negatively charged sulphone or carboxyl group. This helps the membranes in improving of fouling resistance against hydrophobic colloids, proteins, oils and other organics. In order to increase water flux, a charged hydrophilic layer is attached to a hydrophobic UF support membrane. This makes the membrane favorable for the orientation of water dipoles. Flux is inversely proportional to the membrane thickness. Generally, LPROM contains corrugated skin surface that can improve flux significantly. It produces specific flux more than 60 L/m².h MPa (flux per membrane area and per net driving pressure) at low operating pressure. This flux rate is about double the flux of the previous generations of composite RO membrane.

LPROM has the advantage of removing organic and inorganic species as compared to the conventional RO membranes [8]. According to Hofman [6], LPROM showed high removal efficiency for organic micro pollutants and pesticides. Based on LPROM specifications, the energy capacity could be lower than the conventional RO which is about 30 – 40%. Moreover, LPROM is also used for direct treatment of surface water that contains dissolved salts and organic substances.

In general, EDC in wastewater effluent and surface water has raised substantial concern in the public and regulatory agencies. Therefore, there is a potential for LPROM system to be used as a treatment unit for EDC containing wastewater and could offer high treatment efficiency at low costs. As a result, the main aim of this research was to evaluate the DDT and glucose removal efficiency in a LPROM system that operates at various pressure and pH. In addition, the performance of the membrane system was compared to a modified model using design expert analysis to show whether differences occur between the experimental study and the predicted model.

[II] MATERIALS AND METHODS

2.1. Experimental setup and operation

The experimental design was performed using response surface method (RSM) where it uses mathematical and statistical techniques. A multi-layer thin-film of aromatic polyamide (ES20) membrane was used for the LPROM study using a cross flow module (C10-T) [Figure-1]. These membrane consist of carboxyl and amine with effective surface area of 60 cm². The DDT and glucose concentrations were measured using a UV-spectrophotometer. The experimental study was performed by varying pH (2 – 9) and operating pressure (80 – 120 psi) with Design Expert Version 6.0.4 software [Table-1].

The preparation of medium and stock solution was performed using standard chemical measurement. Initially, a stock solution of 10 mg/L⁻¹ of synthetic wastewater containing DDT or glucose was prepared. The stock solution was used to prepare the required concentration of sample solutions. Later, the sample solutions were mixed with Hydrochloric Acid (HCl) or Sodium Hydroxide (NaOH) for pH

adjustment. The volume of stock solution required to achieve the desired concentration was determined by Molarity (M) balanced equation. Both samples (DDT or glucose) and hydrochloric acid (HCl) or Sodium Hydroxide (NaOH) were also prepared using the same procedures and formula.

2.2. Data analysis

The experimental data obtained from this study was calculated using the following formula:

i. Flux rate

$$F = \frac{\text{Average permeate}}{A \times t} \quad \dots \text{(Eq. 1)}$$

Where;

F = permeate flux (L/m².h)

A = effective area of membrane (60 cm²)

t = internal time when each permeate is collected (0.5 hours)

ii. Removal efficiency [Eq. 2]

$$R = \frac{C_f - C_p}{C_f} \times 100\% \quad \dots \text{(Eq. 2)}$$

Where;

C_f = feed concentration (mg/L)

C_p = permeate concentration (mg/L)

iii. Recovery rate (Eq. 3)

$$\text{Recovery Rate (\%)} = \frac{Q_p}{Q_f} \times 100\% \quad \dots \text{(Eq. 3)}$$

Where;

Q_p = permeate flow rate (ml/min)

Q_f = feed flow rate (ml/min)

The feed flow rate can be determined using mass balance equation:

$$Q_f = Q_p + Q_c \quad \dots \text{(Eq. 4)}$$

Q_c = flow rate of the concentration / retentate (L/min).

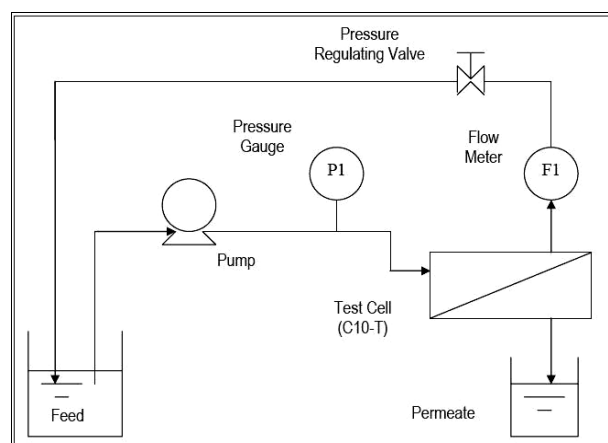
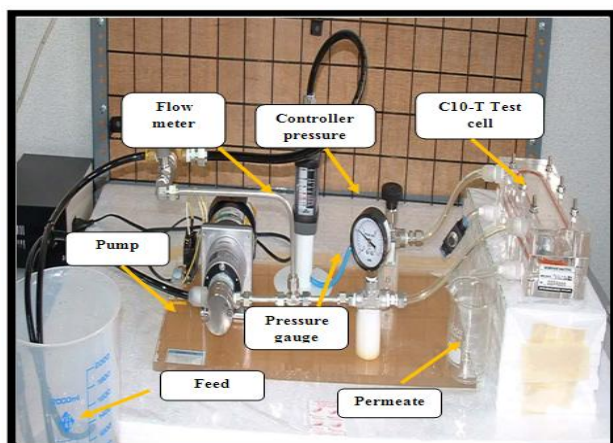


Fig. 1. LPROM set-up, Actual (left) and Schematic (right)

Table: 1. Operating characteristics during experimental study for DDT and glucose samples

Run Order	Operating Pressure (psi)	pH
1	114.14	3.03
2	100.00	5.50
3	80.00	5.50
4	100.00	9.00
5	120.00	5.50
6	100.00	2.00
7	85.86	3.03
8	114.14	7.97
9	85.86	7.97

[III] RESULTS AND DISCUSSION

3.1. DDT removal

Table-2 illustrates the DDT removal efficiency in the LPROM system treating synthetic wastewater at various operating pressure (80 - 120psi) and pH (2 - 9). The results showed that an average removal efficiency of 89.74% was achieved in the membrane system, indicating efficient performance of the system. The highest DDT removal efficiency (94.6%) was achieved at an operating pressure of 100 psi (pH 9, run order 3, **Table-2**). During this period, the flux rate was 32.67 L/m².h, however, when the membrane system was operated at high pressure (120 psi, pH 5.5, run order 6), the DDT removal efficiency decreased slightly to 91.2 %, indicating operating pressure effected the DDT removal efficiency and the flux rate (increased to 41 L/m².h, **Table 1**). One important observation during the study was the effect of pH on the treatment efficiency, where high removal efficiency (above 90%) was noted at elevated pH levels (e.g. pH 9) at operating pressure of 100 psi, except at pH 5.5, when the membrane system was operated at 120 psi. Since factors such as pH and operating pressure could affect the removal efficiencies of the LPROM system, it is important to control the flux rate for continuous operation and consistent removal of the micro pollutant. In general, the selected operational parameters in the current study [**Table-2**] had contributed to high DDT removal efficiencies

compared to other parameters such as temperature and loading rate.

The design expert is a useful tool to perform statistical analysis, especially for the factorial design during the preliminary study of the LPROM. It should be mentioned here that the modified experiment on the selected operational parameters was previously studied by Hamdzah [9]. **Figure- 2** shows the surface response plots based on the modified model and it can be observed that the flux rate increased from 15.31 to 37.15 L/m².h when the pressure was gradually increased (85.86 to 114.14 psi). Additionally, the effect of controlled parameters on DDT removal efficiency was also investigated by using RSM [**Figure-3**] and showed high removal efficiencies (85.80 - 93.67%) when the LPROM was operated at 85.86 - 114.14 psi, confirming that the LPROM indeed an excellent system for the treatment of EDC containing wastewater. One possible reason for the increased removal efficiency is because of the decrease in the average pore size on membrane surface and increase in the preferential sorption of pure water at elevated pressure. Consequently, the sample molecules would be more difficult to permeate through the membrane at high operating pressure.

Table: 2. Operational parameters and DDT removal efficiency

Run Code	pH	Operating Pressure (psi)	Flux (L/m ² .h)	Removal / Rejection (%)	Final Concentration (mg/L)
1	5.50	80.00	10.00	89.1	1.09
2	7.97	85.86	12.67	92.5	0.75
3	9.00	100.00	32.67	94.6	0.54
4	5.50	100.00	26.00	89.7	1.03
5	5.50	100.00	26.00	89.7	1.03
6	5.50	120.00	41.00	91.2	0.88
7	2.00	100.00	30.67	84.2	1.58
8	5.50	100.00	26.00	89.7	1.03
9	7.97	114.14	34.67	93.2	0.68
10	5.50	100.00	26.00	89.7	1.03
11	5.50	100.00	26.00	89.7	1.03
12	3.03	114.14	35.00	87.0	1.30
13	3.03	85.86	14.33	86.3	1.37

It can be concluded that the DDT removal efficiency was effected by the different operating pressure and pH in the membrane system. Previous study using membrane treatment systems have shown that the operating pressure effected the permeate flux [10, 11, 12, 13]. For example, Ozaki [11] demonstrated that organic compound removal was effected by pH and the molecular weight in a LPROM system. They found an increase in organic compound removal rate at higher molecular weight. In addition, the current study had demonstrated that the LPROM under higher operating pressure encourages high feed flow across the membrane which produces high permeate. In another word, pressure is applied to force the concentrated feed solution to flow across the membrane to produce less concentrated permeate. According to Ujang and Anderson [11], permeate flux was high when pressure was increased in a LPROM system treating synthetic wastewater containing heavy metals. Similar trend was also observed in the current study where high permeate flux was detected at elevated pressure and an increase in DDT removal efficiency.

DESIGN-EXPERT Plot

Flux
 X = A: pH
 Y = B: Pressure

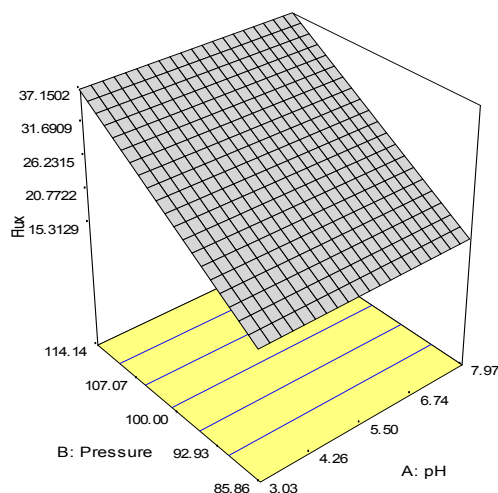


Fig: 2. Surface response plot (relationship between operating pressure, pH and permeate flux for DDT)

3.2. Glucose removal

Glucose is a synthetic organic substance with high carbohydrate compounds which may reduce the effectiveness of LPROM, particularly during the formation of humic acid. Therefore, the possible of glucose removal at a short period is necessary and in the present study, the average glucose removal efficiency was 71.08 % [Table-3]. The highest

removal efficiency (85%) was observed at an operating pressure and pH of 100 psi and 9.0, respectively [run code order 7, Table-3]. The fluctuations in removal efficiency (55.5 – 85%) were mainly attributed to the different operating pressure and pH. On the other hand, the flux range was 3.07 - 16.67 L/m².h and the highest flux was achieved at 120 psi and at pH 5.5 (run code order 9); indicating operating pressure affected the flux rate. Similar to the DDT removal, the glucose removal efficiency was dependent on the pH, where high removal efficiency was observed at elevated pH levels, demonstrating the LPROM system performed well at alkaline conditions. In the following section, several data was presented in a graphical manner to show the flux pattern and glucose removal.

DESIGN-EXPERT Plot

Rejection
 X = A: pH
 Y = B: Pressure

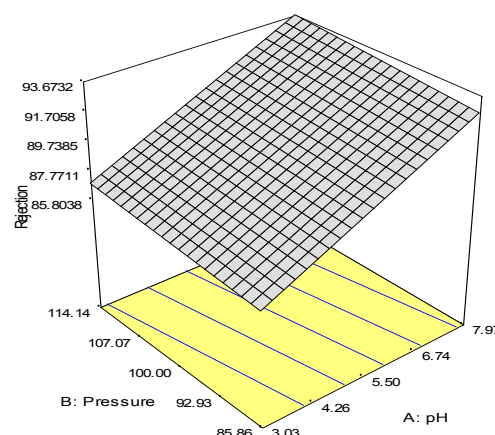


Fig: 3. Surface response plot for the effect of controlled parameters on DDT removal efficiency (relationship between operating pressure, pH and DDT removal efficiency)

3.2.1 Design expert analysis for glucose

Figure-4 shows the surface response and contour plots based on the modified model and shows an increase in flux rate (3.83 to 12.86 L/m².h) when pressure was increased (85.86 to 114.14 psi) gradually in the LPROM system. The effect of controlled parameters on the percentage of glucose removal was also investigated by RSM and the results were illustrated in Figure-5. The glucose removal efficiency was 59.17 - 81.70% when pressure was increased, a trend similar to the DDT removal in the modified model. The results of the modified model agrees with the actual experimental study where high removal efficiency was noted at elevated pressure.

Table: 3. Operational parameter and glucose removal efficiency

Run Code	pH	Operating Pressure (psi)	Flux (L/m ² .h)	Removal (%)	Final Concentration (mg/L)
1	5.50	100.00	6.50	71.5	2.85
2	7.97	114.14	11.67	84.2	1.58
3	5.50	100.00	6.50	71.5	2.85
4	2.00	100.00	6.33	55.5	4.45
5	7.97	85.86	4.00	77.2	2.28
6	5.50	80.00	3.07	67.0	3.30
7	9.00	100.00	7.67	85.0	1.50
8	3.03	85.86	4.33	60.0	4.00
9	5.50	120.00	16.67	75.5	2.45
10	3.03	114.14	10.67	62.2	3.78
11	5.50	100.00	6.50	71.5	2.85
12	5.50	100.00	6.50	71.5	2.85
13	5.50	100.00	6.50	71.5	2.85

DESIGN-EXPERT Plot

Flux
X = A: pH
Y = B: Pressure

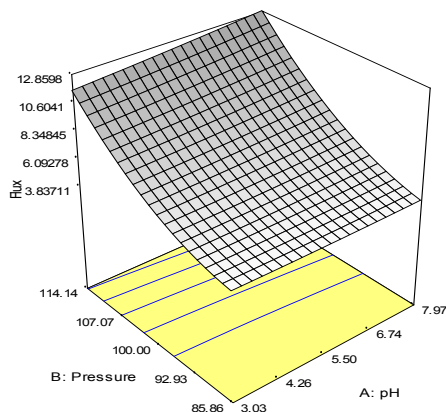


Fig: 4. Response surface plot (relationship between operating pressure, pH and permeate flux for Glucose)

DESIGN-EXPERT Plot

Rejection
= A: pH
= B: Pressure

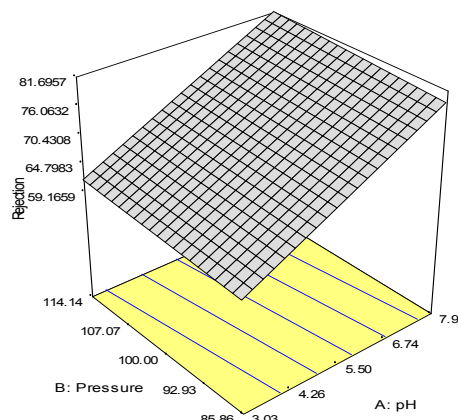


Fig: 5. Response surface plotting for the effect of controlled parameters on glucose removal efficiency

[V] CONCLUSION

The LPRM system is an appropriate option for the treatment of EDC and NOM containing wastewater and could offer high removal efficiency. Up to 94.6% DDT removal was achieved in the membrane system with effluent having a DDT value of 0.54 mg/L⁻¹. As for glucose, a typical removal efficiency of 85.0% was measured with effluent having a value of 1.50 mg/L⁻¹. The flux rate increased when the LPRM system was operated at elevated pressure, and had affected the removal efficiency of micro pollutant. The two parameters that most affected the performance of the membrane system were pH and operating pressure. In general, since the membrane system is considered as a low pressure system with high removal efficiency, it is paramount important to optimize the pH in the

treatment process. Results showed that high removal efficiency was achieved at elevated levels of pH (e.g. at pH 9). In addition, the design expert analysis for both DDT and glucose using RSM have shown an increase in flux when pressure was increased gradually in the LPRM system.

FINANCIAL DISCLOSURE

This research was funded by Universiti Teknologi Malaysia under the postgraduate research scheme.

CONFLICT OF INTERESTS

Authors declare no conflict of interests.

ACKNOWLEDGEMENT

The authors thank Faculty of Civil Engineering, Universiti Teknologi Malaysia and Ministry of Higher Education, Malaysia for their support during the project.

REFERENCES

- [1] Wen X, Ding H, Huang X, et al. [2004] Treatment of Hospital Wastewater using a Submerged Membrane Bioreactor. *Process Biochemistry* 39: 1427–1431.
- [2] Pauwels B, Fru Ngwa F, Deconinck S, et al. [2006] Effluent Quality of a Conventional Activated Sludge and a Membrane Bioreactor System Treating Hospital Wastewater. *Environmental Technology* 27: 395–402.
- [3] Filteau G, Moss P. [1997] Ultra-low pressure RO Membranes: An Analysis of Performance and Cost. *Desalination* 113: 147–152.
- [4] Malaeb L, Ayoub GM. [2010] Reverse osmosis technology for water treatment. State of the art review. *Desalination*. (Unpublished).
- [5] Ujang Z, Anderson GK. [2001] Effect of the Operating Parameters on the Separation of Metal Chelates using Low Pressure Reverse Osmosis Membrane (LPROM). *Water Science & Technology* 41: 135–142.
- [6] Hofman JA, Folmer MHEF, Kruithof JC. [1997] Removal of Pesticides and other Micropollutants with Cellulose-acetate, Polyimide and Ultra-low Pressure Reverse Osmosis Membranes. *Desalination* 113: 209–214.
- [7] Ozaki H, Sharma K, Saktaywin W. [2001] Performance of an Ultra Low Pressure Reverse Osmosis Membrane (ULPROM) for Separating Heavy Metals: Effects of Interference Parameters. *Desalination* 144: 287–294.
- [8] Minett S. [2003] Low Pressure, Reverse Osmosis Membrane for Drinking Water Supplies. *Membrane Technology* 73: 6.
- [9] Hamdzah M. [2007]. Low pressure reverse osmosis membrane for rejection of heavy metals. Masters Thesis. Universiti Teknologi Malaysia, Malaysia
- [10] Ujang Z, Anderson GK. [1998] Performance of Low Pressure Reverse Osmosis Membrane (LPROM) for Separating Mono- and Divalent Ions. *Water Science & Technology* 38: 521–528.
- [11] Ozaki H, Li H. [2002] Rejection of Organic Compounds by Ultra-low Pressure Reverse Osmosis Membrane. *Water Research* 36: 123–130.
- [12] Wu M, Sun DD, Tay JH. [2004] Effect of Operating Variables on Rejection of Indium using Nanofiltration Membranes. *Journal of Membrane Science* 240: 105–111.
- [13] Ku Y, Chen SW, Wang, WY. [2004] Effect of Solution Composition on the Removal of Cooper Ions by Nanofiltration. *Separation and Purification Technology* 43: 135–142.

MICRONUTRIENTS AND MARKERS OF OXIDATIVE STRESS IN SYMPTOMATIC HIV-POSITIVE/AIDS NIGERIANS: A CALL FOR ADJUVANT MICRONUTRIENT THERAPY

Moses Olayemi Akiibinu^{1*}, Adekunle Abiodun Adeshiyan², and Ayodele Olusegun Olalekan³

¹ Department of Chemistry and Biochemistry, Caleb University, Imota, Lagos state, NIGERIA

² Department of Biomedical Sciences, Ladoke Akintola University of Technology, Ogbomosh, Oyo State, NIGERIA

³ Department of Chemical Pathology, University College Hospital, Ibadan, NIGERIA

ABSTRACT

Background: The status of micronutrients and oxidative metabolites have not been fully explored in Nigerian symptomatic HIV-positive/AIDS patients, despite the existing evidences linking micronutrient deficiencies with immune dysfunctions. The present study assessed the plasma levels of selected micronutrients and markers of oxidative stress in symptomatic HIV-seropositive/AIDS patients. **Methods:** Seventy newly diagnosed HIV-positive patients (37 males and 33 females) volunteered to participate in this study. Sixty-five age matched HIV-seronegative, apparently healthy individuals (35 males and 30 females) served as controls. The plasma levels of cobalt (Co), copper (Cu), manganese (Mn), iron (Fe), zinc (Zn), selenium (Se), vitamin C, vitamin E, total antioxidant potential (TAP), total plasma peroxide (TPP), oxidative stress index (OSI) and malondialdehyde (MDA) were determined in them using atomic absorption spectrophotometer and spectrophotometric methods respectively. **Results:** The plasma levels of TAP, Cu, Zn, Fe, Co, Se, vitamin C and vitamin E were significantly lower ($p < 0.05$) in symptomatic HIV-positive/AIDS patients when compared with the controls. The mean values of MDA, TPP and OSI increased significantly ($p < 0.01$) in symptomatic HIV-positive/AIDS patients when compared with the controls. Interestingly, there was no significant change in the mean level of Mn ($p > 0.05$) when compared with the controls. In this study, symptomatic HIV-positive/AIDS patients demonstrated oxidative stress. **Conclusion:** Since most antioxidants regulating the oxidative stress are micronutrient dependent, this study strengthens the evidence and will convince the remnant skeptics that micronutrient supplementation is important in the management of AIDS.

Received on: 9th-Jan-2012

Revised on: 14th-Feb-2012

Accepted on: 21st-Feb-2012

Published on: 8th-Mar-2012

KEY WORDS

symptomatic HIV-infection;
Nigerians; micronutrients;
oxidative stress

*Corresponding author: Email: akiibinumoses@yahoo.com

[1] INTRODUCTION

Acquired immunodeficiency syndrome (AIDS) is the resultant effect of progressive loss of cellular immunity due to metabolic dysfunctions associated with human immunodeficiency virus (HIV) infection [1, 2]. Previous workers associated the progressive loss of cellular immunity in HIV-infection and AIDS with the defect in immunologic activities of monocytes, neutrophils, natural killer cells and significantly decreased level of circulating CD4 +T-cells [2]. Several lines of evidences show that certain micronutrients are important in man and animal due to their dual function for immune modulation and antioxidants or as ligands in the antioxidant enzymes [1, 2, 3]. Previous workers have reported the effects of deficiencies of selenium, zinc, iron and copper on the activities of neutrophils, monocytes, lymphocytes and macrophages [3]. The complex immune dysfunction in HIV-positive individuals predisposes them to both pathogenic and opportunistic infections [4-8]. In the reports of Kochanowski et al [9] and Sherman [10], iron deficiency was implicated as the cause of low cellular immune response and decreased secretion of interferon- γ , tumor necrotic factor- α and interleukin-2.

Arinola et al [11] also reported deficiencies in Cu, Mg, Fe, Se and Cr in HIV-positive patients and associated these with the complications of HIV-infection. Samba et al [1] reported significantly lower levels of Zn and Se in HIV-positive patients and associated the adverse clinical outcome during HIV infection with lower levels of vitamins and micro-mineral deficiencies. Se is a co-factor of several key enzymes, the plasma levels of which determine the activities of glutathione peroxidase, thioredoxin reductase and deiodinase (an enzyme involved in thyroid hormone activation) [12].

HIV is an intracellular pathogen that causes continuous cellular activation which results to free radical and cytokine generation [13, 14]. A number of cytokines up-regulate the HIV expression and cause anorexia in both acute and chronic HIV-infection [14]. The free radicals generation must be controlled at physiological level by the antioxidant system to avoid oxidative stress. Vitamins A, C and E are free radical scavengers while certain trace metals (Fe, Zn, Se, Cu, Mn) are essential in the activities of several antioxidant metalloproteins

that protect the cells against highly toxic reactive oxygen species [3]. Deficiency of selenium reported in HIV-infection has been linked with decrease of glutathione peroxidase activity and the susceptibility of tissues to injury by reactive oxygen species [16]. HIV-infection represents a serious risk factor for the development of metabolic and cellular immune disturbances. Most previous workers only determined the status of micronutrients in uncomplicated HIV-infection, it is therefore necessary to identify the effects of complicated HIV-infection/AIDS on the plasma levels of Cu, Mn, Fe, Co, Zn, Se, vitamin C, vitamin E, total antioxidant potential (TAP), total plasma peroxide (TPP), oxidative stress index (OSI) and malondialdehyde (MDA) in the present study.

[II] MATERIALS AND METHODS

Seventy newly diagnosed HIV-positive patients (37 males and 33 females) with clinical features of AIDS (i.e. chronic diarrhea, weight loss, skin rashes, and persistent fever) were recruited to participate in this study. Another sixty-five age matched HIV-seronegative, apparently healthy individuals (35 males and 30 females) served as controls. The participants (HIV-positive patients and controls) did not test positive to hepatitis B or C viruses and Mycobacterium tuberculosis infections at the time this study was conducted. Five milliliters of blood was withdrawn from each patient and control into a lithium heparin bottle. 0.5 mL of the plasma was immediately transferred into the bottle containing phosphoric acid for the estimation of ascorbic acid. The remaining plasma for the estimation of Cu, Mn, Fe, Co, Zn, Se, vitamin E, TAP, TPP was stored at -200C until analyzed. The experimental protocol was approved by the Research Ethical Committee of the Ministry of Health, Oyo state, Nigeria.

2.1. Determination of ascorbic acid (vitamin C)

Vitamin C concentration was determined by using the method of Briggs [17]. In brief, ascorbic acid in the plasma is oxidized by Cu (II) to form dehydroascorbic acid, which reacts with acidic 2, 4 – dinitrophenylhydrazine to form a reddish – hydrazone, which is measured at 520nm.

2.2. Determination of vitamin E

Vitamin E (α -tocopherol) was assayed by the method of Desai [18]. Briefly, vitamin E was extracted from plasma by addition of 1.6ml ethanol and 2.0ml petroleum ether to 5.0ml plasma and centrifuged. The supernatant was separated and evaporated. To the residue, 0.2ml of 2% α - α -dipyridyl, 0.2ml of 0.5% ferric chloride was added and kept in the dark for 5 min. An intense red coloured layer obtained on addition of 4 ml butanol was read at 520 nm.

2.3. Determination of MDA

Level of lipid peroxidation was determined by measuring the formation MDA using the method of Varshney and Kale [19]. The principle is based on the fact that malondialdehyde (MDA) produced from the peroxidation of membrane fatty acid reacts with the chromogenic reagent; 2-thiobarbituric acid (TBA) under acidic conditions to yield a

pink-coloured complex measured spectrophotometrically at 532nm. 1, 1, 3, 3-tetramethoxypropane was used as standard.

2.4. Determination of TAP

TAP was determined using the ferric reducing / antioxidant power (FRAP) assay [20, 21]. 1.5 ml of working pre-wormed (370C) FRAP reagent (300mM acetate buffer - pH 3.6, 10mM 2,4,6- tripyridyl-s-triazine in 40mM HCl and 20mM FeCl₃ at ratio 10:1:1) was vortex mixed with 50 μ l of test sample and standards. Absorbance was read at 593 nm against a reagent blank. The result was reported as μ mol Trolox equiv. / L.

2.5. Determination of total plasma peroxide (TPP)

Ferrous-butylated hydroxytoluene-xylene orange complex reacts with plasma hydrogen peroxide to form a colour complex measured spectrophotometrically at 560nm. H₂O₂ was used as standard. 1.8ml of reagent 6 (FOX2) was mixed with 200 μ l of plasma. This was incubated at room temperature for 30 minutes. 100 μ Mol H₂O₂ was used as standard. The mixture was centrifuged and the supernatant separated for reading at 560nm [21].

2.6. Determination of oxidative stress index (OSI)

OSI, an indicator of the degree of oxidative stress is the percent ratio of the TPP to the TAP [15].

2.7. Determination of Co, Cu, Mn, Fe, Zn, Se

Trace metals (Fe, Zn, Mn, Co, Cu and Se) were determined using atomic absorption spectrophotometer (AAS) as described by Kaneko et al [22]. The atomization of the element aspirated into the AAS results in the absorption of light of the same wavelength as that emitted by the element when in the excited state.

2.8. Statistical analysis

The statistical analysis of data generated in this study was carried out using SPSS version 10 and the values expressed as mean + 1 SD. Student (t) test was used for comparison. The changes were considered significant, when p-values were less than 0.05.

[III] RESULTS

The results obtained in this study show deregulated levels of certain trace metals in symptomatic HIV-positive patients. The levels of Co, Cu, Zn, Fe and Se [Table– 1] were significantly lower ($p < 0.05$) while no significant change was observed in the mean level of Mn ($p > 0.05$) in the symptomatic HIV-positive/AIDS patients, when compared with controls. Significantly ($p < 0.05$) lower levels of TAP, vitamin C and vitamin E; with significantly higher ($p < 0.05$) levels of TPP, MDA and OSI [Table–2] observed in symptomatic HIV-positive/AIDS patients when compared with the controls is an indication of oxidative stress in them.

Table: 1. levels (Mean + SD) of trace metals in symptomatic HIV-positive/AIDS patients and controls

	N	Co (µg/dL)	Fe (µg/dL)	Zn (µg/dL)	Mn (µg/dL)	Cu (µg/dL)	Se (µg/dL)
Controls	65	63.5+6.8	75.8+8.2	122.1+18.3	65.4+13.1	71.5+16.0	57.8+11.7
HIV-patients	70	38.0+6.5	67.0+11.6	97.4+22.0	62.8+9.5	59.4+12.5	42.3+8.2
p values		<0.01*	<0.05*	<0.05*	>0.05	<0.05*	<0.01*

* = significantly different from the controls. N = number of subjects used in the study

Table: 2. levels (Mean + SD) of antioxidant vitamins and markers of oxidative stress in symptomatic HIV-positive/AIDS patients and controls

	N	TAP (µMol Trolox equiv./ L)	TPP (µMol H ₂ O ₂ / L (%))	OSI (nM/ml)	MDA (mg/L)	Vitamin C (mg/L)	Vitamin E (mg/L)
Controls	65	1652+380	11.8+4.3	0.71+0.46	8.2+3.2	22.6+8.7	12.7+5.3
HIV-patients	70	930+370	33.9+12.0	3.70+1.50	17.5+5.8	12.5+4.1	8.3+4.0
p values		<0.01*	<0.01*	<0.01*	<0.01*	<0.01*	<0.05*

* = significantly different from the controls. N = number of subjects used in the study.

[IV] DISCUSSION

Corneal HIV-infection is capable of modulating the machineries of immune system and causing deranged metabolic activities of macro- and micronutrients molecules. Most of the intra- and extracellular metabolic processes require micronutrients for their optimal activities. The present study demonstrated significantly lower levels of plasma Fe, Co, Zn, Cu and Se in the symptomatic HIV-positive/AIDS patients, when compared with the controls. Meanwhile, there was no significant change in the plasma level of Mn in the symptomatic HIV-positive/AIDS patients, when compared with the controls. Fe, Zn, Se, Cu, Mn are essential in the activities of several antioxidant enzymes that protect the cells against highly toxic reactive oxygen species, and also enhance the immunologic activities of phagocytes and lymphocytes [3]. Since HIV requires large amount of selenium for its replication in the cells [23], the deficiencies of Se observed in these symptomatic HIV-positive/AIDS patients could be due to increased utilization by the HIV. The chronic gastroenteritis and mal-absorption [1] commonly encountered in HIV-positive patients may contribute to micronutrients metabolic disturbances observed in our HIV-positive/AIDS patients. This observation appears to corroborate the report of Bilbis et al [24] who reported lower levels of Fe, Cu and Zn in HIV-positive patients, and associated the levels with the severity of HIV-infection. A considerable number of previous investigators have reported significantly lower levels of certain micronutrients in HIV-positive patients [25, 26]. In a study conducted by Baum et al [25], a significantly lower level

of Zn was observed in HIV/hepatitis C virus co-infected patients when compared with non-infected controls. In another study conducted in Co te d 'Ivoire by Djinhi et al [26], a significantly lower level of Se was reported in HIV-infected patients. The profound decrease in the number and functions of circulating CD₄+T-cells reported by Ammann et al [2] and Groux et al [4] was associated with the consequences of trace metal deficiency in HIV-infected patients. The result of this study is also consistent with the report of Arinola et al [27] that Cu and Zn were significantly lower in HIV-positive patients.

To the knowledge of the authors, this study is the first to report cobalt deficiency in AIDS patients. The fact that cobalt is an essential trace metal linking the four pyrrol rings of cobalamin for effective synthesis of red blood cells [28] makes cobalt deficiency the novel of this study. The megaloblastic anaemia reported earlier by Koduri [29] which responded well to danazol therapy in a patient with AIDS could be ascribed to the cobalt deficiency observed in this study. Therefore, the deficiency of cobalt in our AIDS patients may contribute to anaemia commonly encountered in AIDS patients. Also, cobalt deficiency has been implicated in several neurological disorders such as myeloneuropathy [30], myelopathy [31], myeloneuroencephalopathy and myeloencephalopathy [32]. Neurological and behavioural disorders have been reported in advanced cases of AIDS. This study being the first to report cobalt deficiency in AIDS patients, may suggest that cobalt deficiency has a critical role to play in the development of neurological disorders in AIDS patients.

We observed significantly lower levels of vitamins C and E in our symptomatic HIV-positive /AIDS patients when compared with the controls. These are antioxidant vitamins that scavenge for free radicals in the system. Vitamin E is the cell membrane antioxidant protecting the cell membrane from free radical attack and cell lysis [3]. Depression of vitamins C and E in these patients may be due to increased demand in the detoxification / neutralization of free radicals. The lower levels of these antioxidant vitamins may also be due to mal-absorption and diarrhea that are common complications of AIDS, and secondary to gastro-enteritis and altered gut barrier function. This result agrees with previous workers who reported significantly lower levels of vitamins C and E in HIV-1 sero-positive patients [33]. In the study conducted by Mehta et al [34], significantly lower levels of lipid soluble vitamins were reported in HIV-positive patients. Bilbis et al [24] also reported lower levels of vitamins A, C and E in HIV-positive patients. Significantly lower levels of vitamins E have been reported earlier in asymptomatic HIV-positive/AIDS patients by Djinhi et al [26]. Also, significantly lower levels of vitamins A, C and E were reported in HIV-positive children by Srinivas et al [35]. The significantly lower levels of vitamins A, C and E in the HIV-positive children were associated with increased utilization of antioxidant micronutrients in the neutralization of free radicals in HIV-positive patients [35]. The combination of malnutrition, mal-absorption and exhaustion during detoxification of free radicals could account for the significantly lower levels of vitamins C and E in our symptomatic HIV-positive/AIDS patients.

The symptomatic HIV-positive/AIDS patients showed significantly higher plasma levels of markers of oxidative stress (TPP, OSI and MDA) when compared with the controls. These significantly higher levels of markers of oxidative stress could be due to high free radical load and insufficient antioxidant micronutrients in the HIV-positive patients. High free radical load may cause lipid peroxidation, fragmentation or aggregation of protein and deamination of guanine and adenine in DNA chain to cause gene mutation and cell membrane damage [36]. The data of the present study corroborates the reports of previous workers that markers of oxidative stress are higher in HIV- infected patients. Kameoka et al [37] reported that the reactive oxygen species stimulate oxygen responsive transcription factors that induce HIV replication in the infected T-lymphocyte. Baum et al [28] reported significantly higher level of oxidative stress in HIV-positive patients when compared with non-infected controls. This result also agrees with Suresh et al [33] which reported higher level of MDA in both symptomatic and asymptomatic HIV-1 infected patients in both conditions. Mandas et al [38] reported deranged level of oxidative stress in AIDS patients on anti-retroviral therapy and associated the higher level of oxidative stress to the pro-oxidant effect of the anti-retroviral drugs.

A significantly lower level of TAP was observed in the symptomatic HIV-positive/AIDS patients recruited for this study, when compared with the controls. This study agrees with Suresh et al [33] who reported significantly lower level of total antioxidant capacity in both symptomatic and asymptomatic HIV infections. Stromajar-Racz et al [39] also reported significantly lower level of antioxidant enzymes in HIV-1 infected patients. The lower level of TAP in the present study could be due to excessive free radical generation, mal-absorption due gastro-enteritis, diarrhea and nutritional antioxidant deficiency commonly encountered in HIV-positive patients. Since TAP is an index of all classes of antioxidants, the significantly lower level of TAP observed in this study could be due to significantly lower levels of vitamin C, vitamin E, Cu, Zn, Se and Fe.

In conclusion, micronutrient deficiency possibly contributing disproportionately to the oxidative stress is a feature of AIDS. Therefore, adjuvant micronutrients therapy should be seriously considered in the management of AIDS patients to avert or ameliorate the complications of AIDS and slow the progression of the disease.

FINANCIAL DISCLOSURE

No financial assistance was received for this work.

CONFLICT OF INTERESTS

Authors declare no conflict of interests.

REFERENCES

- [1] Samba RD, Tany AM. [1999] Micronutrients and the pathogenesis of human immunodeficiency virus infection. *British Journal of Nutrition* 81 (3): 181–189.
- [2] Ammann AJ, Abrahams D, Conant M, Chullildwin D, Cowan M, et al. [1983] acquired immune dysfunction in homosexual men: Immunologic profiles. *Clin. Immunol. Immunopathol* 27: 315–325.
- [3] Prasad AS. [1998] *J Trace Elem. Exp. Med* 11:63–87.
- [4] Groux H, Torpier G, Monte D, Mouton Y, Capron A, Amcisen JC [1992]. Activation – induced death by apoptosis in CD4 T-cell from HIV – infected asymptomatic individuals. *J Exp Med* 175: 331– 340.
- [5] Milla A. B, Miller F, Foley NM, Meager A, Semple SJ, Rook GA. [1991] Production of tumour necrosis factor alpha by blood and lung mononuclear phagocytes from patients with HIV – related lung disease. *Amer J. Resp. cell Mol Biol* 5: 144–148.
- [6] Lathey JL, Aagosti JM, Nelson JA, Carroy L, Gnegory A, et al. [1990] A selective defect in tissue factor mRNA expression in monocytes from AIDS patients. *Clin. Immunol. Immunopathol* 54: 1–13.
- [7] Cai Q, Huang X.L, Rappocciolo G. Rina Ido R [1990]. Jn. Natural Killer cell responses in homosexual men with early HIV. *J. AIDS.* 3: 669 – 676.

- [8] Peters AM, Jagger FS, Warneke A, Muller K, Brunkhorst U, et al. [1991] Cytokine Secretion by peripheral blood monocytes from HIV – infected patient. *Clin Immunol. Immunopathol* 61: 343–352.
- [9] Kochanowski BA and Sherman AR [1985] Cellular growth in Fe-deficient rats: effects of pre- and post-weaning Fe repletion. *J Clin. Nutr* 115: 279–287.
- [10] Sherman RA. [1990] Influence of iron on immunity and disease resistance. *Ann. New York Acad. Sci* 587: 123–139.
- [11] Arinola OG, Adedapo KS, Kehinde AO, Olaniyi JA, Akiibinu MO [2004]. Acute phase proteins, trace elements in asymptomatic human immunodeficiency virus infection in Nigerians. *Afr. J Med Sci* 33, 317– 322.
- [12] Kohrle J, Jacob F, Contempre B, Dumont JE. [2005] Selenium, the thyroid and the endocrine system. *Endocrine Review* 26 (7):944–984.
- [13] Poli G, Bressler P, Kinter A, Timmer WC, Rabson A, et al. [1990] Interleukin – 6 induces HIV expression in monocytic cells alone and in synergy with tumour necrosis factor alpha by transcriptional and post transcription Mechanism. *J Exp. Med* 172; 151–158
- [14] Biswas P, Poli G. Kintie A.L, Justement JS, Stanley SK, et al. [1992] Interference – gamma induces the expression of HIV in persistently infected pro-monocytic cell redirects the production of various to intracytoplasmic vacuoles in PMA – differentiated U.I cells. *J Exp. Med.* 176; 739– 750.
- [15] King JC, Keen CL. Zinc. In: Shils M, Olson JA, et al. [1999] Modern Nutrition in Health and Disease. 9th ed. Baltimore: *Williams & Wilkins*: 223–239.
- [16] Roughead ZK, Johnson LK, Hunt JR [1999] Dietary copper primarily affects antioxidant capacity and dietary iron mainly affects iron status in a surface response study of female rats fed varying concentrations of iron, zinc and copper. *J Nutr*, 129:1368–1376.
- [17] Briggs ME. [1981] Vitamin in human biology and medicine. *Boca Raton Fla.* CRC Press inc.
- [18] Desai ID. [1984] Vitamin E methods for animal tissues. *Methods Enzymol* 105: 138–143.
- [19] Varshney R and Kale RK [1990] Effect of calmodulin antagonist on radiation-induced lipid peroxidation in microsomes. *Int. J. Rad. Biol* 58: 733–743.
- [20] Benzie IE, Strain JJ. [1996] The ferric reducing ability of plasma (FRAP) as a measure of antioxidant power (the FRAP assay). *Annals of Biochem.* 239: 70–76.
- [21] Harma M. Harma M. Enel O. [2003] Increased oxidative stress in patients with hydatidiform mole. *Swiss Med. Wkly.* 133:563–566.
- [22] Kaneko J J [1999]. Clinical biochemistry of animals. 4th Edition (ed. J. J. Kaneko), Academic press. Inc New York, 932 pp.
- [23] Arinola OG, Akiibinu MO. [2005] Effect of HIV, urinary schistosomiasis or malaria on the levels of nutritionally essential trace elements in Nigerians. *European Journal of Scientific Research.* 6 (1) 65–73
- [24] Bilbis LS, Idowu DB, Saidu Y, Lawal M, Njoku CH [2010]. Serum Levels of Antioxidant vitamins and mineral elements of human immunodeficiency virus positive subjects in Sokoto Nigeria. *Ann. Afr. Med.* 9 (4); 235–239.
- [25] Baum M, Sales S, Jayaweera D, Lais, Bradwin G, Rafie C, Page J, Campa A [20 11]. Co-infection with hepatitis C virus, oxidative stress and antioxidant status in HIV – positive drug users in Miami. *HIV & Med.* 12 (2) 78–86
- [26] Djinhi J, Tiaheu G, Zirihi G, Lohoues E, Monde A, et al. [2009] Selenium deficiency and oxidative stress in asymptomatic HIV – 1 infected patients in Cote d’ Ivoire. *Bull soc Pathol Exot* 102 (1): 11-3.
- [27] Lyn Patrick ND. [1999] Nutrition and HIV: part one-beta carotene and selenium. *Alternative Medicine Review* 4 (6): 403
- [28] Hall R, Malia RG. [1984] In Textbook of Medical Laboratory Haematology 1st Ed. Butterworths, London. p.32.
- [29] KODURI PR [2005] Refractory megaloblastic anemia in a patient With AIDS: Response to Danazol. *American Journal of Hematology* 80:87–93.
- [30] Adachi H, Hirai Y, Fujiura Y. [2002] Plasma homocysteine levels and atherosclerosis in Japan: epidemiological study by use of carotid ultrasonography. *Stroke* 33(9):2177–2181.
- [31] Kinsella LJ, Green R. 'Anesthesia paresthetica': nitrous oxide-induced cobalamin deficiency. *Neurology.* Aug 1995; 45(8):1608-10.
- [32] Schilling RF. Is nitrous oxide a dangerous anesthetic for vitamin B12-deficient subjects?. *JAMA.* Mar 28 1986; 255(12):1605-6.
- [33] Suresh DR, Annam V, Pratibha K, Prasad BV [2009] Total antioxidant capacity: A novel early bio – chemical marker of oxidative stress in HIV infected individuals. *J Biomed Sci* 16:61
- [34] Mehta S, Epiegelman D, Aboud S, Giovannucci EL, Ms amanga G1, Hertzmark E, Mugusi FM, Hunter DI, Fawzi WW [2010]. Lipid Soluble Vitamins A, D and E in HIV – infected pregnant women in Tanzania. *Eur J Clin. Nutr* 64 (8): 808 – 817
- [35] Srivivas A, Dias BF [2008]. Antioxidants in HIV positive children. *Indian J Pediatr* 75 (4): 347 – 350.
- [36] Farber J.L. (1982). Biology of disease. Membrane injury and calcium homeostasis in the pathogenesis of coagulative necrosis. *Lab. Invest.* 47:114–123.
- [37] Kameoka M, Kimura T, Ikuta K [1993]. Superoxide enhances the spread of HIV-1 infection by cell to cell transmission. *FES Lett.* 331: 182–186.
- [38] Stromajer - Racz T, Gazdag Z, Belagy, J. Vagvolgyi C, Zhao RY, Pesti M [2009]. Oxidative Stress induced by HIV - 1 F341VPr in *Schizosaccharomyces pombe* is one of its multiple functions. *Exp. Mol. Pathol.* (Epub ahead of print)
- [39] Mandas A, Lorio EL, Congiu MG, Balestrieri C, Mereu A, Cau D, Dessi S, Curreli N [2009]. Oxidative Imbalance in HIV-1 Infected patients treated with antiretroviral therapy. *J Biomed Biotechnol:* 749575.

HEAVY METAL DISTRIBUTION IN THE COASTAL SEDIMENT OF CHENNAI COAST

Ramanibai Ravichandran and Shanthi Manickam*

Aquatic Biodiversity Unit, Department of Zoology, University of Madras, Guindy Campus, Chennai 600 025, INDIA

ABSTRACT

Chennai coast is located on the eastern end of east coast of India known as second largest beach of the world. It receives quite good number of inlets, exhibit unique water quality features especially in the near shore coastal areas are of ecologically important. Metals like Pb, Cd, Zn, Ni, Co and Cu were analyzed in sediment collected during pre monsoon season. Present study showed that the heavy metal concentrations were recorded high at near shore station of Ennore during pre monsoon season. This might be due to discharged of industrial effluents, land-based anthropogenic inputs and municipal sewage through the Ennore estuary. The results of the present study suggested the need for a regular monitoring program of the Chennai coast which will help to improve the quality of near shore coastal environment.

Received on: 5th-May-2011

Revised on: 9th-Dec-2011

Accepted on: 13th-Dec-2011

Published on: 15th-Mar - 2012

KEY WORDS

Heavy metals distribution; Chennai coast; Bay of Bengal.

*Corresponding author: Email: jmshanthi@gmail.com; Tel: +91-9444743885

[1] INTRODUCTION

Industrial activities, economic development and urbanization in metropolitan cities all over the world have grown very rapidly in recent years and significant amount of contaminants are introduced in rivers, estuarine and coastal regions. Among the various contaminants heavy metals are serious pollutants of aquatic ecosystems, because of their environmental persistence, toxicity and ability to be incorporated into food chains [1, 2].

Numerous studies have demonstrated from marine sediment are highly polluted by heavy metals; therefore the evaluation of metal distribution in surface sediment is useful to assess pollution in the marine environment [3, 4]. Elevated metals concentrations (e.g. Hg, Cd, Pb, Cu, Ni and Zn) in marine environment are often considered indicators of anthropogenic influence and are themselves of potential risk to the natural environment. Therefore, it is important to assess and track the abundance of these heavy metals in coastal ecosystem [5].

Understanding transfer and distribution of toxic metals between the sediment and water columns is of great importance. Once heavy metals introduced into the aquatic environment, it redistributed throughout the water column, deposited or accumulated in sediments [6]. Heavy metal concentrations profiles in sediments used to identify the history and sources of pollution. The sources of major and minor elements in aquatic sediments area combination of natural weathering, run-off and

riverine and atmospheric input, affected by anthropogenic impact [7, 8].

The Bay of Bengal (BOB) is a semi-enclosed tropical basin in the northern Indian Ocean. It is bounded by the Indian Peninsula and Sri Lanka on the west and by the Andaman-Nicobar Islands and Burma on the east [9]. Chennai (N 13° 15' latitude and E 80° 17' longitude) is a beautiful metropolitan city with high density population of above five millions, and also a major industrial hub in south India. The coastal city where the pollution problem is acute, particularly in the north and central part of the city due to the stress caused by domestic and industrial effluents. Point sources of pollution are mainly from North Chennai Thermal Power Plant, Ennore Port activities, other nearby industries and untreated urban wastes from Chennai Metropolitan [10].

The ever expanding city of Chennai offloads a million liters of sewage, which carried a wide variety of pollutants everyday into the adjoining sea. The information on the coastal hydrograph of Chennai coast is essential in the context of coastal pollution and consequent productivity of the Bay. The present study was therefore undertaken with a view to provide much needed information on the heavy metal distribution in the coastal ecosystem of Chennai and its relation to the prevailing environmental conditions..

[II] MATERIALS AND METHODS

2.1. Study area and sampling stations

The study area covers a part of Chennai coast starting from Ennore (80° 25' E; 13° 14' N) to Kovalam (80° 16' E; 12° 49' N) covering approximately 25km stretch. Fifteen sampling stations were fixed along the Chennai

Coast [Table-1]. Stations 1, 4, 7, 10 and 13 representing near shore stations and its distance covered from 3km from the shore. Stations 2, 5, 8, 11 and 14 represent middle stations where distance covered was 5 km away from the near shore stations. Similarly stations 3, 6, 9, 12 and 15 represent off shore stations with a distance covered 5 km away from middle shore stations [Figure-1].

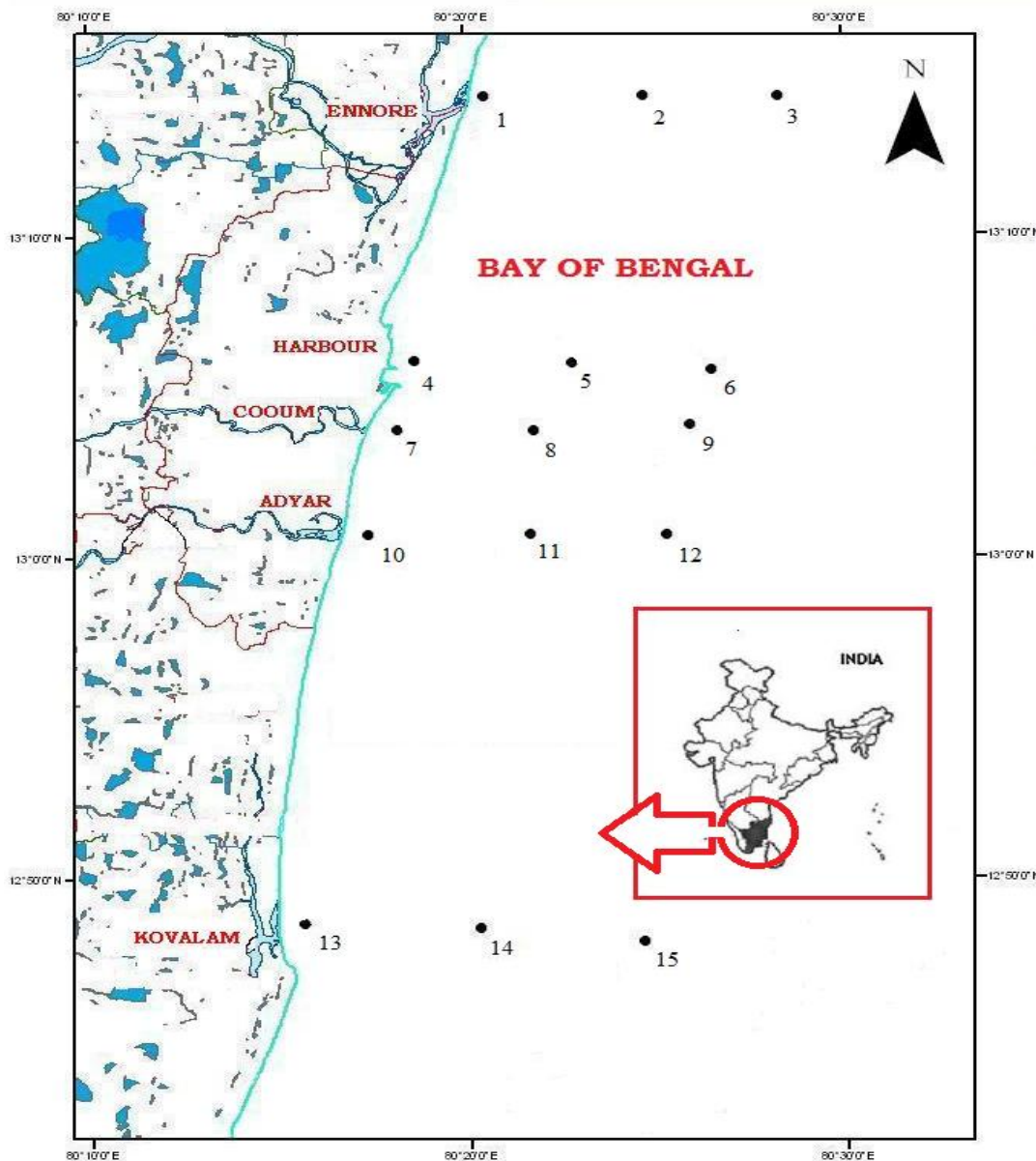


Fig: 1. Location of sampling sites in the study area

- | | | |
|---------------------|---|--------------------|
| Near shore stations | - | 1, 4, 7, 10 and 13 |
| Middle stations | - | 2, 5, 8, 11 and 14 |
| Offshore stations | - | 3, 6, 9, 12 and 15 |

Station 1 located at Ennore receives industrial effluents and station 4 located at harbour receives cargo waste and oil pollution from this region. Station 7 located near the Cooum river mouth and receives large quantities of domestic sewage and industrial effluents through the river Cooum. Station 10 located near the Adyar river mouth and receives domestic and sewage wastes from the river Adyar. Station 13 located at Kovalam, fishing and salt pans are the unique activities carry over here. Station 13 is less polluted when compared with other stations.

Table: 1. Sampling points

Station	Longitude	Latitude
1	80° 20' 25" E	13° 14' 09" N
2	80° 24' 00" E	13° 14' 11" N
3	80° 28' 06" E	13° 14' 10" N
4	80° 19' 95" E	13° 08' 15" N
5	80° 23' 95" E	13° 08' 06" N
6	80° 27' 91" E	13° 08' 22" N
7	80° 20' 06" E	13° 04' 01" N
8	80° 24' 09" E	13° 24' 09" N
9	80° 28' 00" E	13° 04' 00" N
10	80° 18' 14" E	13° 00' 97" N
11	80° 24' 09" E	13° 00' 99" N
12	80° 27' 00" E	13° 01' 00" N
13	80° 16' 98" E	12° 48' 93" N
14	80° 20' 98" E	12° 49' 04" N
15	80° 24' 88" E	12° 49' 00" N

2.2. Sampling and storage

Fifteen sediment samples were collected from Chennai coast, Bay of Bengal. The sampling cruise was conducted pre monsoon (March) 2006 by using the National Institute of Ocean Technology (NIOT) research vessel Sager Pachmi. The sampling locations included areas with different environmental backgrounds for example industrial areas, port, fishing, urban and agriculture areas. The samples from each station were collected using grab. Samples were taken from the central part of the grab sampler to avoid any metallic contamination from the metallic sampler and it was frozen at -4°C immediately onboard until further analysis.

2.3. Sample digestion and Instrumentation

Sediment samples were dried at 105°C for at least 16h until a constant dry weight. Afterwards the dried samples were homogenized with a pestle and mortar in order to normalize for various in grain size. The homogenized samples were sieved through a 250 mm screen and kept in clean plastic container for further analysis. For each sample a known quantity (1 g) of sediment was digested with a solution of concentrated HClO₄ (2 ml) and HF (10 ml) to near dryness. Subsequently, a second addition of HClO₄ (1 ml) and HF (10 ml) was made and the mixture was evaporated to near dryness. Finally, HClO₄ alone was added and the sample was evaporated until white fumes appeared. The residue was dissolved in concentrated HCl and diluted to 25 ml [11].

Heavy metal concentrations Pb, Zn, Co, Ni, Cr and Cu were measured using a flame atomic absorption spectrophotometer (Perkin-Elmer AA700) equipped with a deuterium background corrector. Suitable internal chemical standards (Merck Chemicals, Germany) were used to calibrate the instrument. All the reagents used were analytical grade of high purity. The results of the heavy metal concentrations were determined on a dry weight basis µg g⁻¹.

[III] RESULTS AND DISCUSSION

The accumulation of heavy metals Pb, Zn, Co, Ni, Cr and Cu were presented in Figure 2a-2c and Table-2. The metal concentration in the near shore stations (1 – 13), heavy metals Pb varied from 22.5 to 19.1 µg g⁻¹; Zn 109.02 to 86.3 µg g⁻¹; Co 7.3 to 1.7 µg g⁻¹; Ni 71.1 to 36.6 µg g⁻¹; Cr 88 to 43.7 µg g⁻¹; Cu 92.3 to 40.1 µg g⁻¹ respectively [Figure-2a]. The metals accumulation was recorded high at station 1 and 4. The near shore station (1 and 4) received large quantity of untreated effluents from the industrialized regions. Similarly the metal concentrations were registered low at station 10 and 13.

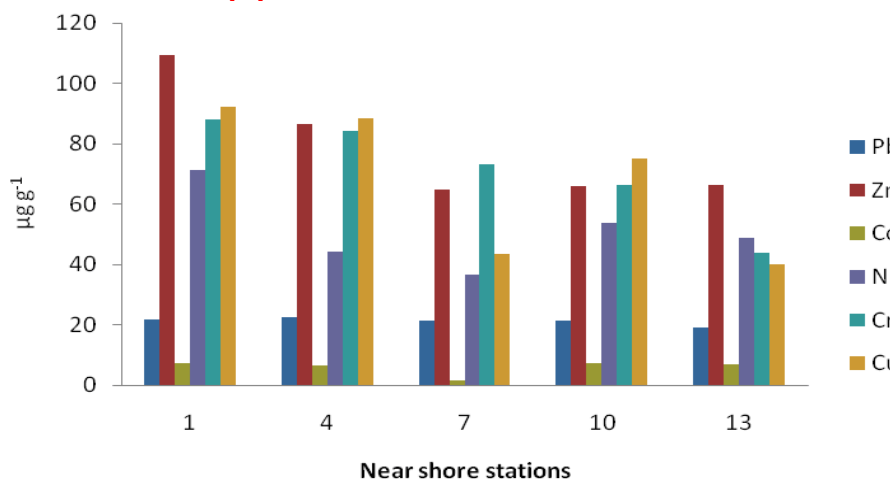


Fig: 2a. Heavy metal concentrations in the near shore sediment samples of Chennai coast

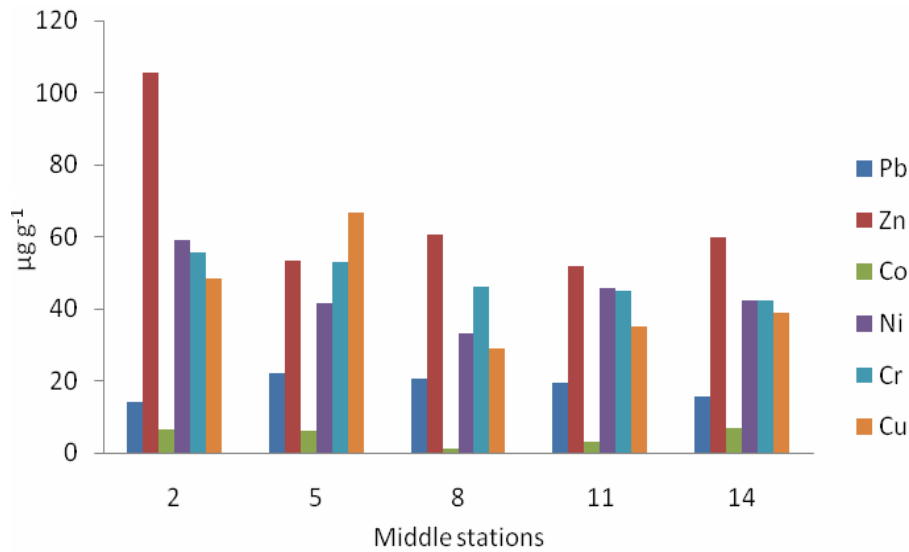


Fig: 2b. Heavy metal concentrations in the middle stations sediment samples of Chennai coast

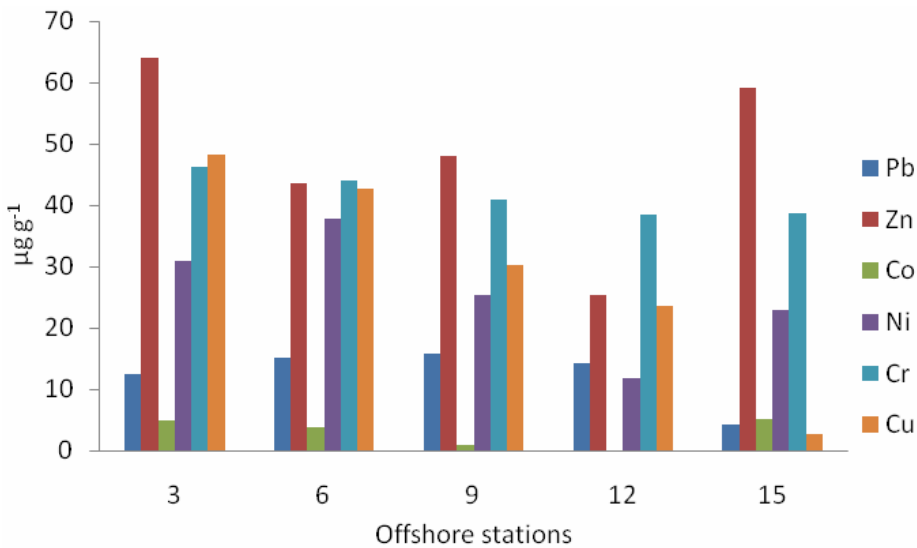


Fig: 2c. Heavy metal concentrations in the offshore sediment samples of Chennai coast

Sediment concentrations in the middle station (2-14), the concentration of metal Pb ranged between 22.1 – 14 µg g⁻¹ ; Zn 105.4 – 53.4 µg g⁻¹; Co 6.8 – 1.3 µg g⁻¹ ; Ni 59.2 – 33.2 µg g⁻¹ 55.6 - 44.9 µg g⁻¹ Cr; Cu 66.8 – 28.8 µg g⁻¹ [Figure-2b]. The metals concentrations were moderately high at all the middle station mainly due to the circulation point from the upstream direction South of Buckingham canal was transporting the organic rich sediment to the middle station. The metal concentrations were recorded low at station 2, 5 and 14 during the study period.

The offshore Stations (3-15), the metal concentrations were comparatively lower than the near and middle stations. The

metal concentration varied from Pb 15.7 to 4.3 µg g⁻¹ ; Zn 64.1 to 25.4 µg g⁻¹; Co 5.2 to 0.12 µg g⁻¹; Ni 37.8 to 11.8 µg g⁻¹; Cr 46.3 to 38.35 µg g⁻¹ and Cu 48.2 to 2.7 µg g⁻¹ [Figure-2c]. Among all the sampling stations, offshore station 12 and 15 showed low accumulation of heavy metals in the sediment samples. Overall the highest metal concentration Zn 109.02 µg g⁻¹; Cu 92.3 µg g⁻¹; Cr 88.0 µg g⁻¹; Ni 71.1 µg g⁻¹; Pb 21.6 µg g⁻¹ and Co 7.3 µg g⁻¹ were recorded high in the sediment samples collected from the near shore stations than the middle and offshore stations.

The high concentration of Pb at near shore station sediments of Ennore are directly related to heavy input of industrial effluents

from the industrial regions of Ennore, north part of the city which are dominated by petrochemical, painting, thermal plant and other chemical industries which also exposed to wave and storm activities [12,13]. Maximum concentration of Zn 109.02 $\mu\text{g g}^{-1}$ in sediment probably due to the discharges of effluents from the petrochemical, painting industries [14] in the Ennore region.

The high concentration of Ni 71.1 $\mu\text{g g}^{-1}$ recorded at the near shore station of Ennore might be due to the petroleum-related activities [15]. Co showed the similar distribution pattern and high concentration in the near shore station of Ennore. This may be due to the discharge of markers of paint industries [12] many are presented in the Ennore region.

The elevated concentration of Cr 88.0 $\mu\text{g g}^{-1}$ recorded in the near shore station 1, mainly from the industrial effluents and it is also associated with the organic particles [16]. Cu and Cr concentrations were elevated at all the near shore stations

indicated that the Cu and Cr mainly discharge of the industry and domestic waste and also iron and steel industries and sewage contribute equally to the contamination in the near shore stations of the study area [17].

The enrichment of heavy metals Zn, Cr, Cu, Ni and Pb in the sediment samples are mainly due to the coal powered thermal power plant, atmospheric deposition of fly ash and anthropogenic sources in the Ennore region of Chennai city, southeast coast of India [18]. Various studies [Table-3] showed the anthropogenic sources of the heavy metal in the Bay of Bengal.

In present study the heavy metals Pb, Cd, Zn, Cu, Co, Ni, and Cr concentrations were recorded high at Ennore and Harbour stations. The high concentrations of the metals during pre monsoon season mainly due to the heavy input of untreated industrial effluents from Ennore area through Pulicat channel and Buckingham canal entry points into the coast.

Table: 2. Concentrations of heavy metals in the sediment samples of Chennai Coast during pre monsoon season 2006.

	Pb ($\mu\text{g g}^{-1}$)	Zn ($\mu\text{g g}^{-1}$)	Co ($\mu\text{g g}^{-1}$)	Ni ($\mu\text{g g}^{-1}$)	Cr ($\mu\text{g g}^{-1}$)	Cu ($\mu\text{g g}^{-1}$)
Near shore stations						
1	21.6	109.2	7.3	71.1	88	92.3
4	22.5	86.3	6.5	44	84.2	88.5
7	21.3	64.6	1.7	36.6	73.1	43.3
10	21.5	66	7.2	53.7	66.4	75.2
13	19.1	66.4	7	48.9	43.7	40.1
Mean	21.2	78.5	5.94	50.86	71.08	67.88
Middle Stations						
2	14	105.4	6.3	59.2	55.6	48.3
5	22.1	53.4	6.1	41.4	52.9	66.8
8	20.4	60.6	1.3	33.2	46.17	28.8
11	19.4	51.8	3.1	45.8	44.9	35
14	15.7	59.7	6.8	42.4	42.4	38.9
Mean	18.32	66.18	4.72	44.4	48.394	43.56
Off shore stations						
3	12.5	64.1	5.1	31	46.3	48.2
6	15.2	43.6	3.8	37.8	43.9	42.7
9	15.7	48	1.1	25.3	40.8	30.3
12	14.3	25.4	0.12	11.8	38.55	23.5
15	4.3	59.1	5.2	23	38.57	2.7
Mean	12.4	48.04	3.064	25.78	41.624	29.48

[IV] CONCLUSION

The accumulation of heavy metals found to be high in the near shore sediment mainly due to the land based activities in

general. The Chennai coastal region should be given great attention to control the anthropogenic input into the coastal environment. Continuous monitoring of the near shore coastal

area of Chennai coast in particularly recommended for future studies.

Table: 3. Comparison of heavy metal concentrations ($\mu\text{g g}^{-1}$) estimated from sediment samples along the Bay of Bengal.

S.No	Sediment type	Place	Pb	Zn	Ni	Cu	Co	Cr	References
1	Shallow sediment	Madras coast	-	-	64	26	-	84	[19]
2	Intertidal sediment	SE Coast	5 - 130	13 -144	-	0 - 105	-	11-394	[20]
3	Near shore sediment	Madras coast	31.7	6.3	-	0.8	-	-	[21]
4	Shore sediment	Coromandel Coast							[22]
5	Core sediment	Madras coast							
6	1.0-5 interval, Muttukadu	East coast	1	68	49	-	8	48	[23]
7	2.0-1 cm interval, Mamallapuram	"	13	106	53	-	9	87	
8	3.0-1 cm interval, Marakkanam	"	11	87	12	-	7	58	
9	Surface sediment	Gulf of Mannar	16	73	24	-	7	167	[15]
10	Shelf sediment	Gulf of Mannar	16	73	24	57	15	177	[24]
11	Innershelf sediment	Madras coast	16	71	30	20	9	57	[13]
12	sediments-Before tsunami	Poompuhar(SE coast)	N.D	5.9	N.D	31.4	N.D	-	[25]
13	Sediment	Ennore, Chennai Coast	24.9-40	71.3-201	19.8-53.4	385-657	-	148.6-243.2	[10]

CONFLICT OF INTERESTS

Authors declare no conflict of interests.

FINANCIAL DISCLOSURE

M.S (author) thank to the University of Madras for the research fellowship under the UGC- JRF Research fellowship in Science for Meritorious programme for the financial support.

ACKNOWLEDGMENT

We thankful to National Institute of Ocean Technology (NIOT) – Chennai, permit to use the vessel (CRV Sager Purvi) for sample collections.

REFERENCES

- [1] Santos IR, Silva-Filho EV, Schaefer CE, Albuquerque-Filho MR, Campos LS. [2005] Heavy metal contamination in coastal sediments and soil near the Brazilian Antarctic Station, King George Island. *Marine Pollution Bulletin* 50:185–194.
- [2] Anna Nikulina, Wolf-Christian Dullo [2009]. Eutrophication and heavy metal pollution in the Flensburg Fjord: A reassessment after 30 years. *Marine Pollution Bulletin* 58: 905–915.
- [3] Cuculic V, Cukrov N, Kwokal Z, Mlakar. [2009] Natural and anthropogenic sources of Hg, Cd, Pb, Cu and Zn in seawater and sediment of Mljet park, Croatia. *Estuarine, Coastal and Shelf Science* 81(3): 311–320.
- [4] Abubakar, MI. [2008] Combining multivariate analysis and geochemical approaches for assessing heavy metal level in sediment from Sudanese harbour along the Red Sea coast. *Microchem. Journal* 90(2):159–163.
- [5] Vlado Cuculic, Neven Cukrov, Zeljko Kwokal, Marina Mlakar [2009]. Natural and anthropogenic sources of Hg, Cd, Pb, Cu and Zn in seawater and sediment of Mljet National Park, Croatia. *Estuarine, Coastal and Shelf Science* 81:311–320.
- [6] Christophoridis C, Dedepeididis D, Fytianos K. [2009] Occurrence and distributed of selected heavy metals in the surface sediments of Thermaikos Gulf, N.Greece. Assessment using pollution indicators. *J. Hazardous Mat* 168: 1082-1091.
- [7] Zhang W feng H, Chang J, Qu J, Xie H, Yu L. [2009] Heavy metal concentration in surface sediments of Yangtze river intertidal zone: An assessment from different indexes. *Environ. Pollut* 157: 1533–1543.
- [8] Yalcin MG, Narin I, Soylak M. [2008] Multivariate analysis of heavy metal contents of sediments from Gumusler creek, Nigde, Turkey. *Environ. Geol.* 54(9): 1155–1163.
- [9] Fernandes LD, Souza F, Matondkar SGP, Bhosle NB. [2006] Amino sugars in suspended particulate matter from the Bay of Bengal during the summer monsoon of 2001. *J Earth Syst Sci* 115(3):363–370.
- [10] Muthuraj S, Jayaprakash M. [2008] Distribution and enrichment of trace metals in marine sediments of Bay of Bengal, off Ennore, south-east coast of India. *Environ Geol* 56:207–217.

- [11] Tessier A, Campbell PGC, Bisson M. [1979] Sequential extraction procedure for the speciation of particulate trace metals. *Anal Chem* 51:844–851.
- [12] Jayaprakash M, Srinivasalu S, Jonathan, MP, Ram Mohan V. [2005] A baseline study of physico-chemical parameters and trace metals in waters of Ennore Creek, Chennai, India. *Marine Pollution Bulletin* 50: 583–608.
- [13] Selvaraj K, Ram-Mohan V, Srinivasalu S, Jonathan, MP, Siddhartha R. [2003] Distribution of non-detrital trace metals in sediment cores from Ennore creek, southeast coast of India. *Journal of Geological Society of India* 62: 191–04.
- [14] Lin YP, Teng TP, Chang TK. [2002] Multivariate analysis of soil heavy metal pollution and land use pattern in Changhua County in Taiwan. *Landsc Urban Plan* 62:19–35.
- [15] Jonathan MP, Ram-Mohan V. [2003] Heavy metals in sediments of the inner shelf off the Gulf of Mannar, southeast coast of India. *Marine Pollution Bulletin* 46: 258–68.
- [16] Forstner U, Wittmann GTW. [1981] Metal pollution in the aquatic environment. Springer, Berlin, 476p
- [17] El Nemr A, Khaled, El Sikaily, A. [2006] Distribution and statistical analysis of leachable and total heavy metals in the sediments of the Suez Gulf. *Environ Monit Assess* 118(1–3):89–112.
- [18] Jayaprakash M, Jonathan MP, Srinivasalu S, Muthuraj S, Ram-Mohan V, Rajeshwara-Rao N [2008] Acid-leachable trace metals in sediments from an industrialized region (Ennore Creek) of Chennai city, SE coast of India: an approach towards regular monitoring. *Estuarine, Coastal and Shelf Science* 76: 692–703.
- [19] Sarin MM, Borole DV, Krishnaswami S. [1979] Geochemistry and geochronology of sediments from the Bay of Bengal and the equatorial Indian Ocean. *Proceedings of the Indian Academy of Science* 8:131-154.
- [20] Subramanian V, Mohanachandran G. [1990] Heavy metals distribution and enrichment in the sediments of southern east coast of India. *Marine Pollution Bulletin* 21: 324-330.
- [21] Sivasamy SN. [1990] Plankton in relation to coastal pollution at Ennore Madras coast. *Indian Journal of Marine Science* 19:115-119.
- [22] Govindasamy C, Azariah J. [1999] Seasonal variation of heavy metals in coastal waters of the Coromandel coast, Bay of Bengal, India. *Indian Journal of Marine Science* 28: 249–56.
- [23] Hema Achyuthan, Richardmohan D, Srinivasalu S, Selvaraj K. [2002] Trace metals in the sediment cores of estuary and tidal zones from northern part of south east coast of India. *Indian Journal of Marine Science* 31: 141–49.
- [24] Jonathan MP, Ram-Mohan V, Srinivasalu S. [2004] Geochemical variations of major and trace elements in recent sediments, off the Gulf of Mannar, southeast coast of India, *Environ. Geol* 45: 466–480
- [25] Prasath PM, Khan TH. [2008] Impact of tsunami on the heavy metal accumulation in water, Sediments and Fish at Poompuhar Coast, Southeast coast of India. *E-Journal of Chem* 5 (1): 16–22.

A ROLE OF GENES IN CRANIOFACIAL GROWTH

Rahul Raman Doshi and Amol Somaji Patil*

Department of Orthodontics and Dentofacial Orthopedics, Bharati Vidyapeeth University, Dental College and Hospital, Pune, Maharashtra, INDIA

ABSTRACT

With the advent in the field of craniofacial biology and with the discovery of the homeobox genes, many research and investigations have shown detailed genetic control for the patterning of the craniofacial region. The Hox gene subfamily important in respect to craniofacial development are – Msx, Dlx, Otx, Gsc, Barx, Prx, and Lim. Msx-1 and Msx-2 are expressed in the brachial arches especially in the region of epithelial mesenchymal organogenesis including the developing teeth and are detected in the development and formation of skull and meninges, the digital aspects of the facial primordia, the associated sense organs and the teeth. Both the Msx-1 and Msx-2 are expressed in the sutural mesenchyme and duramater and Msx-1 is expressed in the bud stage as well as in the morphogenetic cap stage during the tooth development. Dlx-1 and Dlx-2 are expressed in dental mesenchyme, epithelium of the maxillary and mandibular arch mesenchyme. Dlx-5/6 are responsible for cartilage giving rise to the cranial floor (basioccipital, basisphenoid, and sphenoid) and frontonasal prominence. In vertebrates, Goosecoid (Gsc) is expressed transiently at the rostral end of the developing brain and then re-appears in many sites, including the mesenchyme of the branchial arches, nasal capsules and mandible. Barx expression is localized exclusively to the mesenchymal regions around the developing molars. Lim genes (Human LIM class) are related with the expression of the ectomesenchyme of the maxillary and the mandibular process and also suggested to control patterning of the first brachial arch. Prx-1 and Prx-2 coordinately regulate gene expression in cells that contribute to the distal aspects of the mandibular arch mesenchyme. Shh plays an important role in regulating the craniofacial morphogenesis. Pax-9 expression is restricted to prospective tooth mesenchyme at the bud stage, marking the sites of future tooth formation. It is now clear that the role of genes in the craniofacial development is immense. With future advancement in genetic engineering, genetic treatment of craniofacial defects cannot be ruled out. In ultimate analysis, it may prove that reach of the genes is much longer than human beings have ever envisaged.

Received on: 25th-Jan-2012
 Revised on: 26th-Feb-2012
 Accepted on: 04th-March-2012
 Published on: 2nd-Apr-2012

KEY WORDS

Genes; craniofacial growth; homeobox genes; Hox gene

Corresponding author: Email: amolp66@yahoo.com; Tel: +91-9850814846; Fax: +40-9001010012

[I] INTRODUCTION

Rapid advances in molecular genetics and bioinformatics are providing valuable information related to craniofacial growth and its control. The discovery of homeobox genes has helped us to understand its role in establishment of body plan, pattern formation and morphogenesis. The key to the determination of etiology of craniofacial anomalies and its treatability lie in the ability to differentiate the effect of genes and environment on the craniofacial skeleton in a particular individual [1].

Genetic expressions are clearly predominant during embryonic craniofacial morphogenesis, but environment is also thought to influence craniofacial morphology postnatally, particularly during facial growth [2]. It is estimated that about two third of the human genes play a role in craniofacial development. Thus, the systematic review of various genes in the process of embryogenesis and development of maxilla, mandible and craniofacial region.

[II] ROLE OF GENES IN EMBRYOGENESIS

Several major processes are involved in development of

embryo which includes axis specification, pattern formation and organogenesis. The genes responsible for normal development encodes many different products, including i) signaling molecules and their receptors, ii) DNA transcription factors, iii) component of extracellular matrix, enzymes, transport system and other proteins. Each of these genetic mediators is expressed in combination of spatially and temporally overlapping patterns [3].

During embryonic development, the face and neck are derived from swellings or buds of embryonic tissue, the branchial arches that originate bilaterally on the head. The neural crest cells differentiate into most of the skeletal and connective tissue structures of the craniofacial region, while the mesoderm forms the musculature and endothelial lining of arteries of the future face and neck. The establishment of pattern in the craniofacial region is partly determined by the axial origin of the neural crest cells within each arch and partly by regional epithelial mesenchymal interactions [4]. In the mouse embryo, cranial neural crest cells originate from the posterior midbrain-hindbrain regions and migrate ventrolaterally into the branchial

arches [5, 6]. Within the branchial arches, the different populations of crest cells do not intermingle, but instead maintain the positional cues acquired by their rostral-caudal origins in the brain. This segregation of crest cell populations is established early in organogenesis by the apoptotic elimination of crest cells from specific levels of the hindbrain, giving rise to three distinct streams of migratory crest cells. Although this patterning of crest cells depends upon their rostral caudal origin, this pattern does show some level of plasticity [7, 8]. Viz, the knockout of *Hoxa-2* in mice caused the second arch to produce skeletal elements normally found in the first arch. Thus, the Hox genes can specify pattern in arches caudal to the first arch, which does not express this class of genes [9]. Further patterning of the crest cells within the arches involves a reciprocal series of epithelial mesenchymal interactions mediated by several growth factor signaling pathways [10, 11]. The mammalian face develops by the coordinated growth and differentiation of five facial primordia, the single medial frontonasal prominence, the paired maxillary prominences, and paired mandibular prominences, which are located around the primitive mouth or stomodeum. As development proceeds in the frontonasal prominence, localized thickenings of the surface ectoderm called nasal placodes develop. These placodes invaginate, while their margins thicken, to form the nasal pits and the lateral and medial nasal prominences. The maxillary prominences of the first branchial arch grow toward the future midline of the face. They fuse with the lateral nasal prominence on each side, then fuse with the medial nasal prominences, and finally with the intermaxillary segment of the frontonasal process to form the upper jaw and lip. In a similar way, the paired mandibular primordia fuse along their medial edge to form the lower jaw and lip. The frontonasal prominence forms the forehead and nose. Fusion of these approaching primordia results in the formation of a bilateral epithelial seam, which is later replaced by connective tissue giving rise to a confluent lip [12, 13]. Clefts of the upper lip occur as a result of the failure of the maxillary prominence to merge with the medial nasal prominences on one side (producing a unilateral cleft) or on both sides (producing bilateral clefts). Failure of fusion of the paired mandibular prominences occurs far less frequently and results in clefts of the lower lip and jaw [14].

The NCCs are a population of highly migratory multipotent precursors that arise at the junction between the prospective neural tube and epidermis during early stages of vertebrate development [15]. Whatever the initiating mechanism is, execution of a specific differentiation program within CNCCs is likely to require modulating the activity of transcriptional regulators. Several families of transcription factors are expressed in the ectomesenchyme, including Hox, Dlx, Msx, Hand, Pax, Prx, and Fox genes [16]. For inter-BA patterning, *Hoxa-2* has been shown to be necessary (in mouse) and sufficient (in chick and frog) to confer the second BA as opposed to the first BA fate.

2.1. Role of *Shh* in craniofacial development

Facial abnormalities in human *Shh* mutants have implicated the Hedgehog (Hh) pathway in craniofacial development. Although the initial formation of branchial arches (BAs) is normal, expression of several Fox genes, specific targets of Hh signaling in cranial NCCs, is lost in the mutant. The spatially restricted expression of Fox genes suggests that they play an important role in BA patterning. Removing Hh signaling in NCCs also leads to increased apoptosis and decreased cell proliferation in the BAs, which results in facial truncation that is evident by embryonic day.

Shh is expressed in the epithelium of facial primordial [17]. Due to its well established roles in patterning of other organs [18]. *Shh* is a good candidate for one of the molecules that pattern the facial mesenchyme. Indeed, mutations in human *Shh* are responsible for a subset of cases of holoprosencephaly, the congenital defect characterized by forebrain and facial abnormalities. Loss-of-function approaches using function-blocking anti-*Shh* antibody and gain-of-function approaches by ectopic application of *Shh* protein have established the importance of *Shh* for survival and proliferation of ectomesenchyme cells. Adding or blocking the diffusible ligand may affect multiple tissues in the facial primordia, that is, the epithelium, mesodermal mesenchyme and the ectomesenchyme. Therefore, it remains unclear whether there is a direct requirement for Hh signaling within ectomesenchyme to make craniofacial elements, and if this is the case, whether Hh signaling may contribute to molecular patterning of the facial mesenchyme in addition to promoting cell survival and proliferation.

2.2. Expression of *Shh* and *Ptch-1* during craniofacial development

To obtain a detailed understanding of *Shh* signaling during normal craniofacial development, the expression patterns of *Shh* and its transcriptional target Patched-1 (*Ptch-1*) [19] in relation to the distribution of CNCCs in the FNP and BAs was studied. CNCCs were labeled using *Wnt1-Cre*, an NCC-specific Cre-transgene and the R26RLacZ. At embryonic day 9.5 (E9.5) and E10.5, *Shh* is expressed in three epithelial populations in the developing face, that is, the ventral forebrain neuroepithelium the oral ectoderm and the pharyngeal endoderm but is absent from the mesenchyme. Expression of *Ptch-1* indicates that *Shh* signaling occurs in both the epithelium and underlying mesenchyme.

In the MXA and FNP, only the medial half of the mesenchyme is subject to Hh signaling. On the other hand, *Ptch-1* expression extends along the entire mediolateral (proximodistal) axis of the caudal half of the MNA, although its expression is dorsally restricted except at the midline. Additional sites of *Shh* production appear at E12.5, including the ventral nasal pit and tongue epithelium a significant part of

the nasal, oral, and tongue mesenchyme receives Hh signaling at this stage. The mesenchyme expressing Ptch-1 contains a high density of CNCCs at all three stages examined suggesting that direct Hh signaling to this population of cells may have functional importance. In addition to Shh, another member of

Hh family genes, Indian hedgehog (Ihh), has been implicated in craniofacial development; Ihh mutants have mild craniofacial abnormalities. Thus, Shh is exclusively responsible for the Hh signaling in the face prior to E12 19.

2.3. Fox genes as mediators of Hh pathway function

During craniofacial development Hh signaling regulates ectomesenchymal expression of five Fox genes, Foxc-2, Foxd-1, Foxd-2, Foxf-1, and Foxf-2, several of these induced by Shh in somites, foregut, or tissue culture. It has been proposed that the Fox genes are the major mediators of the function of Hh signaling in craniofacial morphogenesis. This hypothesis supported the mutant phenotype of Foxc-2. In particular, the absence of the palate components (palatal process of the maxilla and palatine) and the middle ear ossicles (incus and stapes) correlates with the expression of Foxc-2 in the MXA and second BAs. Foxf-2 mutants also have a cleft palate, although this is likely to be secondary to the influence of Foxf-2 on tongue morphogenesis [20]. In contrast, no craniofacial abnormalities were reported in the mutants of either Foxd-1 or Foxd-2 [21].

2.4. Foxi Class Genes - Early Craniofacial Development

Since the discovery of the highly conserved motif between the Drosophila forkhead gene and the mammalian HNF-3 transcription factor, more than 100 members of the Fox gene family have been identified from yeast to human. Foxi class genes have been identified and analyzed in several species. Mouse Foxi-1, previously called Fkh-10, is expressed in the otic vesicle at the E9.5 and the expression becomes restricted to the epithelium of endolymphatic duct and sac at the later stages. Targeted mutation of Foxi-1 causes an abnormal expansion of the membranous labyrinth, and the resulting mutant mice suffer from hearing impairment and vestibular dysfunction. Mouse Foxi-1 is also expressed in the embryonic and adult kidney from E16.5 [22]. Zebrafish foxi-1 is expressed in the early otic placode and branchial arches, and the zebrafish foxi-1 mutant and morpholino knock-down experiments show that zebrafish foxi-1 regulates dlx and Pax gene expression in the early otic placode and branchial arches. Xenopus foxi-1-a and b are mainly expressed in the neuroectodermal and mesodermal lineage during early embryogenesis and foxi-1c is expressed in the epidermal ring around the neural field and subsequently localized in placodal precursor cells. Solomon and colleagues have identified three other fox-i class genes in zebrafish. Zebrafish foxi-2 is

expressed in the chordamesoderm during early somitogenesis and the retina and branchial arches during later stages. Zebrafish foxi-3-a and foxi-3-b are expressed in the epidermal mucous cells throughout embryogenesis and early larval stages. Zebrafish foxi-2, foxi-3-a, and b are not expressed in the otic lineage. Mouse Foxi genes are expressed in an early pan-placodal ectodermal domain, and also later in particular cranial placodes. Their expression shows some similarities, but also significant differences with the expression of Foxi genes in other vertebrate species.

Foxi-2 is expressed faintly in the ectoderm of the midbrain–hindbrain boundary region at the late pre-somite stage (ss). This expression is no longer visible at later stages. At E 6.5 to E10.5, more distinct but patchy expression is visible in the cranial ectoderm. At this stage, the Foxi-2 expression domain overlaps the Pax-2 expression domain, which marks the presumptive otic region in the cranial ectoderm adjacent to rhombomere 3 to 5. The Foxi-2 expression domain excludes the otic placode at later stages. Thus following hypotheses are proposed. (i) Foxi-2-positive cells in the Pax-2 domain may be future epidermal and epibranchial cells, not otic placodal cells, and migrate away from the otic region as the otic placode forms, (ii) Some of the Foxi-2-positive cells in the Pax-2 domain are future otic placodal cells and (iii) Foxi-2 expression is downregulated in these cells as otic placode forms.

Foxi-2 is expressed faintly in the ectoderm of the midbrain–hindbrain boundary region at the late pre-somite stage (ss). This expression is no longer visible at later stages. At E 6.5 to E10.5, more distinct but patchy expression is visible in the cranial ectoderm. At this stage, the Foxi-2 expression domain overlaps the Pax-2 expression domain, which marks the presumptive otic region in the cranial ectoderm adjacent to rhombomere 3 to 5. The Foxi-2 expression domain excludes the otic placode at later stages. Thus following hypotheses are proposed. (i) Foxi-2-positive cells in the Pax-2 domain may be future epidermal and epibranchial cells, not otic placodal cells, and migrate away from the otic region as the otic placode forms, (ii) Some of the Foxi-2-positive cells in the Pax-2 domain are future otic placodal cells and (iii) Foxi-2 expression is downregulated in these cells as otic placode forms.

Table: 1. Gene abbreviations and references

No	Gene	Abbreviation	Reference
1.	HBG	Homeobox gene family	Burlglin, 1994; Hill, 1989; Sharpe, 1995; Favire, 1997
2.	Hox	Homeobox genes	Burlglin, 1994; Hill, 1989; Sharpe, 1995; Favire, 1997
3.	Msx	Mammalian homology to Drosophila muscle segment Homeobox genes	Alappat, 2003; Bendare, 2000; Akimenko, 1995
4.	Dll	Distal-less Homeobox gene in Drosophila	Cohen, 1998
5.	Dlx	Mammalian homology to Drosophila Distal-less gene	Raymond, 2002; Yang, 1998; Cohen, 1998
6.	OTX	Vertebrate homology to Orthodenticle in drosophila	Simeone, 1998; Acompora, 2002, Bailey-Cuif and Boncinelli 1997
7.	PAX	Paired box domain	Dahl, 1997; Peters, 1998; Mansouri, 1999
8.	Pitx	Pituitary specific transcription factor	Szeto, 1996; Lanctot, 1997; Gage, 1999
9.	PRX	Paired related family of Homeobox genes	Meijlink, 1999; Berge, 1998; Lu, 1999
10.	Barx	Bar class of Homeobox containing genes	Tucker, 1989; Kojima, 1991; Barlow, 1999
11.	Gsc	Goosecoid gene	Yamanda, 1995; Bailey-cuif and Boncinelli 1997
12.	bHLH	Basic helix-loop-helix family of transcription factor	Bailey-cuif and Boncinelli 1997
13.	Osr	Odd skipped related gene	Burlglin, 1994; Hill, 1989;
14.	Shh	Sonic Hedgehog family of genes	Echarld, 1993; Hammerschidt, 1997; Nasse, 1996
15.	Ihh	Indian Hedgehog gene	Belloni, 1996
16.	Fox	Forkhead box gene family	Tukahiro Ohyama and Andrew Grover, 2004; Streit 2002
17.	Wnt	Wingless family of genes	Tomlinson, 1997; Zang and Carthero 1998
18.	Fz	Frizzled family gene	Kuhl 2002
19.	BMPs	Bone Morphogenetic Proteins	Luo, 1995; Kim, 1998
20.	TGFs	Transforming Growth Factors	Dudas, 2004; Xu, 2006; Proetzel, 1995
21.	FGFs	Fibroblast Growth Factors	Trainor, 2002; Kim, 1998
22.	MMPs	Matrix Metalloproteinase	Rasha-Al-Mubarak, 2005
23.	Lhx	LIM-Homeobox containing genes	Maria 1998

2.5. Dlx-5 and Dlx-6 Homeobox genes

2.5.1 Role of Dlx-5 and Dlx-6 HBG in craniofacial development

Dlx homeobox genes (HBG) are mammalian homologs of the Drosophila Distal-less (Dll) gene. The Dlx/Dll gene family is of an ancient origin and appears to play a role in appendage development in essentially all species in which it has been identified. In Drosophila, Dll is expressed in the distal portion of the developing appendages and is critical for the development of distal structures. In addition, human Dlx-5 and Dlx-6 homeobox genes have been identified as possible candidate genes for the autosomal dominant form of the split-hand/split-foot.

2.5.2. Cartilage and bone defects in Dlx5/6-/- mice

Severe craniofacial cartilage defects in Dlx-5/6-/- embryos

are apparent at E14.5. such as- (i) Exencephaly, (ii) Inner ear capsule and middle ear cartilages are fused and severely dysmorphic, (iii) External ear cartilage is absent, (iv) Cartilage giving rise to the cranial floor (basioccipital, basisphenoid, and sphenoid) and frontonasal prominence with severe patterning defects, (v) Cartilage from the exoccipital and ventral temporal bone primordia extending to the distal nasal capsule are distinctly condensed and fused, (vi) Maxillary and Mandibular bones are absent. However, soft tissues (skin, tongue, and muscle) are present in a manner that defined where maxillary and mandibular structures should have developed. Endochondral ossification of the exoccipital bone primordia of Dlx-5/6-/- embryos is present at E18.5. In addition, areas of membranous ossification develop that suggest an attempt to form maxilla, premaxilla and nasal bones [23].

2.5.3 Role of Dlx5/6 in control of craniofacial development

Dlx-5/6-/- mice have a multitude of craniofacial and ear

defects including the failure of Meckel's cartilage, mandible, and calvaria formation. The craniofacial and ear defects are dramatically more severe than those observed in *Dlx-5*-deficient mice. Numerous genes are required for proper ear and craniofacial development, including *Prx-1*, *Prx-2*, *Msx-1*, *Msx-2*, Endothelin-1(*Edn1*), and Endothelin-A receptor (*ETA*). Mice null for *Prx-1/2*, *Msx-2*, *Edn-1*, or *ETA* have craniofacial and ear defects that have some similarity to a portion of the defects in *Dlx-5/6*^{-/-} mice [23].

2.6. *Msx* homeobox genes

2.6.1. Role of *Msx* homeobox gene family in craniofacial development

Vertebrate *Msx* genes are unlinked, homeobox-containing genes that bear homology to the *Drosophila* muscle segment homeobox gene. These genes are expressed at multiple sites of tissue-tissue interactions during vertebrate embryonic development. Inductive interactions mediated by the *Msx* genes are essential for normal craniofacial, limb and ectodermal organ morphogenesis.

Vertebrate craniofacial tissues form multiple embryonic tissues including the cranial neural crest derived cells, prechordal mesoderm, and the embryonic craniofacial ectoderm. Normal craniofacial morphology develops as a consequence of complex interactions between these embryonic tissues, and requires precise regulation of cell movement, growth, patterning, and differentiation of craniofacial tissues. Genetic studies have revealed the involvement of numerous genes in these processes, including genes encoding a variety of transcription factors, growth factors and receptors [24]. Mutations in genes that influence any of these processes would cause craniofacial abnormalities, such as facial clefting and craniosynostosis, which are among the most frequent congenital birth defects in humans. Among the critical factors involved in craniofacial development are members of the *Msx* homeobox gene family. The vertebrate *Msx* genes were initially cloned from mice and identified as homologous to the *Drosophila* muscle segment homeobox gene (*msh*) [25, 26]. Subsequently, *Msx* genes have been isolated from a variety of organisms, including ascidians, sea urchin, zebrafish [27], frogs [28], birds [29], and humans. The mammalian *Msx* gene family consists of 3 physically unlinked members, named *Msx-1*, *Msx-2*, and *Msx-3*. *Msx-3* is only expressed in the dorsal neural tube, in a pattern resembling that of the prototypical *Drosophila* *Msh* gene [30]. However in, developing vertebrate embryos, *Msx-1* and *Msx-2* are widely expressed in many organs, particularly at the sites where epithelial-mesenchymal interactions take place. Most notably, *Msx-1* and *Msx-2* are strongly expressed in the developing *Msx* genes encode transcription repressors. The *Msx* proteins are regulatory proteins that function as transcriptional repressors in vitro and in vivo [31, 32], important modulators of craniofacial, limb, and nervous system development.

Protein-protein interactions, which engage residues within their homeodomain guide target gene selection and transcription regulation [33]. The *Msx* homeodomain interacts directly with the TATA binding protein (TBP), the core component of the general transcription complex to execute transcription repression importantly; this ability to interact with members of the basal transcription machinery and affect transcription is not contingent upon their DNA-binding function. *Msx* proteins also interact with other homeodomain proteins to regulate transcription. Heterodimers formed between *Msx-1* and other homeodomain proteins such as *Dlx-2*, *Dlx-5*, *Lhx-2* and *Pax-3* result in mutual functional antagonism in vitro [34]. The tissues in which expression of *Msx-1* overlaps these other proteins there may be such a regulatory mechanism in place. Although, *Msx-1* and *Msx-2* show similar DNA binding site preference as well as the ability to repress transcription they display different biochemical properties by virtue of unique N-terminal domains, which confer *Msx-2* with a greater affinity for DNA while rendering *Msx-1* a more potent repressor. Three dimensional structure of *Msx-1* homeodomain/DNA complex reveals two major arm of the homeodomain, which tracks the minor groove of the DNA. Secondly, the DNA bound by the *Msx-1* homeodomain with other shows a 28° bend compared to the normal 21° observed homeodomain proteins.

2.6.2. Expression of *Msx* genes during craniofacial development

Expression of *Msx-1* and *Msx-2* are seen at multiple sites of tissue-tissue interaction including the craniofacial regions. Through the course of murine craniofacial development, both *Msx-1* and *Msx-2* are detected in the forming skull and meninges, the distal aspects of the facial primordia, the associated sense organs, and teeth. In the developing skull, *Msx-1* and *Msx-2* are expressed in the suture mesenchyme and dura mater. While *Msx-1* expression extends into the postnatal stages of skull morphogenesis, *Msx-2* registers a sharp decline in expression after birth. Reports of a weak, diffuse expression of *Msx-1* in the palatal mesenchyme provided the first evidence that *Msx-1* may have a direct role in palate development. A more detailed analysis by Zhang et al., (2002) [35] has reported that *Msx-1* expression in the palatal mesenchyme is confined to the anterior portion of the developing palatal shelves [36].

2.7. Role of *Lhx-6* and *Lhx-7*, in craniofacial development

Many homeobox containing genes are, however, found dispersed outside the *HOM-C/Hox* clusters. Such genes often encode polypeptides which, in addition to the homeodomain, contain additional domains (such as paired, POU or LIM domains which can regulate the transcriptional activity of the protein [37]. LIM homeodomain proteins [38], are characterised by the association of two LIM domains

(cysteine-rich motifs involved in intra- and intermolecular interactions) with a homeodomain and constitute a family of transcriptional regulators that were originally identified by sequence homology between the *C. elegans* genes *lin-11* and *mec-3* and the mammalian transcription factor *islet-1*. Genetic studies in both invertebrates and vertebrates have shown that LIM homeodomain encoding genes are required for the control of cell fate specification and differentiation. In vertebrates, targeted mutagenesis of *Lhx* gene has established that they are necessary for the differentiation of specific cell types, such as subclasses of CNS neurons (*isl-1*) or subpopulations of endocrine cells of the anterior pituitary. Finally, misexpression studies have indicated that the *Lmx-1* gene is a critical component of the molecular mechanisms which lead to establishment of the dorsal phenotype of the vertebrate limb bud [39]. *Lhx-6* and *Lhx-7* are expressed in overlapping subdomains of the first branchial arch and the basal forebrain and the expression in the first arch primordia is under the control of signals from the overlying oral epithelium. One of these signals is likely to be *FGF-8*, which is expressed in the oral epithelium and is capable of inducing expression of both *Lhx-6* and *Lhx-7* in mandibular mesenchyme *in vitro*.

Low levels of *Lhx-6* and *Lhx-7* transcripts were first detected by whole-mount *in situ* hybridisation in a subdomain of the first branchial arch of E9.5 embryos. At E10.5; both genes are expressed at high levels, and with an overlapping pattern, in the maxillary and mandibular processes of the first branchial arch. However, expression is restricted to the subdomains bordering the cleft that separates the two facial primordia. Sections of hybridised embryos showed that *Lhx-6* and *Lhx-7* transcripts were restricted to the neural crest-derived ectomesenchyme and were excluded from the overlying oral epithelium. No expression is detectable in other branchial arches. It appears, therefore, that the expression domains of *Lhx-6* and *Lhx-7* coincide with the regions of the first arch mesenchyme which acquire odontogenic potential and contribute to the formation of individual teeth. Consistent with this, expression of *Lhx-6* and *Lhx-7* in the branchial region at subsequent developmental stages is primarily associated with developing teeth. Expression of *Lhx-6* and *Lhx-7* during mouse odontogenesis analysed by *in situ* hybridisation on sections of embryos ranging from E12.5-P2 showed, expression of both genes was identical and distributed uniformly in the ectomesenchyme adjoining the oral epithelium. By the tooth bud stage (E13.5), expression is downregulated from most regions of the mandibular and maxillary mesenchyme, but is maintained (and indeed upregulated) in the mesenchyme adjacent to the epithelial thickenings which constitute the tooth primordia. Similarly, at subsequent stages of tooth cap and bell high levels of *Lhx-6* and *Lhx-7* expression are restricted to the mesenchymal component of the developing tooth. Finally, by postnatal day 2, expression of both *Lhx-6* and *Lhx-7* genes is downregulated in the developing teeth. Overall, data indicates that prior to initiation of tooth development; *Lhx-6* and *Lhx-7* are expressed uniformly in the odontogenic mesenchyme of the

first branchial arch, whereas during odontogenesis, expression is restricted to the mesenchyme participating in the formation of individual teeth.

[III] GENES INVOLVED IN CRANIOFACIAL SUTURE GROWTH

3.1. Expression of BMP-2 and BMP-4

The BMP signaling pathway interacts with FGF, Shh, and Wnt signaling pathways and regulates the expression of several critical transcription factors, such as *Runx-2/Cbfa-1*, *Msx-1*, and *Msx-2*. Although no mutations in the genes encoding the different BMP isoforms have yet been found in human cranial sutures (CS), it has been suggested that BMP signaling is crucial in suture formation of the human bones. Both BMP-2 and BMP-4 are present in the osteogenic fronts of cranial sutures, and high expression of BMP-2 was observed in the mesenchyme during palatal fusion [40]. Deficiency of BMP signaling in mouse neural crest cells shows multiple defects in craniofacial skeleton, such as cleft palate and a hypotrophic mandible. BMP signaling is also found to induce and upregulate the expression of homeobox gene *Dlx-5*, a critical factor for the development of both the craniofacial skeleton and teeth. From early tooth initiation to crown morphogenesis, the BMP/*Msx* signaling loop mediates reciprocal interactions between the epithelium and the mesenchyme.

During embryonic stages, BMP-2 mRNA is detected in the OFs and weakly in parietal bones. After birth, the expression of BMP-2 is greatly reduced. BMP-4 mRNA, on the contrary, is localised in the OFs at high levels and at a lower level in mesenchyme of sagittal suture until E17. At E15 BMP-4 is also expressed in the developing falx cerebri and in the dura. From the end of embryonic stage (E18), the expression of BMP-4 was decreased and the analysis of serial sections showed that expression is not continuous in the OFs, indicating a patched pattern. Both BMP-2 and 4 transcripts are expressed in epidermis of skin and from E16 in hair follicles, however, as with *Msx* probes the hair pigment also contributed somewhat to the authentic expression.

3.2. Expression of Shh and Ptc

The first weak signs of *Shh* gene expression are found at E17 in posteromedial OFs of the parietal bones. From E18 onwards, *Shh* transcripts are expressed in a patched pattern in the OFs in sagittal suture as well as in metopic suture. Expression of *Ptc*, is identified as *Shh* receptor, is not detected by whole-mount *in situ* hybridisation until E18. From E18 onwards, *Ptc* transcripts are localised in the OFs in sagittal and metopic sutures. The patterns of *Ptc* and *Shh* expression were remarkably similar. Control tissues hybridised with sense probes gave negative result. Interestingly, neither *Shh* nor *Ptc* is expressed in the area of the coronal suture during these stages [41].

Table: 2. Genes causing various human birth defects

No	Gene	Syndrome	Birth defect
1.	<i>BORA1</i>	Branchio-oto-renal	External ear anomalies, hearing loss, kidney defects
2.	<i>COL2A1</i>	Stickler	Skeletal dysplasia, cleft palate, nearsightedness
3.	<i>EMX2</i>	Schizencephaly	Clefting of the cerebral cortex
4.	<i>GLI3</i>	Greg	Premature closure of cranial sutures, extra digits
5.	<i>GLI3</i>	Polydactyly type A	Extra posterior digits
6.	<i>HOXA13</i>	Hand-foot-genital	Hypoplasia of first digit, kidney and genital defects
7.	<i>HOXD13</i>	Synpolydactyly A1	Extra digits that are fused with each other
8.	<i>IHH</i>	Brachydactyly	Short finger and toes
9.	<i>IRF6</i>	Van der Woude	Cleft lip/palate, with lip pits
10.	<i>IRF6</i>	Popliteal pterygium	Cleft lip/palate, webbing across joints
11.	<i>LMX1</i>	Nail-patella	Anomalies of bone, kidneys, fingernails
12.	<i>MSX1</i>	-	Cleft lip/palate, missing teeth
13.	<i>NOG</i>	Multiple synostosis	Abnormal fusion of bone, hearing loss
14.	<i>TP63</i>	Ectodermal dysplasia	Limb, teeth, hair defects
15.	<i>PAX2</i>	-	Kidney and optic nerve defects
16.	<i>PAX3</i>	Waardenburg	Hypopigmentation, hearing impairment
17.	<i>PAX6</i>	Aniridia	Hypoplasia or aplasia of the irides
18.	<i>PAX9</i>	Oligodontia	Missing teeth
19.	<i>SHH</i>	Holoprosencephaly	Lack of midline cleavage of brain
20.	<i>SOX9</i>	Campomelic dysplasia	Skeletal defects, sex reversal
21.	<i>SOX10</i>	Hirschsprung	Bowel Hypomotility
22.	<i>TBX3</i>	Ulnar-mammary	Upper limb anomalies, breast and genital anomalies
23.	<i>TBX5</i>	Holt-Oram	Anterior upper limb anomalies, heart defects
24.	<i>TBX22</i>	-	Ankyloglossia, cleft palate
25.	<i>TCOF1</i>	Treacher Collins	Mid-face hypoplasia, small jaw, external ear defects
26.	<i>WT1</i>	Denys-Drash	Kidney defects, sex reversal
27.	<i>DHCR7</i>	Smith-Lemli-Optiz	Mental retardation, Syndactyly, multiple organ defect

3.3. Different signalling pathways may regulate suture maintenance prenatally and postnatally

In situ hybridisation analysis shows that the expression of *Msx-2* and *BMP-4* is correlated with the prenatal activity of dura mater. Postnatally, neither of these genes are detected in this location. Although the expressions of *Msx-1* and *Msx-2* are overlapping, they showed clear differences and, in vitro,

BMP-4 induced the expression of both *Msx-1* and *Msx-2*, whereas *FGF-4* induced the expression of *Msx-1* only. In dental mesenchyme also, *FGFs* preferentially regulate *Msx-1*, but not *Msx-2*. These findings are in line with a showing that the functions of *Msx-1* and *Msx-2* genes are modulated differentially by their non-conserved N-terminal regions. However, it is shown that *Msx-1* and *Msx-2* have similar DNA binding and transcriptional properties suggesting redundant functions of the two genes.

Whole-mount in situ hybridization analysis show that Shh as well as its receptor, Ptc, started to be expressed at the end of embryonic development. Their expression appeared as patches on the OFs of the midline sutures. This indicates that, firstly, the target tissue for Shh signalling is in the OF and, secondly, there are site-specific differences in Shh signalling in the calvaria, which may reflect the difference in sutural architecture. The coronal suture whose OFs are overlapping apparently lacked Shh expression, whereas as Shh is seen in end-to-end type midline sutures. Thus it is suggest that the Shh signalling may be involved in regulating cranial suture development and intramembranous bone formation. It is possible that Shh has an analogous effect on intramembranous bone development as has been shown for Ihh, another hedgehog family member, in endochondral bone formation, where Ihh controls the differentiation of hypertrophic chondrocytes. Postnatally the expression of BMP-2, BMP-4 and Msx-2 is discontinuous along the OFs apparently reflecting a patched pattern thus resembling the expression of Shh and Ptc. It is speculated that Shh may interact with BMPs in the OF through a Ptc-dependent pathway which may be involved in the prevention of precocious sutural closure [41].

3.4. Expression of Bone sialoprotein (Bsp) and Twist

Bsp was first expressed at E12 just lateral to the temporal cartilages, in a strip medial and superior to the eye extending occipitally. From these ossification centres in the frontal and parietal bones, the expression spread toward the apex of the cranium where the osteogenic fronts approximate to form a suture (E15), two osteogenic fronts and intervening mesenchyme. Until E17 Bsp is expressed throughout the calvarial bones, most notably on their outer surfaces. In contrast, osteoclast are found mainly on the endocranial surfaces and so, as the calvaria expands, there is an intimate balance between bone apposition and resorption, thus maintaining bone thickness and shape. After E17, transcripts became more restricted to areas of high activity, notably the sutures. Bsp expression clearly demarcating the developing calvarial bones and illustrated the approximation of their osteogenic fronts. At E10, Twist is intensely expressed in mesenchyme throughout the first and second branchial arches, as well as in the mesenchyme surrounding the developing eye and cranial mesenchyme just beneath the epithelium. Expression then comes more restricted so that, by E14, transcripts are seen bordering areas of condensing calvarial mesenchyme. These condensations consist of osteoprogenitors that differentiate into functioning osteoblasts, the temporal, frontal and parietal bones being thereby initiated. Twist mRNA was also detected close to developing cartilages. From E15 to P1, Twist continued to be expressed in the calvarial mesenchyme and, as in earlier stages, not in mature osteoblasts. Postnatally its intensity is decreased gradually.

3.5. Expression of FGFR-1-B, FGFR-1-C, FGFR-2-B, FGFR-2-C, FGFR-3B, FGFR-3-C and FGFR-4

FGFRs are expressed at numerous locations during early mouse development including the craniofacial area and, although FGFRs have been detected in developing bones and sutures, little is known about their detailed expression during calvarial bone development. Twist proteins are conserved basic helix-loop-helix transcription factors (bHLH) and Inhibitors of differentiation (Ids) are conserved dominant negative helix-loop-helix proteins (dnHLH). Both have been implicated as regulators of mesoderm differentiation and myogenesis in both *Drosophila* and vertebrate development though, in contrast to *Drosophila* Twist, murine Twist is thought to act as a suppresser rather than an activator of myogenesis. Although, Id-1 lacks a DNA binding domain, it inhibits bHLH's function by suppressing their heterodimerization through direct protein-protein interactions. Early osteoblastic cell cultures have been shown to express both Twist and Id, with expression decreasing as maturity increases.

3.6. Expression of FGF-2

FGF-2 demonstrates a more restricted expression patterns, being associated with osteoblast differentiation in the suture. FGF-2 is expressed in the mesenchyme of the calvarial sutures and more weakly in the developing calvarial bones and the underlying dura mater. Expression decreased in intensity after E16. Expression of this potential ligand, although overlapping that of the FGFRs, is not primarily expressed in the osteogenic fronts and is also more extensively expressed in the mid-sutural mesenchyme, suggesting paracrine functions.

BEK, a splicing alternative of FGFR-2, is intensely expressed in the OFs of parietal bones of E15 and E17 mouse embryos, and transcripts are also detected in the superficial dermis of skin. Postnatally BEK is expressed at the same location but its intensity is diminished. Interestingly at P6 these areas of expression appeared to join above and below the mid-sutural mesenchyme, possibly indicating the forming periosteum sheathing this area. At E15, FGF-9 is expressed with high intensity in the dural layers, the calvarial mesenchyme and the overlying epidermis. By E17 transcripts are most notably located in the dura mater and endocranial portion of the mesenchyme and dermis. Postnatally, expression is still noted in the calvarial mesenchyme at a diminished level. FGF-4 is not present in these tissues between E15 and P6.

The FGFRs are high-affinity tyrosine kinase receptors, which together with co-factors mediate the effects of FGFs. They are transmembrane glycoproteins with two or three extracellular immunoglobulin domains. These binding domains differ between alternative splice variants, which are of particular interest as they possess different ligand-binding specificities as well as exhibiting unique temporospatial expression patterns

suggesting unique functions. In addition, many of the human mutations in FGFR-1/FGFR-3 causing disorders in bone development are found in or close to the third immunoglobulin (III) domain. The expression pattern of FGFR-1B is generally weak compared to the other FGFRs and transcripts are not seen in either the developing calvarial bone or sutures.

Very low levels of FGFR-1C expression is detected in the calvarial bones, most notably in the osteogenic fronts between E15 and 17, major sites of osteoblastic condensation and differentiation. FGFR-1C is also expressed in many cartilages in the developing head. FGFR-2B (kgfr) is expressed in the osteogenic fronts of the parietal bones (E15-17). In addition, transcripts are located in developing epithelia, notably the skin including hair follicles. FGFR-2C (bek) is found in similar locations to FGFR-2B but at generally much stronger intensity. Postnatally, expression is at the same locations but diminished in intensity. In comparison to FGFR-2B, FGFR-3B is weakly and FGFR-3C strongly expressed in many cartilages of the head. The majority of this cartilage does not contribute to the calvarial bones, which form directly from mesenchyme. FGFR-3C mRNA is also detected with low intensity in the head periosteum and sutural osteogenic fronts. Transcripts of FGFR-4 are not detected in the developing calvarial bone or mesenchyme. However, FGFR-4 mRNA is detected strongly in developing muscle, notably in the developing temporalis between the epithelium and the underlying calvaria.

3.7. Muscle segment homeobox-containing (Msx) transcription factors

Msx-1 and Msx-2 are transcription factors expressed in overlapping patterns at multiple sites of tissue interactions during vertebrate development. In particular, they have been associated with epithelial–mesenchymal interactions during craniofacial/dental development, as targets of BMP and FGF signaling. For instance, BMP-2 and BMP-4 induce the upregulation of Msx gene expression in tooth explants as well as in rhombomeres and several FGFs induce the expression of Msx-1 in dental mesenchyme. Msx-1 and Msx-2 have also been associated with the differentiation of neural crest-derived intramembraneous bones in the skull. Msx-2 deficient mice exhibit defective proliferation of osteoprogenitors in the developing calvaria and have defects of skull ossification and persistent interparietal foramina. Transgenic mice overexpressing the Msx-2 mutation appear to have different phenotypes depending on which promoter is used, varying from precocious bone formation with accelerated suture closure to craniofacial defects with aplasia of the interparietal bone. Msx-1 and Msx-2 also determine the position and shape of teeth (so-called field model, linking patterning of tooth type to spatial expression of homeobox genes in the dental mesenchyme).

Msx-1 is expressed in the mesenchyme of sagittal suture and the dura mater during embryonic and postnatal stages. Msx-2 is intensely expressed in the sutural mesenchyme and the dura mater during embryonic stages. Interestingly, after birth, the

expression of Msx-2 is dramatically diminished in the mesenchyme and it completely disappeared from the dura mater. Furthermore, analysis of serial sections reveals that the expression of Msx-2 is no longer continuous after birth around the OFs, indicating a patched pattern of expression. Msx-1 and Msx-2 transcripts are intensely expressed in hair follicles. However, the hair pigment also contributed an additional component to the authentic expression.

3.8. Twist transcription factor

Twist is a helix–loop–helix transcription factor that plays a role in cranial neural tube morphogenesis, Twist is expressed very early as a negative regulator of osteoblast differentiation and its expression decreases with maturity, i.e. Twist is expressed by osteoprogenitors but not by mature osteoblasts. FGF-2/FGF-4 and Twist exhibit overlapping expression patterns, both being intensely expressed in the midsutural mesenchyme between the calvarial bones and in the mesenchyme during early tooth initiation. It was shown recently that Twist is one of the integrating parts of the Shh, FGF, BMP, and Msx-2 signaling pathways mediating a number of common effects at the cellular level during development of, e.g. the cranial structures, limbs, the palate, and teeth. Mutations in the Twist gene cause Saethre–Chotzen syndrome, resulting from a loss-of-function mechanism. In contrast to FGFR and Msx-2 mutations, these are mostly deletions or nonsense mutations. Twist knockout mice die before osteogenesis has started, with a failure of the cranial neural folds to fuse and defects in the head mesenchyme. Experimental animal studies further support the idea that FGF signaling may lie both up- and downstream of Twist.

3.9. Otx- Genes

Another family of evolutionary conserved homeodomain factors with critical regulatory roles in the determination of head structures during development is the Otx genes, vertebrate homologs to Orthodenticle in *Drosophila*. The overlapping patterns of expression of Otx and Emx genes in the rostral region of the developing brain, together with functional studies, have suggested that these genes, analogous to the Hox code for hindbrain development, provide a combinatorial code for rostral brain development [42]. Otx-2 homozygous null mutants die early in embryogenesis and fail to develop structures anterior to R3. The phenotypic abnormalities in Otx-1 homozygous mutants indicated its essential role in the formation of cortex in the adult brain.

In addition to its expression in the rostral region of the developing brain, Otx-2 is also expressed in neuroectoderm from the forebrain up to the mid-hind-brain isthmus. Interestingly, Otx-2 heterozygote animals exhibit otocephaly and abnormalities in midbrain crest derivatives of the first arch, suggesting a role for Otx-2 in pre-migratory CNCC originating from the midbrain region. In Otx-2^{+/-} mice, the elements that were shown to be derived solely from midbrain

crest (distal Meckel's cartilage, dentary, maxilla, and palatine) are lacking or severely reduced, suggesting that defects in these animals may be due to deficiencies in CNNC derived from the midbrain region. However, in *Otx-2^{+/-}* mice, the hindbrain-derived, first-arch elements (malleus, incus, and pterygoid) are almost unaffected. Analysis of the knock-in mice in which *Otx-2* was replaced with *Otx-1* showed that most *Otx-2* functions, including the *Otx-2* haploinsufficiency causing the otocephalic phenotype, are replaceable with those of *Otx-1*.

[VI] PALATAL DEVELOPMENT AND FUSION

4.1. Tissue patterning

The wingless (*wnt*) and frizzled (*fz*) family genes were first characterized in *Drosophila*, where they specify tissue patterning and cell-fate determination during embryonic development [40, 41]. The homologous *wnt* and *fz* family members in mammals have also been reported to function in tissue specification [43, 44]. *Wnt-5a* and its receptor, *fz*, are seen to be both down-regulated (−2.7 and −1.9, respectively). This was confirmed by immune-histo-chemistry. Their role in palatogenesis is as yet unidentified; although *Wnt-5a* shows strong expression in the dental papilla mesenchyme [45] and mutant murine embryos have defects in the face and organs that extend from the body [46]. *Barx-1* is a homeobox gene that is expressed in developing facial primordia, including the maxillary mesenchyme [47], targets of fibroblast growth factor *FGF-8*, which in early chick embryo ectoderm defines the maxillo-mandibular region through epithelial–mesenchymal interactions and subsequent upregulation of homeobox genes in the local mesenchyme [48]. Upregulation of *Barx-1* expression before contact of palatal shelves and subsequent downregulation after fusion is seen.

4.2. Neural development

Zic-3 belongs to a class of genes responsible for neural development [49], and the expression of murine *Zic* genes suggests an essential role in body pattern formation. At ED-13.5, *Zic-3* is expressed in peripheral zones of limb mesenchyme and presumptive muscle, but subsequently its expression decreases [50]. *Zic-3* mRNA was downregulated within palatal shelves between ED-13.5 and 14.5, but immunohistochemistry revealed negligible levels of *Zic-3* protein expression at all stages. This suggests that *Zic-3* mRNA levels may be insignificant, and the changes seen may be minimal. The role of *Zic-3* in palate development is unknown, but *Zic-3* null mice have complex congenital heart disease, neural tube defects, disturbances of laterality, and vertebral and rib defects, but no cleft palate [51]. *Sox-1* transcripts are first detected in the neural fold ectoderm at the headfold stage, and during early somitogenesis are expressed in the neuroectoderm [52]. Mesenchyme from the facial

primordia is derived from neural crest cells that have migrated from the neuroectoderm. Proliferation of neural crest cell-derived mesenchyme is an important part of palatal shelf formation. Proteins containing LIM domains play important roles in a variety of fundamental biological processes, including cytoskeleton organization and organ development [53]. It is noted that muscle LIM protein increased fourfold between ED14.5 and 15.5 in the murine palate. *Lhx-8*, a LIM homeobox gene, is expressed in the mesenchyme of the mouse palatal structures throughout their development, and nullizygous mutants for *Lhx-8* are known to have cleft palate [54].

Maternally expressed gene (*Meg-1*) is probably responsible for the imprinted effects of prenatal growth retardation or growth promotion caused by maternal or paternal duplication of proximal chromosome 11, with reciprocal deficiencies.

4.3. Molecular control of secondary palate development

Targeted gene mutations in mice have revealed a number of molecular determinants of PS growth. In these, the PS is hypoplastic and either remain in a vertical position, leading to a wide cleft, or manage to elevate but remain apart. Organogenesis is governed by interactions between adjacent tissues layers. Organs as diverse as the lung, neural tube, tooth, hair and palate share several signaling pathways, although the developmental outcome is different. This emphasizes the notion of ‘common notes—different melodies’, where similar molecular networks are used during ontogeny of several organs but regulate different processes. Thus, insights gained from the biological events operating during embryogenesis of one organ can be used to shed light into those acting in other organs. Early experimental studies indicated a role for epithelial–mesenchymal interactions in the regional specification of PS epithelia and growth of the PS [55, 56]. Studies identified several molecular networks operating between the PS epithelium and mesenchyme during the different steps of palatogenesis. These include signaling molecules and growth factors such as *Shh*, members of the *TGF-β* superfamily, including *BMPs* and *TGF-βs*, *FGFs*, their receptors, effectors and targets. Transcription factors play fundamental roles in tissue patterning, growth and differentiation. *Msx-1*, the LIM-homeobox containing *Lhx-8*, the short stature homeobox *Shox-2* and the odd-skipped related-2 (*Osr-2*) genes have been shown to be expressed in the growing PS. Targeted mutations of these genes generate cleft palate (CP) with minor or no craniofacial anomalies, indicating an intrinsic requirement of these factors during palatogenesis [57, 58]. The CP in mice lacking *Msx-1* (*Msx-1^{-/-}*) has been shown to be caused by altered mesenchymal proliferation [59]. *Msx-1* and *Msx-2* genes are bona fide targets of *BMP* signaling in different developing embryonic sites including the tooth, cranial sutures, hair follicle and neural tube, where they act to regulate morphogenesis and differentiation [60, 61, 62,

63]. Further, in both the embryonic tooth and palate, Msx-1 has been shown to be necessary for expression of BMP-4 and/or BMP-2. Interestingly, exogenous BMP-4 or a mesenchymally expressed BMP-4 transgene are capable to rescue the tooth developmental arrest and CP, respectively, in Msx-1^{-/-} mice. Further elegant experiments 59 indicated that Msx-1 and BMP-4 function in an autoregulatory loop in regulating mesenchymal proliferation in the anterior palate. Nestin-Cre-mediated removal of type I BMP receptor (BMP-R1A; Alk-3) as well as BMP-4 activities demonstrated distinct functions for BMP signaling in lip fusion and secondary palate development in mice [64]. Ablation of BMP-R1A function in both the epithelium and mesenchyme of lip and palate primordia was found to generate bilateral cleft lip and palate. Altered cell proliferation and misexpression of Barx-1 and Pax-9 in the palate as well as precocious cell death in the fusing lip seem to be the cause of the clefting in the BMP-R1a mutants. In these, expression of other important factors such as Msx-1, Tbx-22 and Osr-2 is unchanged. However, conditional removal of BMP-4 activity resulted in isolated cleft lip. The latter phenotype seems at odds with the previously demonstrated important role for mesenchymal BMP-4 in the developing palate. Keratin 14-Cre-mediated targeted mutation of BMP-R1a, which inactivates this receptor in ectodermally derived tissues, including tooth, skin and palatal epithelia, has been shown to affect tooth and hair follicle development. However, the palate seems to develop normally in mutant mice. Altogether, these observations indicate that BMP-R1A functions primarily within the PS mesenchyme. Targeted inactivation of Osr-2 indicates a role for this transcription factor in medio-lateral patterning of the PS. In Osr-2^{-/-} mice, the proliferation defects in the PS mesenchyme and the delayed elevation of the PS seem to be independent of Msx-1, BMP, Shh and Tbx-22 inputs but may be linked to Pax-9 and Osr-1 function.

Other studies addressed the role of FGF signaling during early palate development by analyzing mouse embryos lacking the functions of FGF-10 and FGFR-2b [65]. In the FGF-10^{-/-} and FGFR-2b^{-/-} mutants, altered cell proliferation within both the PS mesenchyme and epithelium as well as increased apoptosis within the epithelium seem to be the primary causes of CP. Those studies also revealed an interesting epithelial-mesenchymal signaling loop. By signaling via its receptor FGFR-2b in the PS epithelium, the mesenchymally derived FGF-10 brings not only about epithelial proliferation and survival but also induces expression of Shh within the epithelium. Shh, in turn, signals to the mesenchyme and stimulates cell proliferation. In general, signaling activities are subject to tight spatio-temporal control and in many instances too much or too little of a good thing can be detrimental to a developing organ. This is well illustrated in anomalies caused by deregulated Hh and FGF signaling. While FGF-10/FGFR-2b activity plays a crucial role during palatogenesis, it appears to be subject to a tight spatio-temporal regulation as shown in mice lacking Shox-2. Shox-2^{-/-} mice develop a very rare type of palatal clefting that may also be found in humans and other

mammals the soft palate is intact, whereas the hard palate is cleft. Abnormal proliferation and apoptosis are likely at the core of the clefting. Surprisingly, a number of protagonists implicated in palatogenesis, including Msx-1, BMP-4, Pax-9, Lhx-8, Osr-2, TGF-β-3 and Jag-2, are found to be expressed normally. In contrast, FGF-10 and FGFR-2c were expressed at ectopic sites within the PS mesenchyme of the Shox-2^{-/-} mice. These studies re-emphasize the importance of a fine tuning of the timing and sites of signaling activities for normal development to take place. TGF-β peptides activate the membrane receptor serine/ threonine kinase quaternary complex made of two type II and two type I receptors. The type I TGF-β receptor Alk-5 has been shown to play a key role in craniofacial and palate development [66]. The craniofacial anomalies of Alk-5 mutants were more severe than those in corresponding mutants lacking the function of the TGF-β type II receptor (TGFβ-RII) in cranial neural crest derivatives [67]. Those striking differences have been suggested to be due to Alk-5 function in mediating signalings by ligands other than TGFβ1-3 and to the ability of Alk-5 to function with type II receptors other than TGF-βRII. In contrast to embryos lacking TGF-β2 in the PS mesenchyme, which displays reduced cell proliferation, the Alk-5-deficient PS mesenchyme seems to be hyperproliferative and to undergo massive apoptosis, again pointing to differences in the signaling functions of these two receptors. In humans, abnormally high TGF-β activity impinges upon palate formation as demonstrated in individuals bearing mutations in TGF-βR1 or TGF-βR2 [68]. These findings indicate that while signaling activities of type I and type II TGF-β receptors are crucial, the amplitude of such signals must be tightly controlled for normal palatogenesis. With the exception of the developing limb, organs consisting of an epithelium and a mesenchyme express the Hedgehog family members, Shh or Ihh, in the epithelial compartment, whereas targets and effectors of the Hedgehog pathway are found in both tissue layers, indicating Shh and Ihh activities at a distance from their sources. In the developing palate, Shh is produced in the PS epithelium, whereas its membrane receptor Patched-1 (Ptc-1) is present in both the epithelium and mesenchyme. The Hedgehog transcriptional effectors Gli1-3 are expressed in the PS mesenchyme but are present at low levels in the PS epithelium as well (AGL). Abrogation of Shh function in the palate epithelium generates CP. In contrast, epithelial loss of function of Smoothed (an obligatory and nonredundant component for all Hh signaling) does not generate CP, implying that the PS mesenchyme is the major target for Shh action. However, this does not exclude the possibility of an indirect action of Shh on the PS epithelium via Shh-induced mesenchymal inputs. Shh has been shown to act as a powerful mitogen in numerous developmental and neoplastic contexts. In vitro cultures show that Shh stimulates PS mesenchymal proliferation. Other in vitro studies have shown that Shh induces/ maintains BMP-2 expression, and that BMP-2 mediates Shh mitogenic effects on PS mesenchyme.

After vertical growth, the PS elevates into a horizontal position, and further extension allows contact between the

opposing PS. Some genetic disruptions affect this second phase of PS growth. For instance, mice lacking TGF- β 2 in the PS mesenchyme develop a CP due to reduced extension of the horizontal PS, and paracrine TGF- β 3 signaling in the PS mesenchyme seems to be required for this growth phase [69]. Similarly, embryos lacking platelet-derived growth factor-c (PDGF-C) activity show normal PS growth up to E13.5; however, after a delayed lifting, the hypoplastic PS are unable to about [70]. Loss of function of single minded-2 (Sim-2) in mice generates either a complete cleft of the secondary palate or a cleft of its posterior-most portion [71]. The complete cleft seems to be caused by lack of outgrowth of the PS which is, however, able to elevate. The PS of Sim-2 $^{-/-}$ mice are hypocellular between E14.5 and E16.5, and histochemical staining suggested the presence of abnormally high amounts of hyaluronan. This aspect is interesting in light of the known role of hyaluronan (hyaluronic acid), a major component of the extracellular matrix, in regulating cell proliferation, differentiation and migration.

Targeted gene ablation in mice identified several factors playing a determinant role in palate fusion. These include TGF- β 3 [72, 73], the forkhead domain-containing transcription factor Foxe-1, epidermal growth factor receptor EGFR and PDGF-C. Loss of function of these factors generates CP with no or minor other craniofacial anomalies. In vitro explant cultures showed that PS from TGF- β 3, EGFR and PDGF-C mutants fail to fuse owing to failure of the MES to degenerate. Importantly, studies in humans identified a mutation within the forkhead domain of FOXE-1 in siblings with thyroid agenesis, CP and choanal atresia and associated TGF- β 3 with nonsyndromic CP. Cell-cell junctional complexes are essential for cell survival, morphogenesis, proliferation and differentiation.

4.4. Molecular control of palatal shelf fusion

During the last few years, extensive efforts have been made to shed light upon the role of TGF- β 3 during palatal fusion. Adhesion of the MEE upon PS contact is a necessary step for fusion. TGF- β 3, which is expressed in the MEE before and during PS fusion, mediates MEE adhesion of the opposing PS through filopodia and chondroitin sulfate proteoglycans at the apical surface of MEE cells and to be necessary for apoptosis of the regressing MES. Importantly, in the absence of TGF- β 3 [74], MEE cells display altered distribution of E-cadherin, α - and β -catenins and impaired cell-cell adhesion. Early studies on fusion processes in different systems consistently show the presence of filopodia at the tip of fusing epithelial sheets. Thus, TGF- β 3 plays a crucial role during the different steps of MEE adhesion and fusion [75]. Other studies implicated TGF- β 3 in controlling the remodeling of the extracellular matrix through regulation of the expression of MMP-13, MP-2 and Tissue inhibitor of metalloproteinase-2. These studies indicate that TGF- β 3 signaling operates not only in the MEE, but is also involved in mediating epithelial mesenchymal interactions leading to tissue changes that regulate palatal fusion. The

effects of TGF- β 3 on MES regression seem to be mediated by the TGF- β type II and the TGF- β type I receptor (Alk-5)/Smad pathway as shown by loss and gain of function studies in vitro and in vivo.

[V] TRANSCRIPTION FACTOR IN MANDIBULAR MORPHOGENESIS

5.1. Msx genes

At early stages of development of mandible, the expression of Msx-1 and Msx-2 in the mandibular arch is limited to the mesenchyme in the medial region and is excluded from the mesenchyme in the lateral region [76, 77]. In addition to its expression in the medial region, Msx-1 is also expressed in the mesenchyme surrounding the hyomandibular cleft. Tissue recombination and bead implantation studies indicate that the expression of Msx genes in the developing mandible and other facial processes is dependent on signals derived from the overlying epithelium [78, 79, 80]. In the developing mandible at early stages, the expression of Msx-1 in the medial region is correlated with areas undergoing expansion which contain highly proliferative and undifferentiated mesenchyme cells. In Msx-1-deficient mice, the medial part of the mandible is truncated. Studies in the developing chick mandible also suggest that Msx genes may be involved in delineating the non-chondrogenic region at the midline region (symphysis).

This possibility is supported by observations that, in contrast to control explants, explants from chick mandibular arches treated with Msx-2 antisense oligonucleotides, formed cartilage in the medial region, resulting in the fusion of the 2 bilateral rods of cartilage at the midline. It is also shown that overexpression of Msx-2 also inhibits chondrogenesis in organocultured mouse mandibles [81]. Although lack of Msx-1 does not appear to disturb the mandibular symphysis, Msx-1/Msx-2 knock-outs display severe abnormalities in the developing mandible. In humans, mutation of one copy of Msx-1 results in single-tooth agenesis, and specific point mutations in the homeodomain in one copy of Msx-2 result in Boston-type craniosynostosis [82].

5.2. Dlx genes

Members of the Dlx family are expressed in the craniofacial region in both ectoderm and mesenchyme [83]. Among these, Dlx-2, Dlx-3, and Dlx-5 are expressed at the junction of the neural plate and surface ectoderm, suggesting that they may be expressed by pre-migratory and migratory CNCC cells [84, 85]. In situ hybridization studies on E9.5-E10 mouse embryos showed that Dlx-1 and Dlx-2 are expressed in the mesenchyme of both proximal and distal regions of all BAs, while Dlx-3, Dlx-5, and Dlx-6 are expressed predominantly in mesenchyme of the distal regions. For example, in the first branchial arch, Dlx-1 and Dlx-2 are expressed in the maxillary processes (the proximally located component) as well as in the mandibular

processes (the distally located component) and *Dlx-3*, *Dlx-5*, and *Dlx-6* are expressed only in the mandibular processes. In the developing mandible, *Dlx* genes are expressed in a lateral-to-medial gradient. Similarly, in the second (hyoid) arch, *Dlx-1* and *Dlx-2* are expressed throughout the proximo-distal axis, while *Dlx-3*, *Dlx-5*, and *Dlx-6* are expressed only in the more distal (close to the midline) region of the second arch. These patterns of expression suggested that *Dlx* genes play essential roles in proximo-distal patterning of the BAs. This possibility is supported by phenotypic abnormalities in mice lacking *Dlx-1*, *Dlx-2*, *Dlx-1/Dlx-2*, and *Dlx-5*. Mice lacking *Dlx-1*, *Dlx-2*, and *Dlx-1/Dlx-2* exhibited abnormalities similar, but not identical, to those of maxillary and proximal (caudal) hyoid arch derived structures. However, in these mutant mice, the skeletal components of the mandibular arch and distal hyoid arch appeared to be normal [86]. On the other hand, one of the most noticeable abnormalities in the mice homozygous for a targeted deletion of *Dlx-5* is in the developing mandible [87]. At early stages (E13-E14), the mandibular arch and the Meckel's cartilage of *Dlx-5* mutants are shorter than those in wild-type embryos and exhibit abnormalities in the caudal region of Meckel's cartilage.

At its caudal end, Meckel's cartilage in *Dlx-5* mutants is bifurcated and gives rise to an ectopic novel cartilage, which becomes surrounded by bone later in development. At birth, the mandibles of *Dlx-5* mutant mice are shortened, lack the coronoid process, and contain mis-shapen condylar and angular processes.

The phenotypic abnormalities in the mandibular arches of *Dlx-5* mutants suggest essential (non-redundant) roles of *Dlx-5* for proper development of mandibular processes and the skeleton of the caudal region of the mandibular arch. Analyses of the branchial arches in *Dlx-5* mutants indicate that the absence of *Dlx-5* did not affect cell proliferation or apoptosis but expanded the territory of the proliferating cells within the first branchial arch. In situ hybridization analysis indicated decreases of *Gsc* expression in the mesenchyme of the frontonasal processes and in the mandibular and hyoid mesenchyme of the *Dlx-5* mutants. Unlike other members of the *Dlx* family, *Dlx-5* and *Dlx-6* are also expressed in developing bones, cartilage, and teeth, suggesting that the *Dlx-5* and *Dlx-6* genes may play roles in the multi-step process of skeletal differentiation and/or morphogenesis [88,89]. *Dlx-5* is also expressed at specific stages of osteoblast differentiation in vitro and could repress osteocalcin gene expression [90]. Interestingly, lack of *Dlx-5* results in hypo-mineralization of calvaria and expression of osteocalcin in the periosteum at birth.

In humans, there is evidence implicating *Dlx-5* and *Dlx-6* genes as candidate genes for ectrodactyly (split hand/foot malformations, SHFM1). Often, these patients also have cleft palate and deafness. A frame-shift mutation in *Dlx-3* is also associated with taurodontism and enamel hypoplasia in humans with Tricho-dento-osseous syndrome [91].

5.3. Goosecoid (*Gsc* genes)

In vertebrates, *Gsc* is expressed transiently at the rostral end of the developing brain and then re-appears at E9.5-E10.5 in many sites, including the mesenchyme of the branchial arches [92]. In the mandibular arch, *Gsc* is strongly expressed in the mesenchyme in the region of the hyomandibular cleft. *Gsc* null mutants die soon after birth, with rib cage malformations and multiple craniofacial defects, including abnormalities in the mandibular arch and middle ear structures. In the mandibles of these mutants, although the condylar process appears normal, the coronoid and angular processes are severely reduced in size, and the mandible is shortened in length. Furthermore, Meckel's cartilage is not enclosed by the mandibular bones but is embedded in a novel groove that extends along the entire length of the mandible. Studies showed that abnormalities in the mandible of *Gsc* null mutants are due to the absence of cells destined to express *Gsc* in these mutants, suggesting the essential roles of *Gsc* in the initial proliferation and/or survival of *Gsc* expressing cells [93].

5.4. Pitx Genes

Pitx-1 (*Ptx-1* /*POTX*) and *Pitx-2* (*RIEG*, *Otx-2*, *Otlx-2*, *Brx-1*, *Arp-1*) are 2 members of a vertebrate multigene family with overlapping and distinctive patterns of expression during embryogenesis. *Pitx-1* was originally identified as a factor interacting with the pituitary-specific transcription factor *Pit-i* and *POMC* promoter. *Pitx-1* is expressed in the pituitary gland throughout its development, in the lateral plate mesoderm of the caudal half of the embryo which leads to its expression exclusively in the hindlimb and not the forelimb, in the first branchial arch as well as its derivatives, and in oral ectoderm. The patterns of expression suggest that *Pitx-1* is a critical transcription factor involved in specification of the hindlimb and development of the pituitary gland and structures derived from the first branchial arch. This possibility was supported by phenotypic abnormalities in null mutants for *Pitx-1* and mis-expression of *Pitx-1* in the chick wing bud. *Pitx-1* null mutants die immediately or shortly after birth and are readily recognizable by their shortened mandibular arch [95]. These mutants exhibit abnormalities in the limb and in the derivatives of the first BA, including cleft palate, significantly shortened tongue and mandible, a novel bone surrounding Meckel's cartilage, and lack of gonial bones. In situ hybridization analysis indicated that the expression of several markers expressed early in the first branchial arch-including *Msx-1*, *Msx-2*, *Gsc*, *Shh*, *BMP-2/4*, *Wnt-5a*, and *Pitx-2*-is unaltered in *Pitx-1* null mutant mice, suggesting that defects in the craniofacial structures similar to those observed in the hindlimb may be due to defects in proliferation and/or abnormal chondrogenesis of mesenchymal cells. Interestingly, it has been suggested that, in humans, mutant *Pitx-1* alleles might be responsible for a subset of patients with Treacher-Collins syndrome (other syndromes shown in table 2). *Pitx-2*/*RIEG* was initially identified by positional cloning of the gene responsible for Rieger Syndrome in humans. This

autosomal dominant haplo insufficiency syndrome is characterized by anterior chamber ocular abnormalities and other features of various degrees of severity, including dental hypodontia, umbilical abnormalities, cardiac defects, and mild craniofacial dysmorphism. Pitx-2 is expressed in many tissues during development, including the craniofacial mesenchyme and epithelium of the first and second branchial arches. Experimental evidence indicated a role for Pitx-2 downstream of sonic hedgehog and nodal in a genetic pathway regulating laterality of heart, gut, and other asymmetric organs. The direct role of Pitx-2 in left-right determination and development of other structures, including the development of the mandibular processes [76], is provided by abnormalities in mice deficient for Pitx-2. Pitx-2 mutant mice die at around E14-15 and exhibit lung isomerization and defects in cardiac positioning and pituitary development. In addition, Pitx-2 null mutants exhibited cleft palate and abnormalities in the maxillary and mandibular arches, including severely hypoplastic mandible and arrested tooth buds. In situ hybridization analysis indicated the absence of FGF-8 and altered domains of expression of BMP-4, Msx-1, and Msx-2 in the developing facial processes in Pitx-2 null mutants, suggesting that the facial abnormalities may be mediated by changes in the patterns of expression of these genes.

5.5. Pax genes

Pax genes encode a family of transcription factors characterized by an evolutionary conserved paired box domain, a 384-bp DNA binding motif that regulates embryonic development by the control of target genes. In mammals, the Pax gene family consists of 9 members that, based on the presence or absence of structural motifs, are divided into 4 subgroups. The function and role of Pax genes in embryonic development have been elucidated by analysis of naturally occurring mouse mutants, targeted inactivation of several Pax genes in mice, and human syndromes. A common feature of all Pax mutants is reduction in size and malformation or loss of specific organs [96]. Among all Pax genes, members of group I (Pax-1, Pax-9), group III (Pax-3, Pax-7), and group IV (Pax-6) are expressed in the developing facial processes. Analyses of various mutants have indicated essential roles for Pax-3, Pax-6, and Pax-7 in the development of CNCC-derived structures in the upper face. However, in these mutants, no abnormalities were observed in CNCC-derived structures of the lower face [76]. On the other hand, phenotypic abnormalities in the Pax-9 null mutant indicate essential roles for Pax-9 for the lower face. Pax-9-deficient mice lacked structures derived from pharyngeal pouches, such as thymus and parathyroid glands. In the developing mandible, in addition to abnormalities in the developing teeth, the alveolar ridge and the coronoid process are absent in Pax-9 null mutants.

5.6. Prx genes

Prx-1 (previously called Mhox) and Prx-2 (previously called

S8) are closely related members of the paired-related family of homeobox genes that are co-expressed in a variety of sites, including the craniofacial mesenchyme. Studies in developing mice and chickens indicate that Prx-1 and Prx-2 are co-expressed in the CNCC-derived mesenchyme of the frontonasal process, in the mesenchyme of the first and second branchial arches, and in the pre-osteogenic areas [97]. In the developing mandible, at early stages of development, high levels of expression of both genes are detected in the mesenchyme of the medial region. In addition to the medial region, Prx-1 is also expressed in the cells around the first branchial groove. As development proceeds, the expression of both genes is downregulated in the mandibular process but maintained in the maxillary and nasal processes.

Although Prx-2 null mutant mice show no obvious craniofacial and skeletal abnormalities, Prx-1 null mutant mice show defects in skeletal elements derived from the maxillary processes and the caudal part of the mandibular processes, including hypoplastic coronoid, condylar, and angular processes and malformed malleus. In addition, Meckel's cartilage in Prx-1 mutants displayed abnormal sigmoidal morphology. Studies indicate that, in the Prx-1 null mutants, cells fated to express Prx-1 are initially present in the regions that give rise to the defective structures, but disappear later, suggesting that Prx-1 product may be required for the maintenance (proliferation and/or survival) of specific subpopulations of CNCC-derived mesenchymal cells in the branchial arches. In contrast to single mutants, Prx-1/Prx-2 double-knock-out mice exhibited severe craniofacial abnormalities, including pointed snout, the absence of external ears, and severely shortened lower jaws. Double-mutant mice also had novel phenotypes, including abnormalities in the medial region of the developing mandibles, lower incisors, and Meckel's cartilage. Approximately 8% of the newborn double-mutants generated exhibited clefts in the mandible and tongue, whereas the mandibular processes of the double-mutant mice generated lacked the midline symphysis and were fused. In these double-mutants, either a single incisor arrested in the bud stage or no incisors were present. The arrested incisor tooth buds showed decreases in the expression of Pax-9 and patched. Furthermore, in these doublemutants, most of Meckel's cartilage was absent. The phenotypic abnormalities in Prx-1 and Prx-1/Prx-2 mutants indicate redundant but essential roles for Prx-1 and Prx-2 in the signaling network regulating epithelial-mesenchymal interactions that promote outgrowth and skeletogenesis in the mandible. Other members of the paired-related family of homeobox genes in vertebrates include Alx-3, Alx-4, and Cart-1. These genes are also expressed in the distal part of the mandibular arch. However, no phenotypic abnormalities in the developing mandible have been reported in mice lacking these genes. It is possible that, similar to Prx-1 and Prx-2, the absence of abnormalities in the mandibular arch in these knock-outs may be due to functional redundancies.

5.7. Barx genes

Barx-1 and Barx-2 are members of the vertebrate Bar class of homeobox-containing genes homologous to *Drosophila* BarH-1 and BarH-2. Three mouse and two chick homologues of the Barx genes have been isolated. Tissue distribution studies showed that these genes are expressed in many sites, including the facial processes. Studies in developing mice showed that, in the developing maxilla and mandible, Barx-1 is expressed in the mesenchyme, and Barx-2 is expressed in the overlying epithelium [98].

However, studies in chick embryos indicate that, unlike in the mouse, Barx-1 is expressed in both epithelium and mesenchyme of the maxillary and mandibular processes. Furthermore, in chick embryos, Barx-2b-which is 80% and 61% identical to mouse Barx-2 and Barx-1, respectively-is expressed prominently in myogenic populations in the craniofacial region, in the mesoderm of the BA, and in areas of the forming bones. During embryogenesis, Barx-2b is expressed at the tips of the outgrowing maxilla and mandible but disappears by stage 30. In both the chick and mouse, the mesenchymal domain of Barx-1 expression is restricted to the lateral region, where FGF-8 is expressed by the overlying epithelium. The expression of Barx-1 is excluded from the mesenchyme in the medial region in which BMP-4 is expressed in the overlying epithelium. The expression of Barx-1 is also excluded from the central core corresponding to the regions forming Meckel's cartilage and the muscle of the mandibular process.

These patterns of expression suggest the involvement of signals derived from the overlying epithelium (FGF-8/BMP-4) in regulating the spatial patterns of Barx-1 expression in the mandibular mesenchyme. In fact, studies in mouse mandibles indicate that beads soaked in FGF-8 can induce/maintain expression of Barx-1 in the lateral mandibular mesenchyme. On the other hand, beads soaked in BMP-4 inhibited expression of Barx-1 in the lateral mandibular mesenchyme expression. Inhibition of BMP-4 signaling by application of Noggin protein during the early stages of mandibular development resulted in ectopic expression of Barx-1 in the mesenchyme in the medial region. Similar antagonistic interactions between BMP and FGF signaling also restrict expression of Barx-1 to the maxillary mesenchyme in the posterior region, suggestive of the involvement of Barx-1 in patterning of the facial processes.

5.8. HAND genes

dHAND and eHAND, 2 members of the bHLH (basic helixloop- helix) family of transcription factors, are co-expressed in many regions, including the medial region of the developing mandible. Deletion of the dHAND gene in mice resulted in embryonic death at E11 secondary to cardiac failure and many abnormalities, including severely hypoplastic first and second BAs. Molecular analyses indicated that although

Prx-1, Dlx-2, eHand, and Msx-2 are expressed at normal levels, Msx-1 expression is not detectable in the medial region of the developing mandible of E9.5 dHAND null mutants.

Studies indicate that the hypoplastic mandible in the dHand-/- mutant is not due to defects in the migration of neural crest cells into the branchial arch and occurs secondary to programmed cell death. The unchanged patterns of expression of eHAND in the dHAND mutant suggest that eHAND is unable to compensate fully for dHAND in the branchial arch and that these genes may have some unique roles in the development of the developing mandible [99].

[VI] CONCLUSION

Considering the embryogenesis of craniofacial form, development is genetically determined through neural crest cell migration and through the expression of homeobox gene information. Epithelial-mesenchymal interaction during the process of craniofacial patterning, induction and programmed cell death is mediated by regulatory molecules and growth factor super families controlled by gene expression. So role of genes in craniofacial development is immense and further studies in future may suggest more specific genes. The practical application of this knowledge in the diagnosis and treatment planning will be beneficial. With further advancement in genetic engineering genetic treatment planning of craniofacial defects cannot be ruled out.

FINANCIAL DISCLOSURE

No financial assistance was received for this work.

CONFLICT OF INTERESTS

Authors declare no conflict of interests.

REFERENCES

- [1] Patil AS, Sable RB, Kothari RM. Occurrence, biochemical profile of vascular endothelial growth factor (VEGF) isoforms and their functions in endochondral ossification. *J Cell Physiol* (In Press).
- [2] Patil AS, Sable RB, Kothari RM. Role of Insulin-like growth factors (IGFs), their receptors and genetic regulation in the chondrogenesis and growth of the mandibular condylar cartilage. *J Cell Physiol* (In Press).
- [3] Jorley LB, Cary JC, Bamshad MJ, White RL. [2003] Medical Genetics. 3rd ed. St Louis (Missouri): *Mosby*: p. 4.
- [4] Grapha PA, Koentges G, Cumsden A. [1996] Neural crest apoptosis and the establishment of craniofacial pattern: an honorable death. *Mol Cell Neurosci* 8:76–83.
- [5] Nicholas DH. [1986] Neural crest formation in head of the mouse as observed using new histologic technique. *J Embryol Exp Morphol* 98: 21–58.
- [6] Tann SS, Morris-Kay GM. [1986] Analysis of cranial neural crest cell migration and early fates in postimplantation rat chimaeras. *J Embryol Exp Morphol* 98: 21–58.

- [7] Hunt P, Clarke JD, Buxton P, Ferretti P, Thorogood P. [1998] Segmentation, crest prespecification and the control of facial form. *Eur J Oral Sci* 106: 12–18.
- [8] Trianor PA, Ariza-Mc Naughton L, Krumlauf R. [2002] Role of the isthmus and FGFs in resolving the paradox of neural crest plasticity and pre-patterning. *Science* 295:1288–1291.
- [9] Rijli FM, Mark M, Lakkaraju S, Dierich A, Dolle P, Chambon P. [1993] A homeotic transformation is generated in the rostral branchial region of the head by disruption of Hox-a-2, which acts as a selector genes. *Cell* 75:1333–1349.
- [10] Bronner-Fraser M. [1995] Patterning of the vertebrate neural crest. *Perspect Dev Neurobiol* 3:53–62.
- [11] Sharpe PT. [1995] Homeobox genes and orofacial development. *Connect Tissue Res* 32:17–25.
- [12] Diwert VM, Shiota K. [1990] Morphological observations in normal primary palate and cleft lip embryos in the Kyoto collection. *Teratology* 41:663–677.
- [13] Wang KY, Juriloff DM, Diwert VM. [1995] Deficient and delayed primary palatal fusion and mesenchymal bridge formation in the cleft lip- liable strains of mice. *J Craniofac Genet Dev Biol* 15: 99–116.
- [14] Alappat S, Zang Z, Chen P. [2003] Msx homeobox gene family and craniofacial development. *Cell Res* 13(6):429–442.
- [15] Gammil LS, Bronner-Fraser M. [2003] Neural crest specification: Migration into genomics. *Nat Rev Neurosci* 4:795–805.
- [16] Depew MJ, Tucker AS, Sharpe PT. [2002] In mouse development, patterning, morphogenesis and organogenesis. *Craniofacial Development* 46:421–498.
- [17] Echard Y, Vassileva G, McMohan AP. [1994] Cis acting regulatory sequences governing Wnt-1 expression in the developing mouse CNS. *Development* 120:2213–2224.
- [18] McMahon AP, Ingham PW, Tabin CJ. [2003] Developmental roles and clinical significance of hedgehog signaling. *Curr Top Dev Biol* 53:1–114.
- [19] Goodrich LV, Johnson RL, Milenkovic L, McMahon JA Scott MP. Conservation of hedgehog/patched signaling pathway from flies to mice: induction of mouse patched gene by hedgehog. *Genes Dev* 1996; 10: 301–312.
- [20] Wang T, Tamakoshi T, Vezato T, Shu F, Fu NY, Koseki H, et al., [2003] Forkhead transcription factor Fox-F-2(LUN) deficient mice exhibit abnormal development of secondary palate. *Dev Biol* 259:83–94.
- [21] Jeong J, Mao J, Tenzen T. [2004] Hedgehog signaling in the neural crest cells regulates the patterning and growth of facial primordium. *Genes Dev* 18:937–951.
- [22] Takashi Ohyama and Andrew k. Grover. [2004] Expression of mouse Foxi genes in early craniofacial development. *Development dynamics* 231:640–646
- [23] Raymond P, Rajan L, Xui Li. [2002] The Dlx-5 and Dlx-6 homeobox genes are essential for craniofacial, axial and appendicular skeletal development. *Genes Dev* 16:1089–1101.
- [24] Davidson D. [1995] The function and evolution of Msx genes: pointers and paradoxes. *Trends Genet* 11:407–410.
- [25] Mooney MP, Siegel MI. [2002] Understanding craniofacial anomalies. The etiopathogenesis of craniosynostoses and facial clefting. New York: *Wiley-liss*. p.532–579.
- [26] Hill RE, Jones PF, Rees AR. [1989] A new family of mouse homeobox containing molecular structure, chromosomal location and developmental expression of Hox-7. *Gene Dev* 3:26–37.
- [27] Akimenko MA, Johnson SL, Westerfield M, Ekker M. [1995] Differential induction of four Msx homeobox genes during fin development and regeneration in zebra fish. *Development* 121:347–357.
- [28] Suzuki HR, Padanilam BJ, Vitale E, Ramiriz F, Solursh M. [1991] Repeating development expression of G-Hox-7, a novel homeobox containing gene in the chicken. *Dev Biol* 148:375–388.
- [29] Takahashi Y, Le Doualin N. [1990] CDNA cloning of quail homeobox gene and expression in neural crest derived mesenchyme and lateral palate mesoderm. *Proc Natl Acad Sci* 87:7482–7488.
- [30] Shimeld SM, McKay JJ, Sharpe PT. [1996] The murine homeobox gene Msx-3 shows highly restricted expression in the developing neural tube. *Mech Dev* 55:201–210.
- [31] Carton KM, Iler N, Abate C. [1993] Nucleotides flanking a conserved TAAT core dictate the DNA binding specificity of the murine homeodomain protein. *Mol Cell Biol* 13:2354–2365.
- [32] Bendare AS, Abate C. [2000] Roles for Msx and Dlx homeoprotein in vertebrate development. *Gene* 247:17–31.
- [33] Semenza GL, Wang GL, Kundu R. [1995] DNA binding and transcriptional properties of wild type and mutant forms of homeodomain protein Msx-2. *Biochem Biophys Res Commun* 209:257–262.
- [34] Zang H, Hu G, Wang H. [1997] Heterodimerization of Msx and Dlx homeoprotein results in functional antagonism. *Mol Cell Biol* 17:2920–2932.
- [35] Zang Z, Sang Y, Zhao X, Fermin C, Chen Y. [2002] Rescue of cleft palate in Msx-1 deficient mice by transgenic BMP-4 reveals network of BMP and Shh signaling in regulation of mammalian palatogenesis. *Development* 129:4135–4146.
- [36] Alappat S, Zang ZY, Chen YP. [2003] Msx homeobox gene family and craniofacial development. *Cell Research* 13:429–442.
- [37] Burlglin TR. [1994] A comprehensive classification of homeobox genes. In guide book to homeobox genes. *Sambrook and Tooze publications*. p. 457–69.
- [38] Taira M, Otani H, Jamrich M, Dawid IB. [1994] Expression of the LIM class homeobox genes Xlim-1 in pronephrons and CNS cell lineages of *Xenopus* embryos is affected by retinoic acid and exogastrulation. *Development* 120:1525–1536.
- [39] Vogel A, Rodriguez C, Warnken W, Izpissua Belmonte JC. [1995] Dorsal cell fate specified by chick Lmx-1 during vertebrate limb development. *Nature* 378:716–720.
- [40] Liu YH, Kundu R, Wu L, Luo W, Ignelzi MA Jr, Snead ML. [1995] Premature suture closure and ectopic cranial base in mice expression Msx-2 transgenes in developing skull. *Proc Natl Acad Sci* 92:6137–6141.
- [41] Stone DM. [1996] The tumor suppressor gene patched encodes a candidate receptor for sonic hedgehog. *Nature* 80:129–134.
- [42] Bally Cuif L, Boncinelli E. [1997] Transcription factors and head formation in vertebrates. *Bioessays* 19:127–135.
- [43] Tomlinson A, Strapps WR, Heemskark J. [1997] Linking Frizzled and Wnt signaling in dorsophilia development. *Development* 124:4515–4521.
- [44] Zang J, Carthew RW. [1998] Interaction between wingless and DFZ-2 during dorsophilia wing development. *Development* 125:3075–3085.
- [45] Cadigan KM, Nusse R. [1997] Wnt signaling: a common theme in animal development. *Genes Dev* 11:3286–3305.
- [46] Wodarz A, Nusse R. [1998] Mechanics of Wnt signaling in development. *Annu Rev Cell Dev* 14:59–88.

- [47] Sarkar L, Sharpe PT. [1999] Expression of Wnt signaling pathway genes during tooth development. *Mech Dev* 85:197–200.
- [48] Yamaguchi TP, Bradley A, McMohan AP, Jones S. [1999] A Wnt-5a pathway underlies outgrowth of multiple structures in vertebrate embryo. *Development* 126:1211–1223.
- [49] Barlow AJ, Bogardi JP, Ladher R, Francis West PH, Gibbs S. [1999] Expression of chick Barx-1 and its differential regulation by FGF-8 and BMP signaling in the maxillary primordium. *Dev Dyn* 214:291–302.
- [50] Shigetani Y, Nobusada Y, Kuratani S. [2000] Ectodermally derived FGF-8 defines the maxillomandibular region in the early chick embryo: epithelial mesenchymal interaction in the specification of craniofacial ecto mesenchyme. *Dev Biol* 228:73–85.
- [51] Nakata K, Nagai T, Aruqa J, Mikoshiba K. [1999] Xenopus Zic-3 a primary regulator both in neural and neural crest development. *Proc Natl Acad Sci* 94:11980–11985.
- [52] Nagai T, Aruqa J, Takada S. [1997] The expression of the mouse Zic-1, Zic-2 and Zic-3 suggest an essential role of Zic gene in body pattern formation. *Dev Biol* 182:299–313.
- [53] Purundare SM, Ware SM, Kwan KM. [2002] A complex syndrome of left-right axis, central nervous system and axial skeleton defects in Zic-3 mutant mice. *Development* 129:2293–2302.
- [54] Pevny LH, Sockanathan S, Placzek M, Lovell-Badge R. [1998] A role of Sox-1 in neural determination. *Development* 125:1967–1978.
- [55] Bach I. [2000] The LIM domain: regulation by association. *Mec Dev* 91:5–17.
- [56] Zhao Y, Guo YJ, Tomac AC, Taylor NR, Grinberg A, Lee EJ, et al. [1999] Isolated cleft palate in mice with targeted mutation of the LIM homeobox gene Lhx-8. *Proc Natl Acad Sci* 96:15002–15006.
- [57] Tyler MS, Koch WE. [1997] In vitro development of palatal tissue from embryonic mice II. Tissue isolation and recombination studies. *J Embryol Exp Morphol* 38:37–48.
- [58] Ferguson MWJ, Honig LS. [1984] Epithelial mesenchymal interactions during vertebrate pathogenesis. *Curr Top Dev Biol* 19:138–164.
- [59] Satokasa I, Maas R. [1994] Msx-1 deficient mice exhibit cleft palate and abnormalities of craniofacial and tooth development. *Nat Genet* 6:348–356.
- [60] Yu L, Allapat S, Song S, Yan Y, Zang M, et al. [2005] Sox-2 deficient mice exhibit a rare type of incomplete clefting of secondary palate. *Development* 132:4393–4408.
- [61] Zang Z, Song Y, Zhao X, Zhang X, Fermin C, Chen YP. [2002] Rescue of cleft palate in Msx-1 deficient mice by transgenic BMP and reveals a network of BMP and Shh signaling in the regulation of mammalian pathogenesis. *Development* 129:4135–4146.
- [62] Vainio S, Karavanova I, Jowett A, Thesleff I. [1993] Identification of BMP for a signal mediating between epithelial and mesenchymal tissue during early tooth development. *Cell* 75:45–58.
- [63] Kim HJ, Rice DP, Kettunen PJ, Theseleff I. [1998] FGF, BMP and Shh mediated signaling pathways in the regulation of cranial suture morphogenesis and calvarial bone development. *Development* 125:1241–1251.
- [64] Kulesa H, Turk G, Hogan BLM. [2000] Inhibition of BMP signaling affects growth and differentiation in the anagen hair follicle. *Embo J* 19:6664–6674.
- [65] Ramos C, Robert B. [2005] MSH/MSx gene family in neural development. *Trends Genet* 21:624–632.
- [66] Liu W, Sun X, Brant A, Mishina Y, Behringer RR, Mina M, et al. [2005] Distinct functions for BMP signaling in lip and palate fusion in mice. *Development* 132:1453–1461.
- [67] Rice R, Spencer-Dene B, Connor EC, Gritli Linde A, McMahon AP, Dickson C. [2004] Disruption of FGF-10/FGF-R-2-b-coordinated epithelial mesenchymal interactions causes cleft palate. *J Clin Invest* 113:1692–1700.
- [68] Dudas M, Nagy A, Laping NJ, Moustakers A, Kaartinen V. [2004] TGF-β3 induced palatal fusion is mediated by Alk-5/smad pathway. *Dev Biol* 266:96–108.
- [69] Ito Y, Chytil A, Han J, Bringas P, Nakajima A, Shaler CP, et al. [2003] Conditional inactivation of TGFB-R-2 in cranial neural crest causes cleft palate and calvarial defects. *Development* 130:5269–5280.
- [70] Loeys BL, Chen J, Neptune ER, Judge DP, Podowski M, Holm T, et al. [2005] A syndrome of altered cardiovascular, craniofacial, neurocognitive and skeletal development caused by mutation in TGFB-R-1 or TGFB-R-2. *Nat Genet* 37:275–281.
- [71] Xu X, Han J, Yoshihiro I, Bringas JR, Urata MM, Chai Y. [2006] Cell autonomous requirement of TGFB-R-2 in the disappearance of medial edge epithelium during palatal fusion. *Dev Biol* 102:1223–1229.
- [72] Ding H, Wu X, Brstrom H, Kim I, Wong N, et al. [2004] A specific requirement for PDGF-c in palate formation and PGDFR-α signalling. *Nat Genet* 36:1111–1116.
- [73] Shambloot MJ, Bugg EM, Lawler AM, Gearhart JD. [2002] Craniofacial abnormalities resulting from targeted disruption of the murine sim-2 gene. *Dev Dyn* 224:373–380.
- [74] Patil AS, Sable RB, Kothari RM. 2011. An update on transforming growth factor-β (TGF-β): Sources, types, functions and clinical applicability for cartilage/bone healing. *J Cell Physiol* 226:3094–3103.
- [75] Kaartinen V, Cui XM, Heisterkamp N, Groffer J, Schuller CF. [1997] Transforming growth factor-β3 regulators transdifferentiation of medial edge epithelium during palatal fusion and associated degradation of basement membrane. *Development Dynamics* 209:255–260.
- [76] Proetzel G, Pawlowski SA, Wiles MV, Yin M, Biovin GP, Howles PN. [1995] Transforming growth factor-β3 required for secondary palatal fusion. *Nat Genet* 11:409–414.
- [77] MacKenzi A, Ferguson MW, Sharpe PT. [1992] Expression patterns of the homeobox gene, Hox-8 in mouse embryo suggests a role in specifying tooth initiation and shape. *Development* 115:403–420.
- [78] Nishikawa K, Nakanishi T, Aolci C, Hattori T, Takahashi K, Taniguchi S. [1994] Differential expression of homeobox containing genes Msx-1 and Msx-2 gene expression during chick craniofacial development. *Biochem Mol Biol Int* 32:763–771.
- [79] Mina M, Gluhak J, Upholt WB, Kollar EJ, Rogers B. [1995] Experimental analysis of Msx-1 and Msx-2 gene expression during chick mandibular morphogenesis. *Dev Dyn* 202:195–214.
- [80] Mina M. Regulation of mandibular growth and morphogenesis. [2001] *Crit Rev Oral Biol Med* 12(4) 276–300.
- [81] Brown JM, Wedden SE, Millburn GH, Robson LG, Hill RE, Davidson DR. [1993] Experimental analysis of the control of expression of the homeobox gene Msx-1 in the developing limb and face. *Development* 119:41–48.

- [82] Bei M, Maas R. [1997] FGFs and BMP-4 induced both Msx-1 independent and Msx-1 dependent signaling pathways in early tooth development. *Development* 125:4325–4333.
- [83] Semba I, Nonaka K, Takahashi I, Takahashi K, Dashnu R, Shum L. [2000] Positionally dependent condrogenesis induced by BMP-4 is co-regulated by Sox-9 and Msx-2. *Dev Dyn* 217:401–414.
- [84] Cohen Jr MM. [2000] Craniofacial disorders causes by mutation in Homeobox genes Msx-1 and Msx-2. *J Craniofac Genet Dev Biol* 20:19–25.
- [85] Davidue JL, Demri P, Gu TT, Simmons D, Nessman C, Forest N. [1999] Expression of Dlx-5 during human embryonic craniofacial development. *Mech Dev* 81:183–186.
- [86] Robinson GW, Mahon KA. [1994] Differential and overlapping expression domains of Dlx-2 and Dlx-3 suggests distinct role of distal-less homeobox genes in craniofacial development. *Mech Dev* 48:199–215.
- [87] Qui M, Bukfane A, Ghattas I, Meneses JJ, Chirsten L, Sharpe PT. [1997] Role of Dlx homeobox gene in proximodistal patterning of the branchial arches: mutation of Dlx-1 and Dlx-2 altered morphogenesis of proximal skeleton and soft tissue structures derived from the first and second arches. *Dev Biol* 185:165–184.
- [88] Thomas BL, Tucker AS, Qui M, Ferguson CA, Hardcastle Z, Rubenstine JL. [1997] Role of Dlx-1 and Dlx-2 in patterning of the murine dentition. *Development* 124:48811–48818.
- [89] Acampora D, Mazon S, Lalumand Y, Avantaggiato V, Maury M, Simeone A. [1995] Forebrain and midbrain regions and deleted in Otx-2^{-/-} mutants due to a defective anterior neuroectoderm specification during gastrulation. *Development* 121:3279–3790.
- [90] Zhao GQ, Zhao S, Zhou X, Eberspaechhu H, Solursh M, Crombrughe B. [1994] RDlx-1 a novel distal-less like homeoprotein is expressed in cartilages and discrete neuronal tissues. *Dev Biol* 164:37–51.
- [91] Ferrari D, Sumoy L, Gannons J, Sun H, Brown AM, Upholt WB. [1995] The expression pattern of distal-less homeobox containing genes Dlx-5 in the developing chick limb bud suggest it involvement in apical ectoderm ridge activity, pattern formation and cartilage differentiation. *Mech Dev* 52:257–264.
- [92] Ryoo HM, Hoffman HM, Beumer T, Frenker B, Towler DA, Stains GS. [1997] Stage specific expression of Dlx-5 during osteoblast differentiation: involvement in regulation of osteocalcin gene expression. *Mol Endocrinolo* 11:1681–1694.
- [93] Gaunt SJ, Blum M, De Robertis EM. [1993] Expression of the mouse gooseoid gene during mid embryogenesis may mark mesenchymal cell lineages in the developing head, limbs and body wall. *Development* 117:769–778.
- [94] Yamada G, Mansouri A, Torres M, Stuart ET, Blum M, Schultz M. [1995] Targeted mutation of the murine gooseoid gene results in craniofacial defects and neonatal death. *Development* 121:2917–2922.
- [95] Lanctot C, Lamolet B, Drouin J. [1997] The bicoid-related homeoprotein Ptx-1 defines the most anterior domain of the embryo and differentiate posterior from anterior lateral mesoderm. *Development* 124:2807–2817.
- [96] Dahl E, Koseki H, Balling R. [1997] Pax genes and embryogenesis. *Bioessays* 19:755–765.
- [97] Meijlink F, Beverdam A, Brouwer A, Oosterveen TL, Berge DT. [1999] Vertebrate airstaless-related genes. *Int J Dev Biol* 43:651–663.
- [98] Smith DM, Tabin CJ. [1999] Chick Barx2b, a marker for myogenic cells also expressed in branchial arches and neural structures. *Mech Dev* 80:203–206.
- [99] Thomas T, Kurihara H, Yamagishi H, Kurihara Y, Yazaki Y, et al. [1998] A signaling cascade involving endothelin-1, dHAND and Msx1 regulates development of neural-crest-derived branchial arch mesenchyme. *Development* 125:3005–3014.

ABOUT AUTHORS



Dr. Amol Patil (MDS, Ph.D.) Associate Professor, Dept. of Orthodontics and Dentofacial Orthopedics, Bharati Vidyapeeth Dental College and Hospital, Bharati Vidyapeeth Deemed University, Pune, Maharashtra, India.



Dr. Rahul Doshi, Postgraduate student, Dept. of Orthodontics and Dentofacial Orthopedics, Bharati Vidyapeeth Dental College and Hospital, Bharati Vidyapeeth Deemed University, Pune, Maharashtra, India.

EVIDENCES OF INTERACTION BETWEEN PANCREAS, HEART AND SPLEEN IN THE PATHOGENESIS OF COXSACKIEVIRUS CARDIOMYOPATHY

Minghui Li, Yeqing Xie, Xinggang Wang, Yunzeng Zou, Junbo Ge, Ruizhen Chen*

Key Laboratory of Viral Heart Diseases, Ministry of Public Health, Shanghai Institute of Cardiovascular Diseases, Zhongshan Hospital, Fudan University, Shanghai-200032, CHINA

ABSTRACT

Pathogenesis of coxsackievirus cardiomyopathy has not yet been clarified. Evidences from clinical practices and laboratory researches have hinted a pathologic association among organs of pancreas, spleen and heart, underlying a probable new pathogenesis. We summarized these evidences here and proposed the probable mechanism, which might bring about some changes to the diagnosis and treatment of viral cardiomyopathy.

Received on: 1st-Feb-2012

Revised on: 16th-Feb-2012

Accepted on: 22nd-Feb-2012

Published on: 10th-Apr-2012

KEY WORDS

coxsackievirus, pathogenesis, cardiomyopathy, pancreas, spleen

*Corresponding author: Email: chen.ruizhen@zs-hospital.sh; Tel: 86-21-64041990 ext. 2104; Fax: 86-21-64223006

[I] INTRODUCTION

Cardiomyopathy is a major cause of sudden unexpected death in young patients, it contributes significantly to the societal burden of heart failure. Now significant evidences from animal models and clinical studies suggests that viral myocarditis is important in the etiology of dilated cardiomyopathy. Enterovirus, and especially Coxsackieviruses of group B (CVB), is the most common infectious agent [1, 2].

Enteroviruses (family Picornaviridae) are nonenveloped icosahedral viruses that contain a single plus-strand RNA genome of about 7,500bp. The CVB are typical enteroviruses and 5' end of the genome is not capped but is linked covalently to the viral protein, VPg. The virus receptor, human coxsackievirus and adenovirus receptor (CAR), a protein of the immunoglobulin superfamily [3-5], most likely interacts with virus capsid in the depression that surrounds the 5-fold axes of symmetry.

In clinical, progression of coxsackievirus myocarditis to dilated cardiomyopathy has always been a deteriorating outcome which usually resorts to heart transplant [1]. Pathogenesis of coxsackievirus cardiomyopathy hasn't yet been clarified and the diagnosis is conventionally based on clinical presentations [2]. Although endomyocardium biopsy (EMB) evidences have been the gold standard, this Dallas criteria has been questioned in practice [6, 7]. New pathogenesis viewpoint may help in diagnosis and treatment of

the disease. Based on current evidences of a pathologic association between pancreas, spleen and heart, such a viewpoint is proposed as a hypothesis in this review.

[II] COEXISTENCE OF PANCREAS DISEASES AND MYOCARDIAL INJURY IN CLINICAL PRACTICE

The phenomenon of myocardial injury accompanying pancreas diseases has been noticed for a long time in clinical practice. A wide spectrum of the related pancreas diseases have been mentioned including cystic fibrosis [8], pancreas carcinoma [9] and acute pancreatitis caused by toxic substances [10]. A large sample autopsy in children covering 2,000 cases carried out by Nezelof C et al. [11] found that children's pancreatic diseases were usually associated with multifocal myocardial necrosis and fibrosis, in which the pancreatic diseases include cystic fibrosis, pancreatic lipomatosis and extensive small bowel resection.

Pancreas injuries resulting from various reasons usually accompany heart inflammation. This is also the case with regard to coxsackievirus cardiomyopathy.

[III] EXISTENCE OF A PATHOLOGIC ASSOCIATION BETWEEN PANCREAS AND HEART WITH REGARD TO COXSACKIEVIRUS

INFECTION

Among the various causative agents of cardiomyopathy, enterovirus infection, especially coxsackievirus infection is the most common reason [2]. Coincidentally, coxsackievirus infection of the heart is often accompanied by pancreas infection. In 1998, an outbreak of enterovirus 71 infection was evoked in Taiwan, a comprehensive study on death cases revealed that hearts and pancreas suffered infection at the same time [12]. A case report of neonate death in Germany in 2006 was attributed eventually to enterovirus myocarditis complicated by pancreatitis [13]. Early in the 1970's, it has been found that coxsackievirus infection could lead to myocarditis and necrosis of the endocrine part of pancreas causing the simultaneous secondary diabetes [14]. An autopsy research [15] found that enterovirus infection, while causing the onset of myocarditis, almost simultaneously led to the inflammation of pancreas. These evidences are all implying a correlation between pancreas diseases and myocardium injury in the background of virus infection.

Such a correlation was also observed in animals. Gómez RM et al. [16] infected Balb/c mouse with coxsackievirus B3 and 1 week post infection all mouse were found pancreas glandular duct inflammation and focal myocarditis. Such organ injuries were restricted in pancreas and heart selectively and was absent in other organs like liver etc. This "targeted-organ-injury" property of coxsackievirus was attributed to at least one important cell structure component- coxsackie and adenovirus receptor (CAR) [17, 18]. After the depletion of CAR from pancreas and heart, coxsackievirus titers decreased significantly both in vitro and in vivo and the related organs injury ameliorated as well [19]. Besides coxsackievirus, another myocarditis-causing agent encephalomyocarditis virus (EMV) could also injury pancreas and lead to the secondary diabetes [20].

Mouse infected with fatal doses of CVB3 after expressing IFN γ in pancreas via transgenic method survived without suffering myocarditis [21]. Suppressing the replication of virus in the pancreas prevented the onset of myocarditis. There must be some connection between pancreas and heart pathologically. Tracy et al. [22] used 8 different strains of CVB3 to infect mouse respectively, and 3 strains induced myocarditis. All strains replicated and persisted in pancreas 8 days post infection, but the cardiotropic strains of CVB3 tended to reach a higher titer level in the early phase and persist longer in serum, pancreas and heart than the non-cardiotropic strains.

From the above evidences, we could see that pancreas diseases and myocardium injuries associated with each other.

[IV] PANCREAS: RESERVOIR OF COXSACKIEVIRUS COMPARING WITH HEART

A study [23] focusing on coxsackievirus B 5's injury to mouse organs revealed that virus clearance rate was slow in both pancreas and heart than in liver. And virus RNA reached to peak value more earlier in pancreas than in heart (2.5 days V.S. 4 days), and the pathologic injury was also more serious (acute pancreatitis V.S. marginal myocarditis). Cheung et al. [24] found that as for the mouse 4 weeks and 8 weeks post infection, heart and pancreas were the most seriously injured organs, which implied the susceptibility to CVB5 infection of both organs. However, along with age growing susceptibility of the heart tissue decreased gradually. "Comparatively, susceptibility of the pancreas exocrine part to the virus didn't change. Pancreas is vulnerable to virus infection and favors virus replication. This is true not only for the enteroviruses but also for the encephalomyocarditis virus (EMV), which was supported by the fact that 28 days post EMV infection virus antigen could still be detected in the pancreas and pancreas suffered from chronic obstructive pancreatitis, but the inflammation focuses were almost healed completely except for some virus antigen detected in the valves.

Various recombinant CVBs had been used to clarify the pathogenesis of viral myocarditis. Henke et al. [25] designed a recombinant CVB3 expressing IFN γ and IL10. This recombinant virus could infect mouse, but its appearance is only restricted in pancreas rather than heart tissue. Pancreas seemed to be friendlier to CVB instinctively. Similarly, Slifka et al. [26] inserted one of the cytotoxic T-lymphocyte (CTL) epitopes from lymphocytic choriomeningitis virus (LCMV) into the genome of CVB3 and infected wild type neonate mouse and LCMV immunized mouse"respectively with this recombinant virus. The authors found that the latter displayed significant anti-virus effect with a 50 fold decrease of virus titer in the heart but only 6 fold in the pancreas. Besides, the authors found that the inserted epitope of this recombinant virus disappeared in vivo organ specifically with only 0~1.8% maintained in heart and rather more in pancreas. Although the authors addressed the immune pathogenesis of virus infection, these data emphasized on the other hand that pancreas is more vulnerable to CVB3 than heart and more compatible with the invaded virus. Another experiment using a recombinant CVB3 (CVB3-PL2-Ad2L1) [27] concluded that the recombinant coxsackievirus evoked viremia without inducing significant pathological changes in pancreas and heart, but in the pancreas rather than heart the authors found the persistent replication of this virus. This also indicated that pancreas seemed to be friendlier than heart to CVBs. Pancreas tends to be a reservoir of CVBs.

Why pancreas is seemed to be friendlier than heart to CVBs? The mechanism has not yet been clarified. Evidence hinted that it might be associated with the pattern pancreas activates the immune response. Vella et al. [28] studied pancreas sensitivity of 8 different mouse genotypes to CVB4 and found that the innate immunity, represented by NK cells, could inhibit virus replication in the early phase while the humoral response in the late phase failed inhibiting the virus replication. Further research found an inability of pancreatic

acinar cells to express the MHC I molecules. So it seemed that the comparative inability of the pancreas immunity pattern determines its compatibility with CVBs. Besides, low doses of virus infection of NK cell-depleted C3H/HeJ mouse led to pancreatitis in all mouse but myocarditis only in one case, which also implied a more vulnerable property of pancreas than heart.

Summarily, pancreas' susceptibility to coxsackievirus and compatibility with its proliferation seemed to be an intrinsic property determined by some mechanisms not yet clarified. The above evidences direct us to regard pancreas as a reservoir of CVBs.

[V] THE HEART IS MORE VULNERABLE THAN THE PANCREAS TO THE IMMUNOPATHOLOGIC INJURY AROUSED BY COXSACKIEVIRUS INFECTION

In the late phase of cardiomyopathy, viral genome may persist in many cases [29]. However the deterioration of heart function couldn't merely be explained by direct injury effect of virus and brought out the mechanism of pathologic immunity [30, 31]. Comparing with pancreas, heart is more vulnerable to pathologic immunity attack with regard to CVB infection. And related mechanisms have been summarized in a series of reviews elsewhere [32-36].

One of the mechanisms we focused here is the autoimmunity mechanism, which is still controversial. Although some investigator questioned the role of autoimmunity in the pathogenesis coxsackievirus cardiomyopathy [32], heart reactive autoantibodies indeed exist like autoantibodies to $\beta 1$ receptor [37], muscarinic acetylcholine receptor-2 [38], α - and β -cardiac myosin heavy chain [39] and ADP/ATP carrier (adenine nucleotide translocator, ANT) [40]. One of the mechanisms involved in the production of these autoantibodies is antigenic mimicry [34]. Some CVB protein components are structurally similar with related heart proteins. For example, the amino acid residues of ANT protein on 27-36 position are homologous to that of CVB3 capsid protein on 1218-1228 position [41].

Immune cells' intracellular signal transduction might also be associated with susceptibility of heart to myocarditis [42]. Inhibiting the NFAT in CD4+ T cells could prevent the onset of myocarditis but not pancreatitis. Virus titers in wild type mouse and NFAT-inhibited mouse were in the same level in pancreas but increased in NFAT-inhibited mouse's heart, indicating the difference of these two organs' responses to virus infection, in which pancreas' injury seemed not owing to immune factors like the heart was involved.

[VI] COMPROMISE OF SPLEEN B CELLS WITH COXSACKIEVIRUS

Basically, B cell humoral immunity plays a dual role in the injury of coxsackievirus to heart. On one hand, humoral immunity plays a certain role in defense against virus infection. Agamaglobulinemia patients are most vulnerable to coxsackievirus infection because of inability to produce antibody due to abnormal genes [43]. Despite B cells' lacking CARs on membrane surface, researches [44, 45] found that CVBs could infect spleen B cells in a passive way of been phagocytized in the procedure of antigen processing and presentation.

On the other hand, humoral immunity could facilitate the dissemination and replication of the infected CVBs [46, 47]. In mouse whose B cells were knocked out, virus dissemination and replication was delayed and chronic infection were observed in various organs including heart, liver, brain, kidney, lung, pancreas and spleen, which demonstrate B cells' roles in facilitating CVB replication and dissemination besides their killing effect [44].

Considering the compatibility of pancreas with CVBs and vulnerability of heart to pathologic immune injuries, such a compromise between B cells and CVBs might promote the formation of a vicious circle.

[VII] SUMMARY AND HYPOTHESIS: CAUSE AND EFFECT CHAIN OF "PANCREAS-SPLEEN-HEART"

In summary [Figure-1], we hypothesize that coxsackievirus invade the digestive tract, infect pancreas, and invade myocardium via viremia causing myocarditis and pancreatitis. After the acute phase, virus in the heart are cleared while still persist in pancreas. Anatomically adjoining, immune cells in spleen, especially B cells, are activated continually or at intervals by virus or virus components from pancreas, which results in synthesis and release of anti-virus products like antibodies to the peripheral circulation. Due to the similarity of heart structure proteins to virus epitopes, heart tissue is injured simultaneously. Besides, compatibility of pancreas with virus keeps on the above malignant events and forms the vicious cycle in specific individuals causing the progression of myocarditis to cardiomyopathy eventually. In short, cause and effect chain of "pancreas virus infection- spleen immunity activation- heart tissue pathologic immune injury" finally leads to the irreversible heart insufficiency.

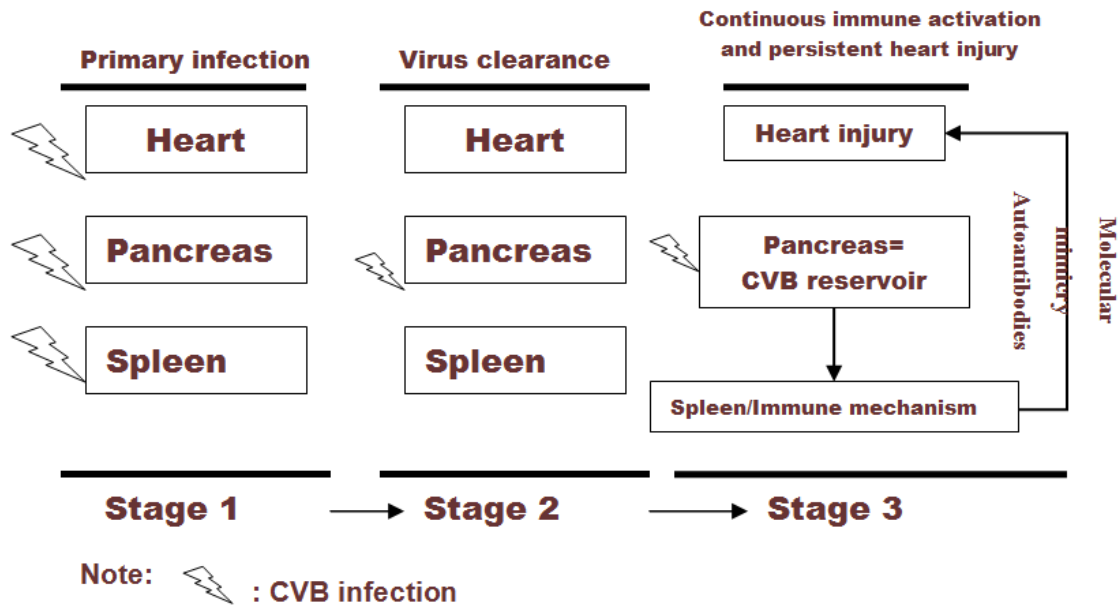


Fig. 1. Probable mechanism of interaction between heart, pancreas and spleen causes continuous heart injury after virus clearance in the heart via immune mechanisms. At stage 1, heart, pancreas and spleen are all infected by CVBs. Immune system is evoked and viruses are cleared at namely stage 2 completely in heart and spleen and only partially in pancreas. CVBs incubate in pancreas for a certain period and active immune system represented by spleen functions continuously or at intervals at stage 3. Via molecular mimicry mechanism, autoantibodies to heart proteins are also produced continuously or at intervals and cause persistent heart injury leading to the evolvement of myocarditis to cardiomyopathy.

FINANCIAL DISCLOSURE

This project was supported by grants from National Natural Science Foundation of China (No. 31070786), International Cooperation and Exchanges NSFC (No.81010007) and Research Fund for the Doctoral Program of Higher Education of China (No.20090071110076).

CONFLICTS OF INTEREST

All authors declare that we have no conflicts of interest.

REFERENCES

- [1] Cooper LT Jr. Myocarditis. [2009] *N Engl J Med* 360(15):1526–1538.
- [2] Schultz JC, Hilliard AA, Cooper LT Jr, Rihal CS. [2009] Diagnosis and treatment of viral myocarditis. *Mayo Clin Proc* 84(11):1001–1009.
- [3] Kim DS, Nam JH. [2011] Application of attenuated coxsackievirus B3 as a viral vector system for vaccines and gene therapy. *Hum Vaccine* 7(4):410–416.
- [4] Pan J, Narayanan B, Shah S, Yoder JD, Cifuentes JO, et al. [2011] Single amino acid changes in the virus capsid permit coxsackievirus B3 to bind decay-accelerating factor. *J Virol* 85(14):7436–7443.
- [5] Carson SD, Chapman NM, Hafenstein S, Tracy S. [2011] Variations of coxsackievirus B3 capsid primary structure, ligands, and stability are selected for in a coxsackievirus and adenovirus receptor-limited environment. *J Virol* 85(7):3306–3314.
- [6] Hauck AJ, Kearney DL, Edwards WD. [1989] Evaluation of postmortem endomyocardial biopsy specimens from 38 patients with lymphocytic myocarditis: implications for role of sampling error. *Mayo Clin Proc* 64(10):1235–1245
- [7] Baughman KL. [2006] Diagnosis of myocarditis: death of Dallas criteria. *Circulation* 113(4):593–595.
- [8] Oppenheimer EH, Esterly JR. [1973] Myocardial lesions in patients with cystic fibrosis of the pancreas. *Johns Hopkins Med J* 133(5):252–261.
- [9] Williams JO, Pollitzer RS, Green HD. [1952] Acute interstitial myocarditis associated with carcinoma of the body of the pancreas; report of a case. *N C Med J* 13(3):147–150.
- [10] Verma SK, Ahmad S, Shirazi N, Barthwal SP, Khurana D, et al. [2007] Acute pancreatitis: a lesser-known complication of aluminum phosphide poisoning. *Hum Exp Toxicol* 26(12):979–981.
- [11] Nezelof C, LeSec G. [1979] Multifocal myocardial necrosis and fibrosis in pancreatic diseases of children. *Pediatrics* 63(3):361–368.
- [12] Yan JJ, Wang JR, Liu CC, Yang HB, Su IJ. [2000] An outbreak of enterovirus 71 infection in Taiwan 1998: a comprehensive pathological, virological, and molecular study on a case of fulminant encephalitis. *J Clin Virol* 17(1):13–22.
- [13] Dettmeyer RB, Padosch SA, Madea B. [2006] Lethal enterovirus-induced myocarditis and pancreatitis in a 4-month-old boy. *Forensic Sci Int* 156(1):51–54.
- [14] Foulis AK, McGill M, Farquharson MA, Hilton DA. [1997] A search for evidence of viral infection in pancreases of newly diagnosed patients with IDDM. *Diabetologia* 40(1):53–61.
- [15] Gladisch R, Hofmann W, Waldherr R. [1976] Myocarditis and insulinitis following coxsackie virus infection. *Z Kardiol* 65(10):837–849.
- [16] Gómez RM, Lopez Costa JJ, Pecci Saavedra G, Berria MI. [1993] Ultrastructural study of cell injury induced by coxsackievirus B3 in pancreatic and cardiac tissues. *Medicina (B Aires)* 53(4):300–306.
- [17] Raschperger E, Thyberg J, Pettersson S, Philipson L, Fuxe J, Pettersson RF. [2006] The coxsackie- and adenovirus receptor

- (CAR) is an in vivo marker for epithelial tight junctions, with a potential role in regulating permeability and tissue homeostasis. *Exp Cell Res* 312(9):1566–1580.
- [18] Ashbourne Excoffon KJ, Moninger T, Zabner J. [2003] The coxsackie B virus and adenovirus receptor resides in a distinct membrane microdomain. *J Virol* 77(4):2559–2567.
- [19] Kallewaard NL, Zhang L, Chen JW, Guttenberg M, Sanchez MD, Bergelson JM. [2009] Tissue-specific deletion of the coxsackievirus and adenovirus receptor protects mice from virus-induced pancreatitis and myocarditis. *Cell Host Microbe* 6(1):91–98.
- [20] Ujevich MM, Jaffe R. [1980] Pancreatic islet cell damage. Its occurrence in neonatal Cocksackievirus encephalomyocarditis. *Arch Pathol Lab Med* 104(8):438–441.
- [21] Horwitz MS, La Cava A, Fine C, Rodriguez E, Ilic A, Sarvetnick N. [2000] Pancreatic expression of interferon-gamma protects mice from lethal coxsackievirus B3 infection and subsequent myocarditis. *Nat Med* 6(6):693–697.
- [22] Tracy S, Höfling K, Pirruccello S, Lane PH, Reyna SM, Gauntt CJ. [2000] Group B coxsackievirus myocarditis and pancreatitis: connection between viral virulence phenotypes in mice. *J Med Virol* 62(1):70–81.
- [23] Moon MS, Joo CH, Hwang IS, Ye JS, Jun EJ, et al. [2005] Distribution of viral RNA in mouse tissues during acute phase of Cocksackievirus B5 infection. *Intervirology* 48(2-3):153–160.
- [24] Cheung PK, Yuan J, Zhang HM, Chau D, Yanagawa B, et al. [2005] Specific interactions of mouse organ proteins with the 5'untranslated region of coxsackievirus B3: potential determinants of viral tissue tropism. *J Med Virol* 77(3):414–424.
- [25] Henke A, Zell R, Ehrlich G, Stelzner A. [2001] Expression of immunoregulatory cytokines by recombinant coxsackievirus B3 variants confers protection against virus-caused myocarditis. *J Virol* 75(17):8187–8194.
- [26] Slička MK, Pagarigan R, Mena I, Feuer R, Whitton JL. [2001] Using recombinant coxsackievirus B3 to evaluate the induction and protective efficacy of CD8+ T cells during picornavirus infection. *J Virol* 75(5):2377–2387.
- [27] Höfling K, Tracy S, Chapman N, Kim KS, Smith Leser J. [2000] Expression of an antigenic adenovirus epitope in a group B coxsackievirus. *J Virol* 74(10):4570–4578.
- [28] Vella C, Festenstein H. [1992] Cocksackievirus B4 infection of the mouse pancreas: the role of natural killer cells in the control of virus replication and resistance to infection. *J Gen Virol* 73:1379–1386.
- [29] Chapman NM, Kim KS. [2008] Persistent coxsackievirus infection: enterovirus persistence in chronic myocarditis and dilated cardiomyopathy. *Curr Top Microbiol Immunol* 323:275–292.
- [30] Olson JK, Croxford JL, Miller SD. [2001] Virus-induced autoimmunity: potential role of viruses in initiation, perpetuation, and progression of T-cell-mediated autoimmune disease. *Viral Immunol* 14(3):227–250.
- [31] Richer MJ, Horwitz MS. [2008] Viral infections in the pathogenesis of autoimmune diseases: focus on type 1 diabetes. *Front Biosci* 13:4241–4257.
- [32] Fujinami RS, von Herrath MG, Christen U, Whitton JL. [2006] Molecular mimicry, bystander activation, or viral persistence: infections and autoimmune disease. *Clin Microbiol Rev* 19(1):80–94.
- [33] Horwitz MS, Sarvetnick N. [1999] Viruses, host responses, and autoimmunity. *Immunol Rev* 169:241–253.
- [34] Münz C, Lünemann JD, Getts MT, Miller SD. [2009] Antiviral immune responses: triggers of or triggered by autoimmunity? *Nat Rev Immunol* 9(4):246–258.
- [35] Olson JK, Ercolini AM, Miller SD. [2005] A virus-induced molecular mimicry model of multiple sclerosis. *Curr Top Microbiol Immunol* 296:39–53.
- [36] Olson JK, Croxford JL, Miller SD. [2001] Virus-induced autoimmunity: potential role of viruses in initiation, perpetuation, and progression of T-cell-mediated autoimmune disease. *Viral Immunol* 14(3):227–250.
- [37] Limas C, Goldenberg I, Limas C. [1991] Effect of anti β 1 receptor antibodies in dilated cardiomyopathy on the cycling of cardiac beta receptors. *Am Heart J* 122:108–114.
- [38] Fu L, Magnusson Y, Bergh C, et al. [1993] Localization of a functional autoimmune epitope on the muscarinic acetylcholine receptor-2 in patients with idiopathic dilated cardiomyopathy. *J Clin Invest* 91:1964–1968.
- [39] Caforio A, Grazzini M, Mann J, et al. [1992] Identification of α - and β -cardiac myosin heavy chain isoforms as major autoantigens in dilated cardiomyopathy. *Circulation* 85:1734–1742.
- [40] Schulze K, Becker BF, Schultheiss HP. [1989] Antibodies to the ADP/ATP carrier, an autoantigen in myocarditis and dilated cardiomyopathy, penetrate into myocardial cells and disturb energy metabolism in vivo. *Circ Res* 64(2):179–192.
- [41] Caforio AL, Vinci A, Iliceto S. [2008] Anti-heart autoantibodies in familial dilated cardiomyopathy. *Autoimmunity* 41(6):462–469.
- [42] Huber SA, Rincon M. [2008] Cocksackievirus B3 induction of NFAT: requirement for myocarditis susceptibility. *Virology* 381(2):155–160.
- [43] Winkelstein JA, Marino MC, Lederman HM, Jones SM, Sullivan K, et al. [2006] X-linked agammaglobulinemia: report on a United States registry of 201 patients. *Medicine (Baltimore)* 85(4):193–202.
- [44] Mena I, Perry CM, Harkins S, Rodriguez F, Gebhard J, Whitton JL. [1999] The role of B lymphocytes in coxsackievirus B3 infection. *Am J Pathol* 155(4):1205–1215.
- [45] Klingel K, Stephan S, Sauter M, Zell R, McManus BM, Bültmann B, Kandolf R. [1996] Pathogenesis of murine enterovirus myocarditis: virus dissemination and immune cell targets. *J Virol* 70(12):8888–8895.
- [46] Kemball CC, Alirezaei M, Whitton JL. [2010] Type B coxsackieviruses and their interactions with the innate and adaptive immune systems. *Future Microbiol* 5(9):1329–1347.
- [47] Huber S. [2008] Host immune responses to coxsackievirus B3. *Curr Top Microbiol Immunol* 323:199–221.

THE RELATIONSHIP OF ZONOTIC CUTANEOUS LEISHMANIASIS TO ABO BLOOD GROUP

Safar Ali Talari, Mohammad Reza Talari, Zahra behzadi, Hossin Hooshyar, Rezvan Soltani, Hassan Ehteram*

Department of Parasitology, School of Medicine, Kashan University of Medical Sciences, Kashan, IRAN

ABSTRACT

*It has been hypothesized that leishmania parasites escape the host defence mechanisms by mimicry of human blood group antigen, conflicting reports have been published. The distribution of blood group types of human infected with cutaneous leishmaniasis was compared with control subjects. For each patient and control the following data were collected: age, sex, ethnic origin frequency of contamination with plant materials. In total number of infected persons 51.7% were males and 48.3% females. The highest rate of leishmaniasis were seen in the group of less than 10 years old and the least rate were in the age group of 40 to 55 year. We tested the hypothesis in cutaneous leishmaniasis, due to *Leishmania major*, by comparing to distribution of blood groups (ABO and Rhesus) among 482 patients in Isfahan central Iran with that among 1032 healthy controls. No association between blood groups and disease was found in this study, but further studies are needed with strains of the *Leishmania donovani* infantum.*

Received on: 19th-Jul-2011

Revised on: 7th-Aug-2011

Accepted on: 8th-Aug-2011

Published on: 12th-Apr-2012

KEY WORDS

Cutaneous leishmaniasis; ABO blood group type; Leishmania major; Kashan-Iran

*Corresponding author: Email: h_ehteram@yahoo.com; Tel: + 00989121910309; Fax: 00983614465055

[I] INTRODUCTION

Leishmaniasis remains an important cause of morbidity and mortality in numerous areas throughout the world. The association of certain human blood groups with parasites is a controversial subject. In some cases positive relations have been demonstrated, as in schistosomiasis [1] and Giardiasis [2], while in other cases, such as filariasis [3], no evidence of association appeared to the investigators. In particular case of leishmaniasis the same discrepancy occurs: Walton and Valverde noted racial differences in the evolution of mucocutaneous leishmaniasis (MCL) due to *Leishmania braziliencensis* [4]. Decker –Jacson and Honigberg [5] found that surface glycoproteins of *L. tropica* and *L. donovani* were comparable to certain ABO blood groups, suggesting a possible escape mechanism for these comparable to certain ABO blood groups of the patient [6]. On the contrary, a study of Brazilian patients with American visceral leishmaniasis (AVL) due to *L. donovani chagasi* did not show any significant relation between ABO blood groups and the development of the disease [7].

In order to determine whether there is an association between blood group types and zoonotic cutaneous leishmaniasis (ZCL) due to *L. major*, the distribution of blood groups in patients with this leishmaniasis observed in Isfahan Iran was compared with that in a control group of individuals living in province of Isfahan, with special attention being paid to ethnic origin and way of life.

[II] MATERIALS AND METHODS

A descriptive study was performed by random cluster. The distribution of blood group types in two groups isolated of infected patients was compared with that in two groups of control subjects.

The first group of ZCL patients group (group1) was composed of worker individual of Afghan refugees. These individuals have relatively frequent contact with the plant materials and the kind of soil which can infect the human and vectors. The second group (group2), ZCL patients of Iranian origin, was composed of individuals contaminated referring to Central Health Care of Shohada in Isfahan. This group had very frequent contact with infected sandflies, and they made up the majority of the patients examined at the laboratory of center health care of Shohada Isfahan.

A first control group was composed of afghan origin healthy individual having the same criteria as the first group of patients live in the same located Isfahan area. In a similar way, we used a second control group with a composition similar to that of the corresponding patients group: healthy persons of Iranian origin.

Zoonotic cutaneous leishmaniasis is endemic in Isfahan located in central Iran [8-11]. For infected patients, the diagnosis of ZCL was parasitologically confirmed by examination of positive smears. In the majority of cases identification of the parasite was made by measurement of the amastigotes in the smear, by behavior of the parasites in culture and by isoenzyme characterization.

In the two groups of infected patients (Group 1 and 2) and in control group 3 and 4, peripheral blood was taken by vene puncture and placed on slide. Commercially available anti A, anti B, and Rh (Blood Research and Fractionation Co) was used to determine the blood type. For the subjects in Groups 3 and 4, ABO and Rhesus blood groups

were obtained from the records of blood bank of Isfahan. For each patient and control the following data were collected: age, sex, ethnic origin, frequency of contamination with plant material and the kind of soil which can infect the human and vectors, location of habitation.

All the data were put into a computer based analysis, using a commercial software package, and then chi-square test statistical comparisons were made to assess the association of blood group types with other parameters. The p-value less than 0.05 considered statistically significant.

[III] RESULTS

In total number of 1514 infected persons, 51.7% were male and 48.3% female ($p < 0.5$). The highest rate of leishmaniasis were seen in the age group of less than 10 years old (43.7%) and the least rate were in the age group of 40 to 55 (1.2%). The distribution of the active lesions in relation to the age is shown in **Figure-1**.

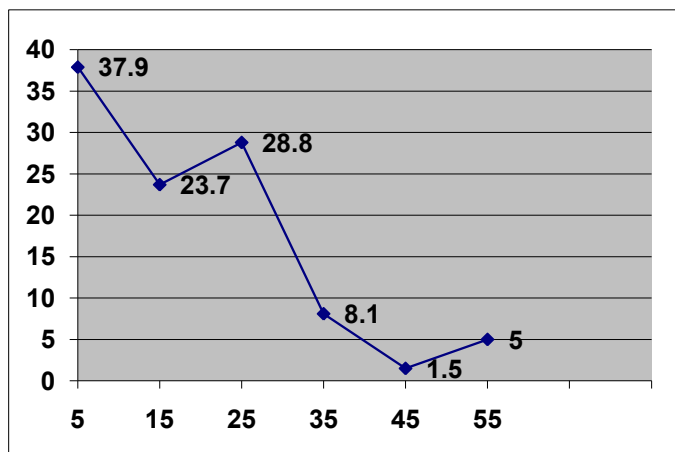


Fig: 1. Distribution of Zoonotic cutaneous leishmaniasis according to the age

Forty seven of the lesions were found on the hands, 21.4% on the face, 18% on the legs and 13.6% on other site of the body. From all infected patients, 1069 patients (70.6%) had only one lesion, 340 patients (22.4%), 2 lesions, 60 patients (4%), 3 lesions and 45 patients (3%) had 4 active lesions. According to these findings, 25.6% of the have living patients in north-eastern of Isfahan, 35.7% in west and 38.7% of them were referred from other clinics. 56% of patients were successfully treated.

The ABO and Rhesus blood group distributions are shown in **Supplementary Table-1** for patients with ZCL and the two groups. There was no significant difference ($P < 0.5$) with chi-square between the distribution of ABO, Rh blood group types in patients (Group 1 and 2). Likewise, there was no difference in all patients (Group 1 and 2) during this period and all controls (group 3 and 4).

[IV] DISCUSSION

The data show suggestive evidence there is not relation between blood group type and zoonotic cutaneous leishmaniasis. The findings thus fail to support the hypothesis of based on serotyping of leishmania excreted factors and studies of leishmanial surface glycoprotein's, that there is a relationship between ABO blood group and leishmaniasis in humans [6]. Our statistical evaluation was done with as many relevant comparisons as possible, and in no grouping could there be shown any association between ABO blood group type and ZCL.

In accordance with the comments of several authors of population – based studies we gave special attention in this study to statistical problems [7, 12, 13]. First, we were very careful with the selection of the different samples. One solution is the enter patients and control randomly cluster sampling in the study, as did [13], but we considered that the case / control method could be used with a minimum of precautions, particularly by selection control groups very similar to the patients group and seconds, we used sufficient numbers of controls and checked that the ratio of patients to control was not low.

The infections with *Leishmania* were evaluated by trained scientists in a laboratory, and not based on clinical features. The patients groups were homogeneously infected with *L. major*, which is the dominant subspecies in Isfahan–Iran. Where 117 of 1514 isolates obtained from human lesions were characterized as *L. major* by isoenzyme techniques [14]. The conclusion of our study is similar to that of [7] on AVL due to American cutaneous leishmaniasis (ACL) and [12] on ACL due to *L. braziliensis guyanensis*, which fails to support the hypothesis of camouflage by using blood group antigens. In their studies on AVL and ACL, these authors suggest that the susceptibility of humans of species other than *L. donovani infantum* may possibly be related to ABO blood type. Apparently this is not true for *L. major*, but further studies are needed with strains of the *L. tropica*.

Rather than a association between leishmaniasis in humans and the presence of red blood cell antigens other than ABO, we prefer to envisage the alternative hypothesis also suggested by

[7], that susceptibility to leishmaniasis, whether visceral or cutaneous leishmaniasis, might be related to surface antigens on human mononuclear phagocytes.

[V] CONCLUSION

Our results showed that the blood group was not a risk factor in the occurrence of ZCL. The ABO-Rh blood groups were not associated with the occurrence of ZCL in Iranian patients.

ACKNOWLEDGEMENTS

We are especially grateful to the physicians and staffs of the central health care Shohada and Blood Bank of Isfahan, and the patients who participated in this study.

FINANCIAL DISCLOSURE

This work was carried out with out any grant.

CONFLICTS OF INTEREST

All authors declare that we have no conflicts of interest.

REFERENCES

[1] Pereria FEL, Bortoloni EP, Carneiro JL, and Neves RC.[1979] ABO blood groups and hepatosplenic form of shistosomiasis mansoni . *Trans Of Royal Society of Tropical Med Hyg* 73: 238–241.

[2] Barnes and GL, Kay R. [1997] Blood groups in giardiasis. *Lancet* 1: 808–812.

[3] Higgins DA, Jenkins DJ, and Partono F. [1983] Timorian filariasis and ABO blood groups. *Trans. Of Royal Society of Tropical Medicine Hyg.* 79: 537–538.

[4] Walton BC, and Valverde L. [1979] Racial difference in espundia. *Annals of Trop Med and Parasitology.* 73:23–29.

[5] Decker-Jackson JE, Honigberg BM. [1978], Glycoproteins released by Leishmania donovani. Immunological relationships with host and bacterial antigens and preliminary biochemical analysis. *J of Parasitol* 25: 514–525.

[6] Greenblatt CL, Kark JD, Schnur LF, Slutzky GM. [1981] Do leishmania serotypes mimic human blood group antigens. *Lancet.*1: 505–506.

[7] Evans T, Talapala GN, Pearson RD. [1984] The relationship of American visceral leishmaniasis to ABO blood group type. *Am J Trop Med Hyg.* 33:805–807.

[8] Nadim MA, Faghiih DJ. [1968] The epidemiology of cutaneous leishmaniasis in Isfahan province of Iran. *Trans Royal Society of Trop Med Hyg.* 62: 534–542.

[9] Salimi M. [2000], A clinical and epidemiological comparison on the cutaneous leishmaniasis in the city and villages of Isfahan. *Iranian Journal of Public Health.* 2: 214–219.

[10] Yaghoobi MR, Jafari R, and Hanafi AA. [2004] A new epidemic focus of zoonotic cutaneous leishmaniasis in central Iran. *Annals of Saudi Medicine* 24: 98–101.

[11] Momeni A. [1994] Clinical picture of cutaneous leishmaniasis in Isfahan, Iran. *International J Dermatology.* 33: 260-265.

[12] Esterre P, and Dedet JP.[1989] The relationship of blood group type to American cutaneous leishmaniasis. *Annals of Trop Med and Parasitol.* 83: 345–348.

[13] Gyorkos TW, Sukul NC, and Dasdal A. [1983] Filariasis and ABO blood group: a critical appraisal. *Trans. Of Royal Society of Trop Med Hygiene.* 77:565–569.

[14] Farid Moaer H, Talari SA, Haghghi B, and Samadi A. [1997] Taxonomic determination of various type of leishmania isolated from Isfahan area using isoenzyme method, *Journal of Isfahan Medical School.* 14: 1–4.

Supplementary Table (As supplied by authors)

Supplementary Table: 1. Distribution of blood groups in patients with Zoonotic Cutaneous Leishmaniasis and in controls from Isfahan-Iran. Comparison was made between the distribution of all patients with ZCL (Group 1 and 2) and all control groups (Group 3 and 4) and no significant difference was found.

Group	No	No (%) in blood group		No (%) Rh		In	A	O	B	AB
+	-									
Group										
Infected group										
Group 1	42	14(33.3)	19(45.2)	7(16.7)	2(4.8)	38(90.5)	4(9.5)			
Group 2	75	29(38.7)	34(46.3)	11(14.7)	4(5.3)	69(92)	6(8)			
Control group										
Group 3	90	30(33.3)	42(46.7)	15(16.7)	3(3.3)	81(90)	9(10)			
Group 4	160	59(36.8)	70(43.7)	23(14.5)	8(5)	145(90.6)	15(9.4)			